International Pyrheliometer Comparison
IPC-X
26 September - 14 October 2005
Davos, Switzerland

Preliminary Results

Wolfgang Finsterle

PMOD/WRC Internal Report, Davos, 13 January 2006

Contents

Part I

RESULTS

Chapter 1 Organization and Procedures

1.1 Introduction

The Tenth International Pyrheliometer Comparison (IPC-X) was held from 26 September through 14 October 2005 at the Physikalisch-Meteorologisches Observatorium Davos/World Radiation Center (PMOD/WRC) in Davos, Switzerland.

The results presented in this report are based on the measurements carried out during the 3 weeks assigned to the IPC-X. The favorable weather conditions yielded a record number of calibration points for most participating instruments. Cloudy and overcast days were used for technical preparations and training of participants as well as for a the IPC-X symposium.

1.2 Participation

72 participants took part in the comparison and operated a total number of 101 pyrheliometers (including the WSG instruments).

1.3 Data Acquisition and Evaluation

The WSG instruments and additional radiometers of the WRC as well as auxiliary parameters were measured by an analog data acquisition system based on eight HP3478A voltmeters with relay scanners that are controlled by the data acquisition PC.

The remaining instruments were operated with their standard equipment in order to avoid electrical interface problems and mutual interferences. The data from the participating instruments were acquired via a number of micro-terminals operated by the participants and controlled by the data acquisition PC. Each terminal could accept up to 3 different values from two instruments. After each series, a summary of the values entered by micro-terminal was printed and distributed to be checked by the participants. If necessary, the raw data could be edited manually to correct typing errors.

The participants having their own computer controlled systems (synchronized to the timing of the IPC's measurement series) had the possibility to up-load their data to a dedicated directory on the IPC-X FTP site. LAN/WLAN, floppy disks, or USB memory sticks were accepted means of data transfer. All data on the FTP site were ingested into the data acquisition and evaluation system at the end of each day.

1.3.1 Timing of the Measurements

The measurements were taken in series of 21 minutes with a basic cadence of 90 seconds. Voice announcements and buzzer signals were used to inform the participants about the sequence of operations. All data acquisition systems were synchronized to Central European Time either by connecting them to a network time server or by manually adjusting to the reference clock, which was set up on the measuring field. The timing for the different instrument types was as follows:

- Ångström pyrheliometers: Before the start and after the end of the run the zero of the instrument was established. Alternating right and left strip readings were performed, starting with the right hand strip exposed to the sun. The following readings were paired as L-R, R-L, etc., yielding a total of 12 irradiance values per run.

- PACRAD: the run started with the shutter closed, after 60 s the heater was turned on for 40 s (this was introduced after IPC-III in order to have a well defined thermal state of the instrument independent of the operation sequence before the run). At 270 s the zero of the thermopile was read and the heater switched on again. At 450 s the heater voltage, current and thermopile was read, the heater turned off and the shutter opened. From 540 s on readings were taken every 90 s yielding 8 irradiance values per run. After the last reading the shutter was closed.

- HF type pyrheliometers: the run started with the shutter closed, after 90 s the zero was read and the heater turned on until at 180 s the voltage, current and thermopile were read. The heater was then turned off and the shutter opened. From 270 s onward the instrument was read every 90 s yielding 11 irradiance values per run. Some instruments which were providing their data with diskettes performed the calibration between the series and consequently measured 13 irradiance values per run.

- TMI type pyrheliometers: the run started with the shutter closed and the calibration procedure was performed until the end of the first 90 s. Starting at 180 s readings were taken every 90 s yielding 12 irradiance values per run.

- Active cavity type pyrheliometers: the run started with a reference phase (shutter closed) of 90 s, followed by a measurement phase (shutter open) of 90 s. This was repeated for the next 18 minutes. A total of 6 open and 7 closed readings were taken yielding a total of 6 irradiance values during a run. PMO2 was read at twice that pace, with a reference phase of 32 s and a measurement phase of 58 s, producing 13 irradiance values per run so that for all readings of the basic sequence a PMO2 irradiance was available.

- Normal Incidence Pyrheliometers (NIP): it took 12 irradiance values every 90 s after an initial zero reading at 90 seconds.

1.3.2 Data Evaluation

For each instrument the irradiance was obtained with the appropriate evaluation procedure as listed below. After each day a summary of the computed irradiances was printed and distributed to be checked by the participants. As indication the mean and standard deviation of the ratios to PMO2 were also given for each series. PMO2 was used as the local reference during the time of the comparison.

The procedure used to calculate the irradiance *S* of each instrument type is described below. The notations are:

V_{th}	output of the thermopile
U_h, U_i	voltage across the heater (h) or across the standard resistor (i)
R_n	standard resistor
C	calibration factor
C_2	correction factor for lead heating
P	electrical power in the active cavities

- Ångström-pyrheliometers: the current through the right or left strip was measured as voltage drop across a standard resistor and the irradiance was obtained as:

$$S = C\frac{U_i(\text{left})U_i(\text{right})}{R_n^2}$$

This corresponds to the geometric mean of the irradiances at the time of right and left readings. Thus, the ratio to WRR was calculated using the geometric mean of the WSG irradiances at the corresponding instances.

- PACRAD and HF type pyrheliometers: the irradiance was calculated from the thermopile output V_{th}(irrad) when the receiver was irradiated. The sensitivity was determined by the calibration during which the cavity was shaded and electrically heated and U_h and U_i were measured together with the corresponding thermopile output V_{th}(cal). Furthermore, the zero of the thermopile V_{th}(zero) was measured and subtracted.

$$S = C\frac{V_{th}(\text{irrad}) - V_{th}(\text{zero})}{V_{th}(\text{cal}) - V_{th}(\text{zero})}\frac{U_i}{R_n}\left(U_h - \frac{U_i}{R_n}C_2\right)$$

- TMI type pyrheliometers: most were operated in the "normal" way, that is by calibrating the readout directly in units of $\mathrm{mW\,cm^{-2}}$. The values were entered in $\mathrm{Wm^{-2}}$ and no irradiance calculation was needed. Others were operated and evaluated like HF pyrheliometers.

- Active cavity pyrheliometers: the irradiance was obtained from P(closed) averaged from the closed values before and after the open reading P(open).

$$S = C(P(\text{closed}) - P(\text{open}))$$

The power calculation was done according to the prescription of the instrument type with

$$P = U_h^2 \qquad \text{or} \qquad P = U_h U_i \qquad \text{or} \qquad P = U_h\frac{U_i}{R_n}$$

- Normal Incidence Pyrheliometer (NIP): the thermopile reading was divided by the calibration factor after subtraction of the zero point reading.

- PMO2: As during preceding IPCs, PMO2 was used as the local reference instrument because it can be operated fast enough to provide an irradiance value every 90 seconds. The values of PMO2 were obtained with the algorithm for active cavity radiometers. At the end of the open phase, 8 readings were taken in rapid succession. For the on-line calculations the first value was used as reference for the values entered by the terminals. The standard deviation of the 8 readings was used during the final evaluation as a quality control parameter to judge the stability of the radiation during each acquisition sequence (see Sect. 2.1).

1.3.3 Auxiliary Data

The meteorological parameters (air temperature, relative humidity, atmospheric pressure) were obtained from the automatied weather station ASTA of MeteoSwiss located at PMOD/WRC. The ASTA values are 10-minute averages. A cloud sensor flagged all data points when clouds were within 15 degrees of the Sun. No such points were used to evaluate ngstrom type pyrheliometers.

1.4 Approvement and Dissemination of the Results

According to Resolution 1 of CIMO-XI an Ad-hoc Group was established to discuss the preliminary results of the IPC-X, based upon criteria defined by the WRC, evaluate the above reference and recommend the updating of the calibration factors of the participating instruments. It was chaired by the Bruce W. Forgan, (Australia, Region V) and composed as follows: Mohamed Hussein Korany (Egypt, Region I), Kohei Honda (Japan, II), Pedro Mostraj Aquilera (Chile, III), Augustin Muhlia (Mexico, IV), Don Nelson (USA, IV), Zlotan Nagy (Hungary, VI), Klaus Behrens (Germany, CIMO Expert Team). The WRC was represented by Wolfgang Finsterle and Werner Schmutz.

The procedures used to compute the new WRR factors of the WSG and participating instruments have been approved by the Ad-hoc Group and the final results of IPC-X were calculated accordingly.

Besides its official duties, the Ad-hoc Group also discussed the future of the IPCs and the most efficient way of transferring the WRR worldwide.

Chapter 2 Measurements and Results

Measurements were taken on 10 days (September 26, 28, and 30, October 4, 9, 10, 11, 12, 13, and 14).

2.1 Data Selection Criteria for the Final Evaluation

At the beginning of the IPC, the Ad-hoc Group responsible for the approval of the final evaluation procedure (c.f. Sect. 1.4) met and set the following criteria for the acceptance of IPC data:

1. Only observations falling within the appropriate measurement periods be accepted and that the last series for any group of instruments stop before the end of the period is reached (based on calculations associated with the instrument field of view).
2. That no measurements be used for Ångstrom pyrheliometers if a cloud is within 15 degrees of the sun. No measurements will be used for the absolute cavity radiometers (field-of-view = 5°) if a cloud is within 8 degrees of the sun.
3. That no measurements be used if the measured wind speed is greater than 2.5 m/s.
4. That no data be used if the 500 nm AOD is greater than 0.12.
5. That an individual point be excluded from a series if the variation of the 8 fast PMO2 measurements is greater than $0.5\,\mathrm{Wm^{-2}}$.
6. That an entire series be removed from consideration if more than two (out of 13) individual observations do not meet criterion (5).
7. That the minimum number of acceptable data points be 150 for the PMO2 taken over a minimum of three days during the comparison period.

All measurements which have been selected for the preliminary evaluation are in conformity with criteria 1, 2, 5, and 7. The remaining criteria will be considered for the final evaluation.

2.2 Status of the WSG

The main objective of the periodic International Pyrheliometer Comparisons is the dissemination of the World Radiometric Reference (WRR) in order to ensure worldwide homogeneity of meteorological radiation measurements. The WRR is realized by the World Standard Group (WSG) which is frequently inter-compared at PMOD/WRC to detect possible deviations of individual members of the group and to ensure the stability of the WRR. Independently, the stability of the WRR can be checked by instruments that have participated in previous IPC's.

Since IPC-IX, which was held in 2000, three member instruments of the World Standard Group showed a linear trend of about -185 ppm/yr (PMO2), +130 ppm/yr (HF18748), and +100 ppm/yr (PAC3), respectively. The drift in PMO2 is suspected to be caused by degradation of the electronics amplifier. An almost identical drift occured in PMO5 five year ago and was corrected by removing the signal amplifier. Suitability tests for a similar repair of PMO2 are under way. In the case of HF18748 the manufacturer suggested to check and clean all connections. This will be postponed until after PMO2 is fully functional again.

2.3 Transfer of the WRR

Since the instrumental drifts described in Sect. 2.2 nearly compensate all six WSG member instruments (i.e. PMO2, PMO5, CROM2L, PAC3, TMI67814, HF18748) were included in the transfer of the WRR.

Table 2.1: New WRR-factors for the WSG instruments computed using PMO2, PMO5, CROM2L, PAC3, HF18748 and TMI67814 and the IPC-IX WRR-factors.

Instrument	*WRR factors IPC-IX*	*WRR factors IPC-X*	*Standard Uncertainty* (σ/N)*[ppm]*	*N*	*Change [ppm] IPC-X - IPC-IX*
PMO2	0.999548	0.998614	12	1037	-934
CROM2L	1.00301	1.002991	36	497	-19
TMI67814	1.00066	1.000702	13	940	42
HF18748	0.995675	0.996293	14	939	612
PAC3	1.00065	1.001135	15	680	485
PMO5	.998974	0.998984	25	516	10

2.4 Computation of the New WRR-Factors

For the preliminary evaluation of the instruments participating in IPC-X the factors of Table 2.1 were used to calculate the WRR for each sequence as the mean of at least 3 instruments from the WSG.

2.5 Stability of the WRR and Recommendations for the WSG

The WRR factors for the tree WSG member instruments PMO5, MK67814, and CROM2L changed since last IPC by less than 42 ppm (Tab. 2.1). The remaining three WSG member instruments showed obvious longterm linear drifts of -934 ppm (PMO2), 612 ppm (HF18748), and 485 ppm (PAC3), which alomst cancel out each other. The short-term stability of all three of these instruments is not affected by their drift. The stability of the WRR could be further checked by calculating the average change of the WRR reduction factors of all pyrheliometers which had participated in IPC-IX and IPC-X (42 instruments, not counting the WSG). On average the WRR reduction factor of those 42 instruments changed by -292 ppm with a standard uncertainty of 410 ppm. One instrument (PMO6-850410) shows a large change of -1.3% and can be considered an outlier. Excluding it from the analysis yields an average change of $+17\pm276$ ppm. If we only use those instruments which changed by less than 0.3% we get -58$\pm$215 ppm (39 instruments). These results are certainly confirming the stability of the WRR derived by the results of the WSG alone. The observed changes are also very well in agreement with results from previous IPCs. It is therefore reasonable at this stage to conclude that a) the WRR was stable over the past five years and b) to use all six WSG member instruments for the transfer of the WRR.

Chapter 3 Graphics

3.1 Graphical Representation of the Results

The following figures show the performances of the instruments. The deviation from WRR (i.e. "ratio to WRR"-1) is plotted. All the points which may be used for the analysis (i.e. the points fulfilling the selection criterion mentioned in Sect. 2.1) have been plotted with a corresponding histogram on the side. The horizontal solid line represents the derived ratio to WRR and the dashed lines its 1-σ standard deviation. The values of the ratio to WRR and its standard deviation is printed on top of the plot with the number of points used to determine this value. The number in parentheses corresponds to the total number of points available for the analysis.

Note: Two Ångström type instruments exhibited serious problems. Å8412 was operated in a "actinometric"-type mode, i.e. with no heating power applied to the shaded strip. The reading of the thermocouple was submitted. These data were analyzed using the standard Ångström procedure. The uncertainty of the resulting WRR factor therefore is quite high. Å6549 submitted an almost constant reading corresponding to $\sim 830Wm^{-2}$. The same happened already during IPC-IX and was then attributed to an improper operation of the instrument. Since the instrument was now operated by a different person this was porbably the wrong explanation. The instrument is probably broken. Data from this instrument cannot be evaluated.

3.1.1 WSG Member Instruments

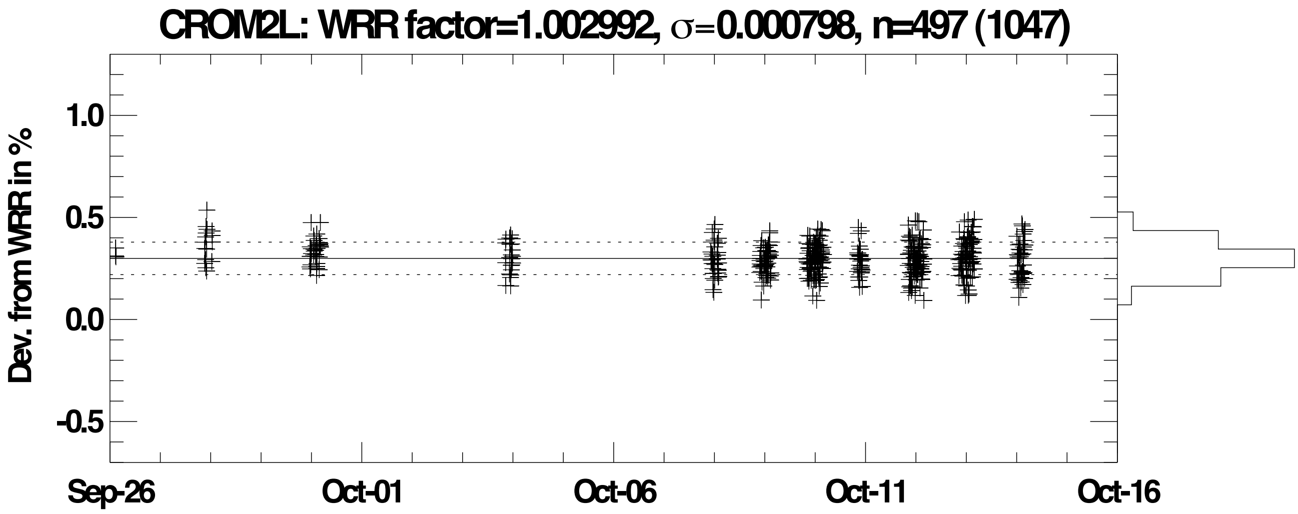

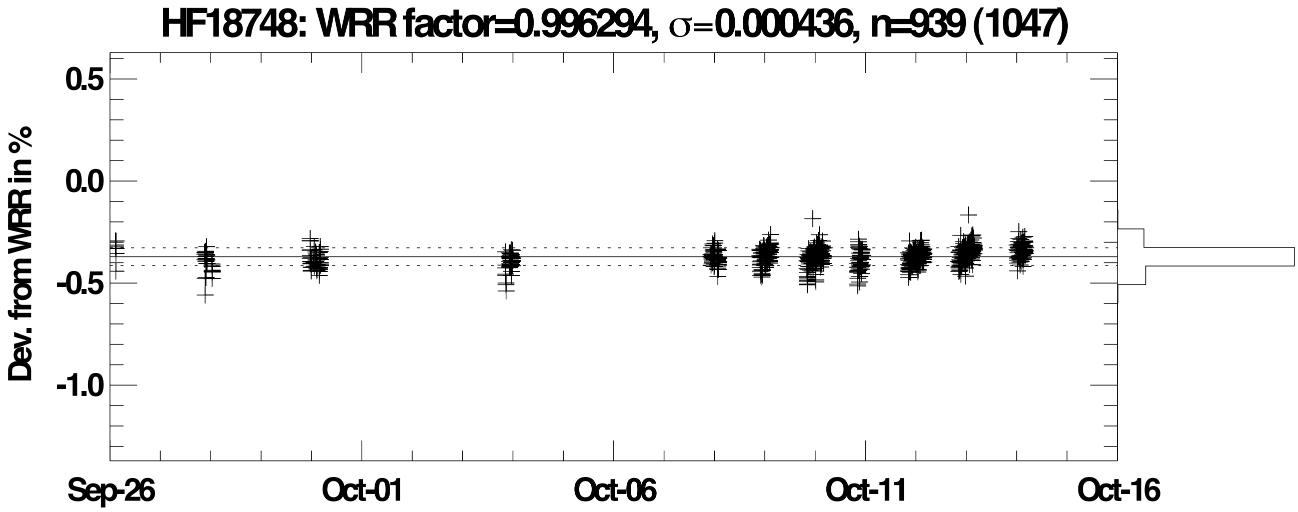

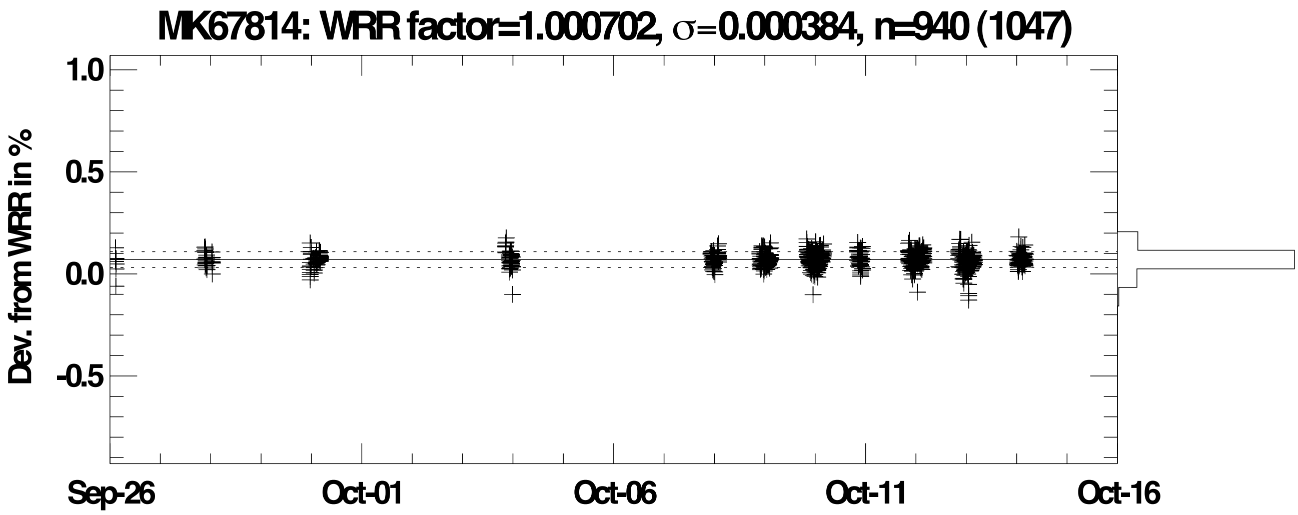

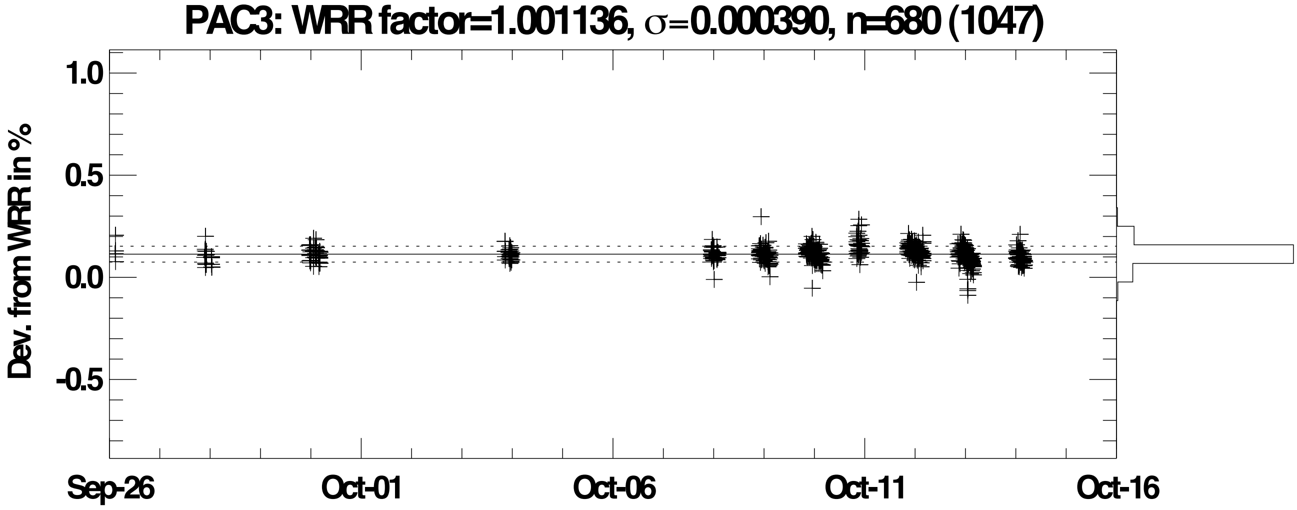
PAC3: WRR factor=1.001136, σ=0.000390, n=680 (1047)
Dev. from WRR in %
1.0
0.5
0.0
-0.5
Sep-26
Oct-01
Oct-06
Oct-11
Oct-16

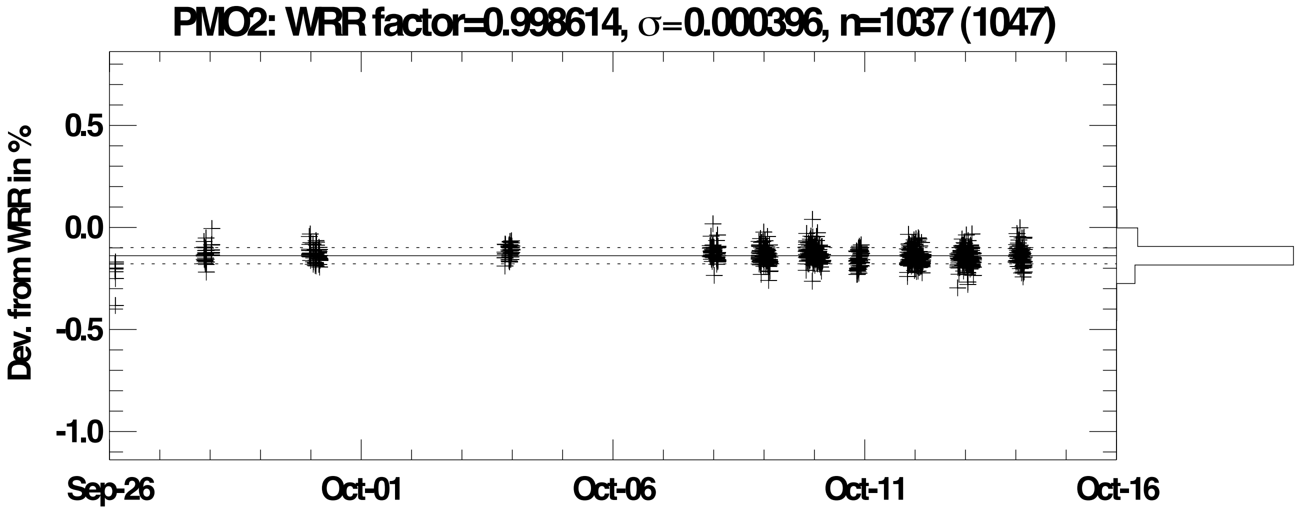
PMO2: WRR factor=0.998614, σ=0.000396, n=1037 (1047)
Dev. from WRR in %
0.5
0.0
-0.5
-1.0
Sep-26
Oct-01
Oct-06
Oct-11
Oct-16

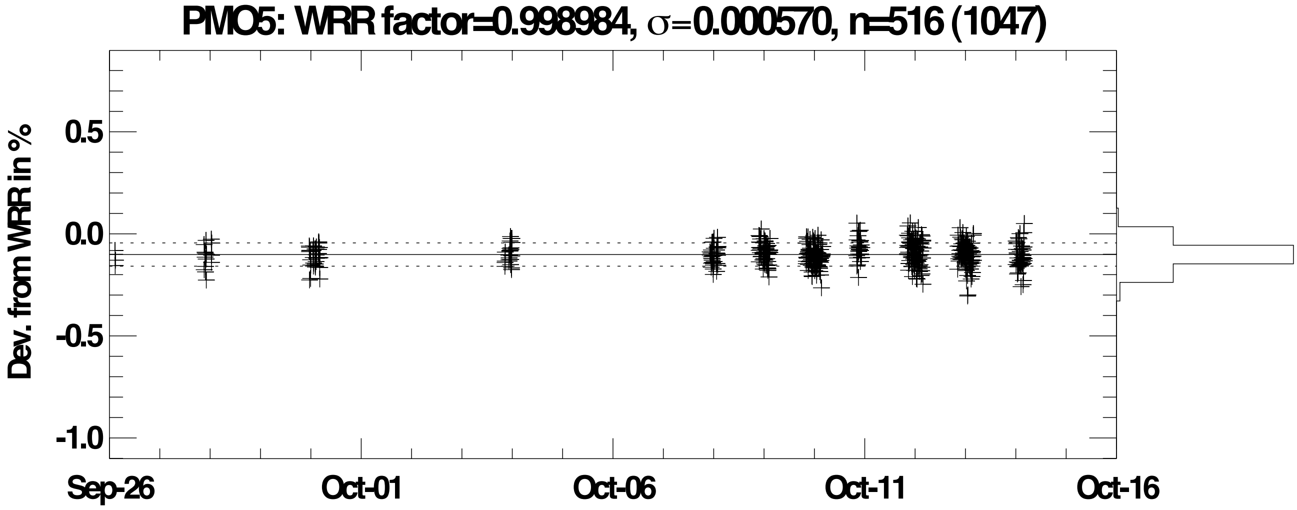
PMO5: WRR factor=0.998984, σ=0.000570, n=516 (1047)
Dev. from WRR in %
0.5
0.0
-0.5
-1.0
Sep-26
Oct-01
Oct-06
Oct-11
Oct-16

3.1.2 Participating Instruments

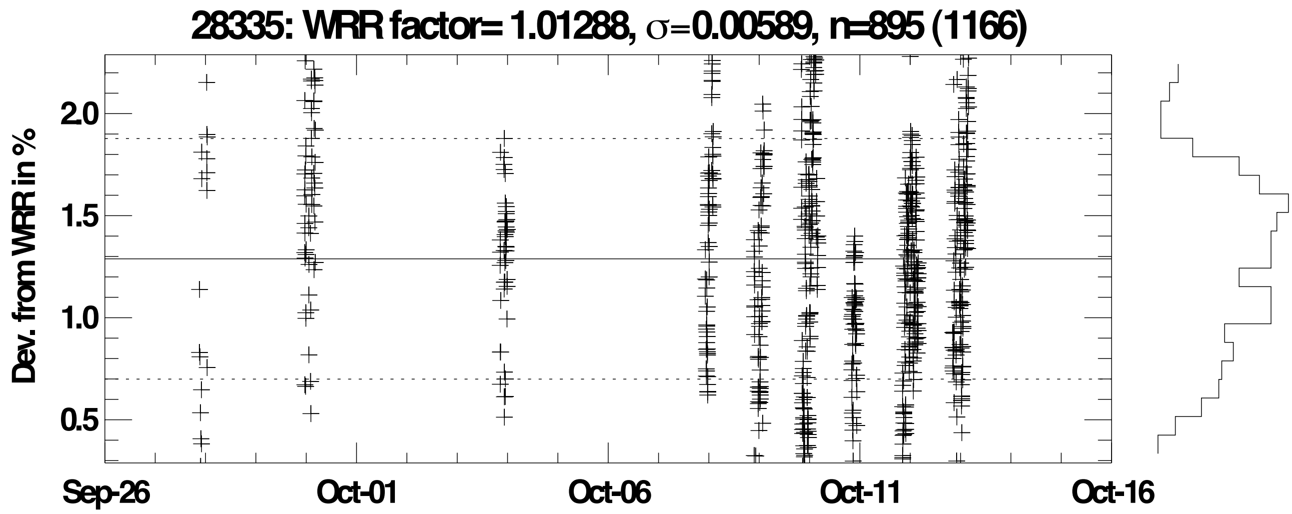

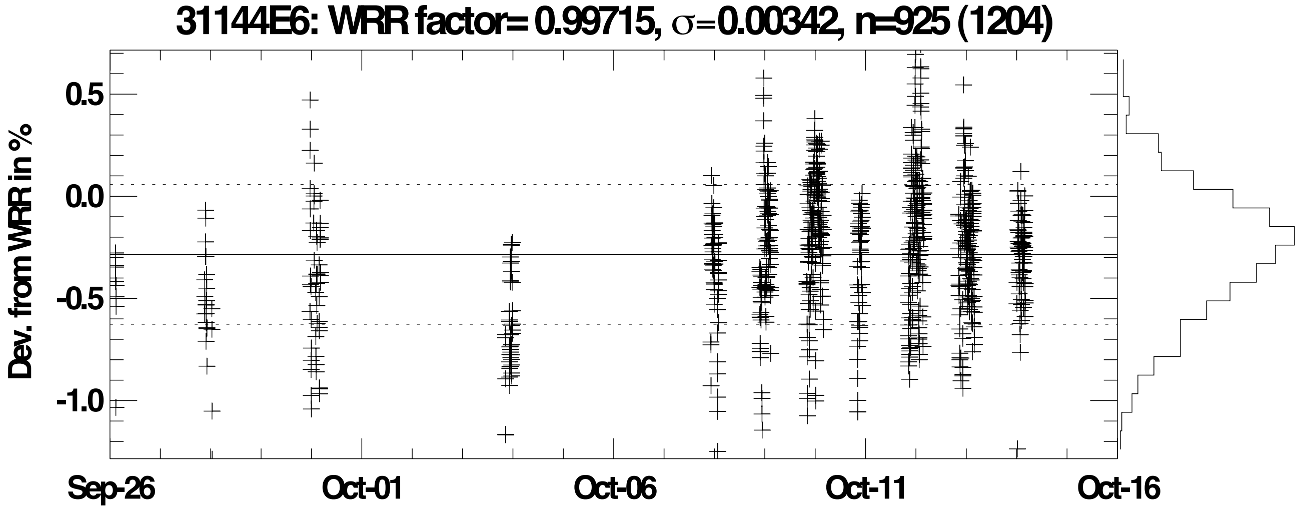

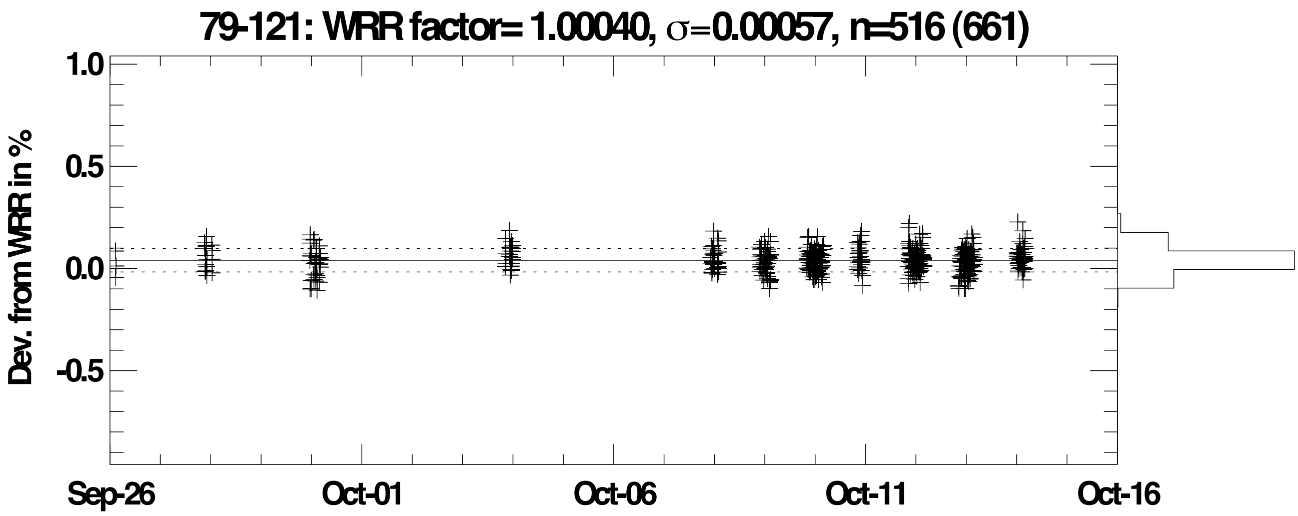

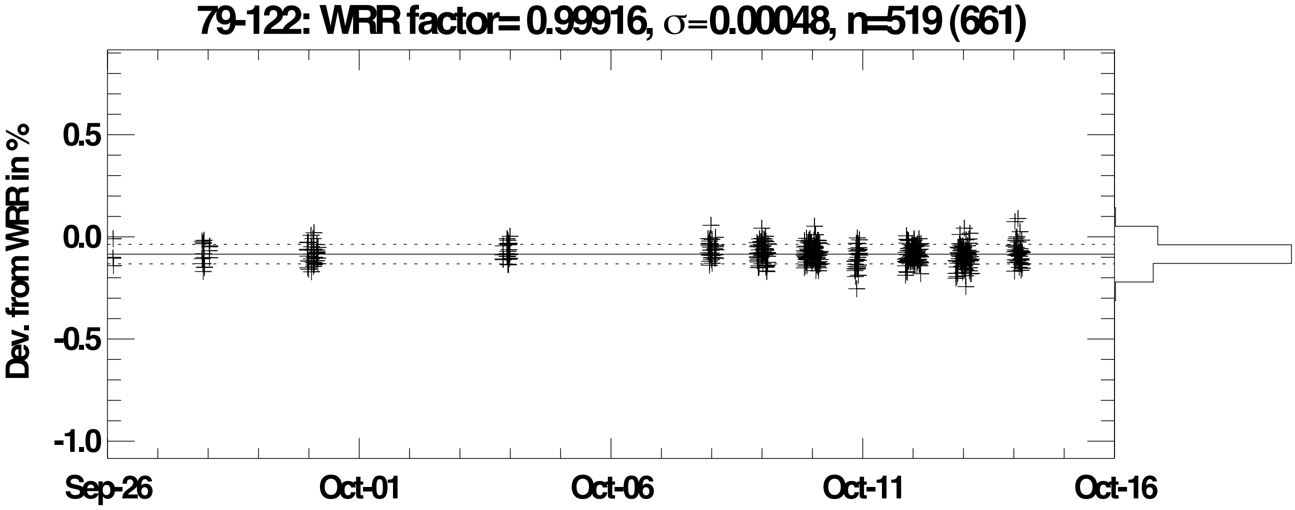
79-122: WRR factor= 0.99916, σ=0.00048, n=519 (661)
Dev. from WRR in %
0.5
0.0
-0.5
-1.0
Sep-26
Oct-01
Oct-06
Oct-11
Oct-16

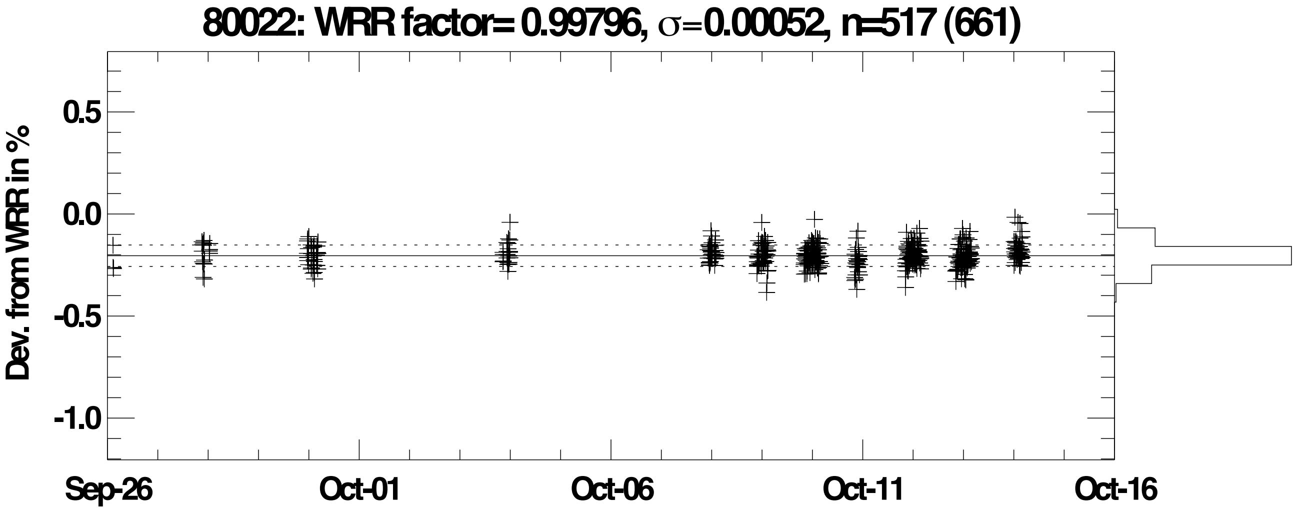
80022: WRR factor= 0.99796, σ=0.00052, n=517 (661)
Dev. from WRR in %
0.5
0.0
-0.5
-1.0
Sep-26
Oct-01
Oct-06
Oct-11
Oct-16

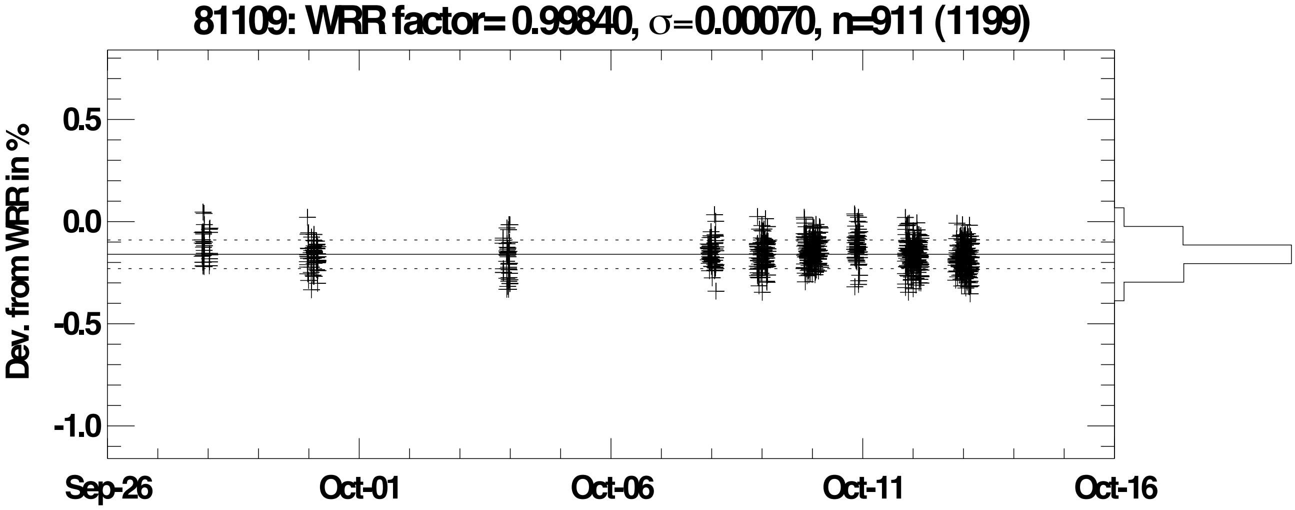
81109: WRR factor= 0.99840, σ=0.00070, n=911 (1199)
Dev. from WRR in %
0.5
0.0
-0.5
-1.0
Sep-26
Oct-01
Oct-06
Oct-11
Oct-16

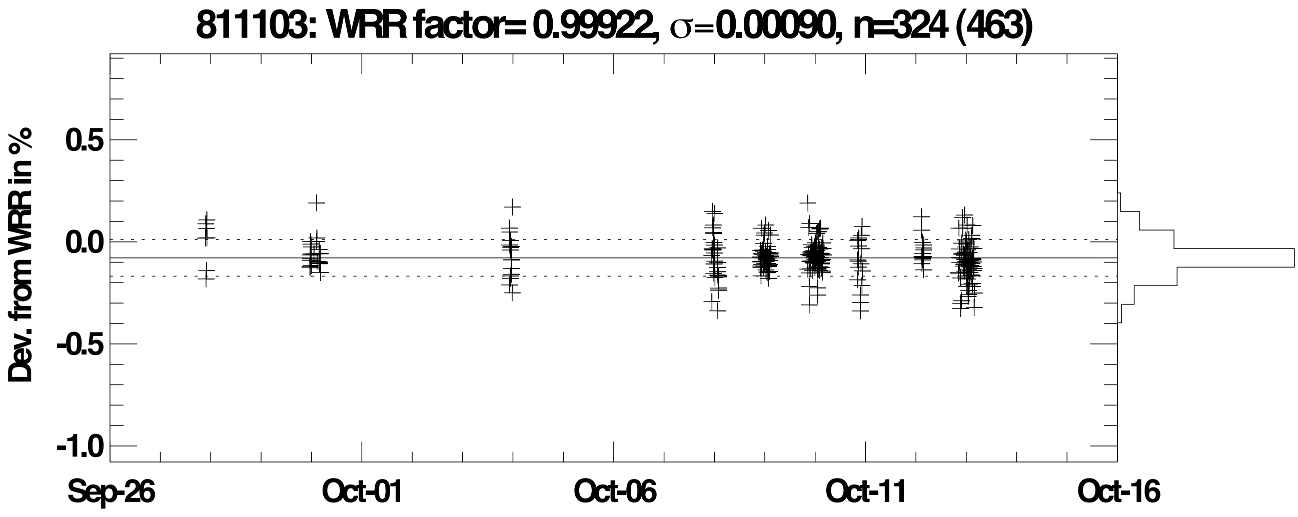
811103: WRR factor= 0.99922, σ=0.00090, n=324 (463)
Dev. from WRR in %
0.5
0.0
-0.5
-1.0
Sep-26
Oct-01
Oct-06
Oct-11
Oct-16

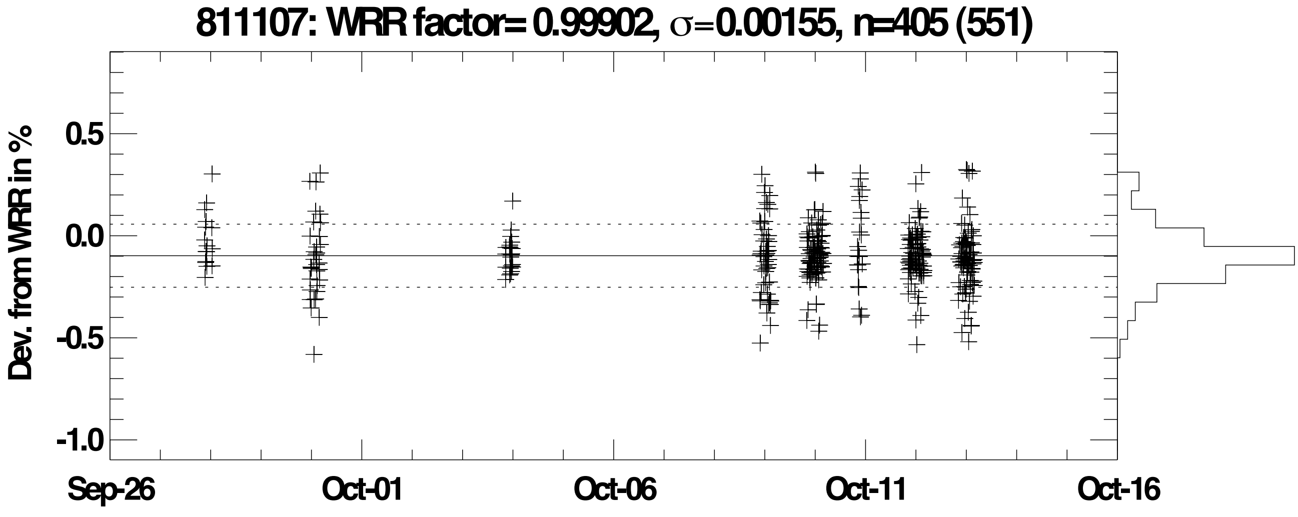
811107: WRR factor= 0.99902, σ=0.00155, n=405 (551)
Dev. from WRR in %
0.5
0.0
-0.5
-1.0
Sep-26
Oct-01
Oct-06
Oct-11
Oct-16

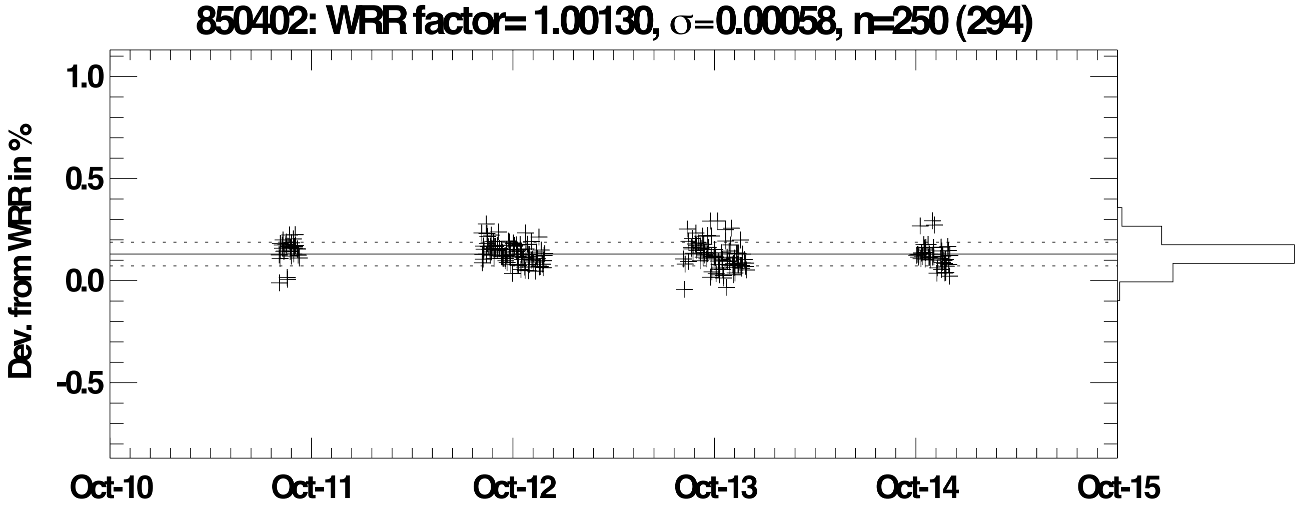
850402: WRR factor= 1.00130, σ=0.00058, n=250 (294)
Dev. from WRR in %
1.0
0.5
0.0
-0.5
Oct-10
Oct-11
Oct-12
Oct-13
Oct-14
Oct-15

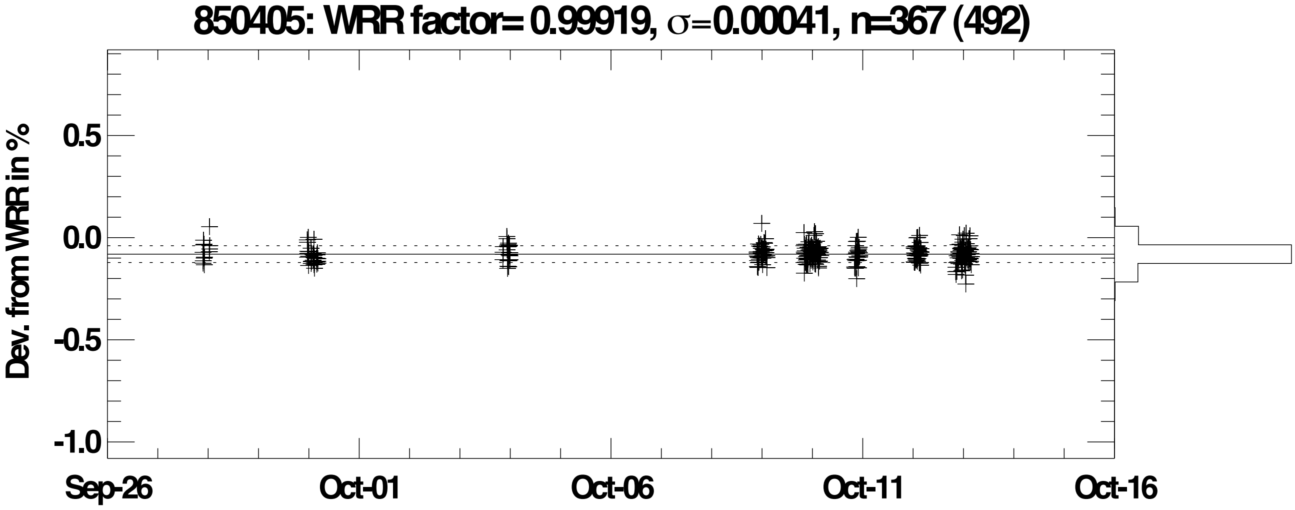
850405: WRR factor= 0.99919, σ=0.00041, n=367 (492)
Dev. from WRR in %
0.5
0.0
-0.5
-1.0
Sep-26
Oct-01
Oct-06
Oct-11
Oct-16

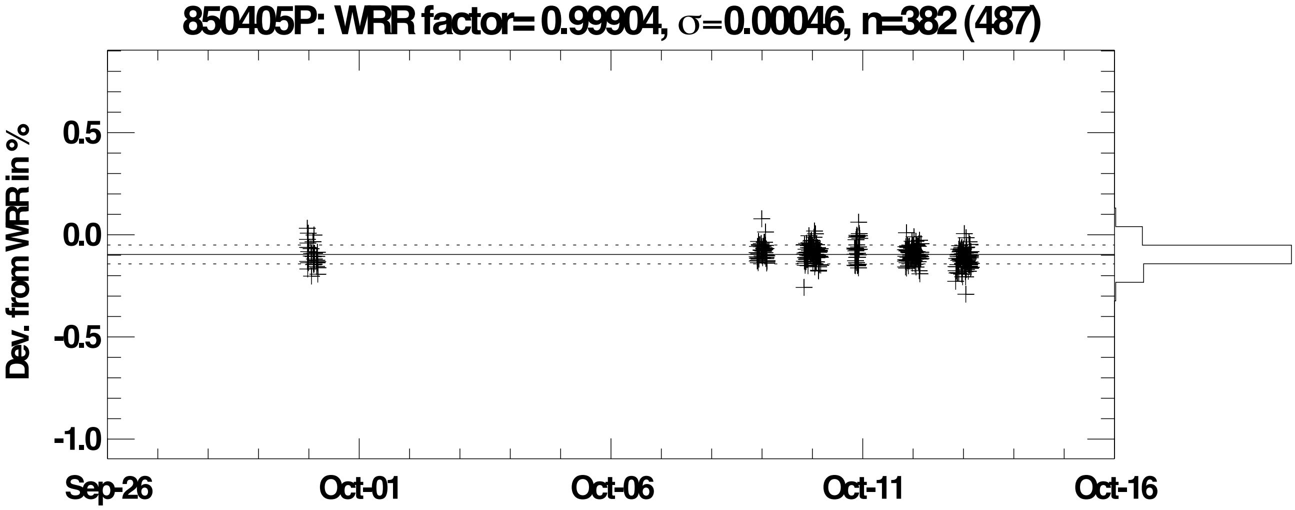
850405P: WRR factor= 0.99904, σ=0.00046, n=382 (487)
Dev. from WRR in %
0.5
0.0
-0.5
-1.0
Sep-26
Oct-01
Oct-06
Oct-11
Oct-16

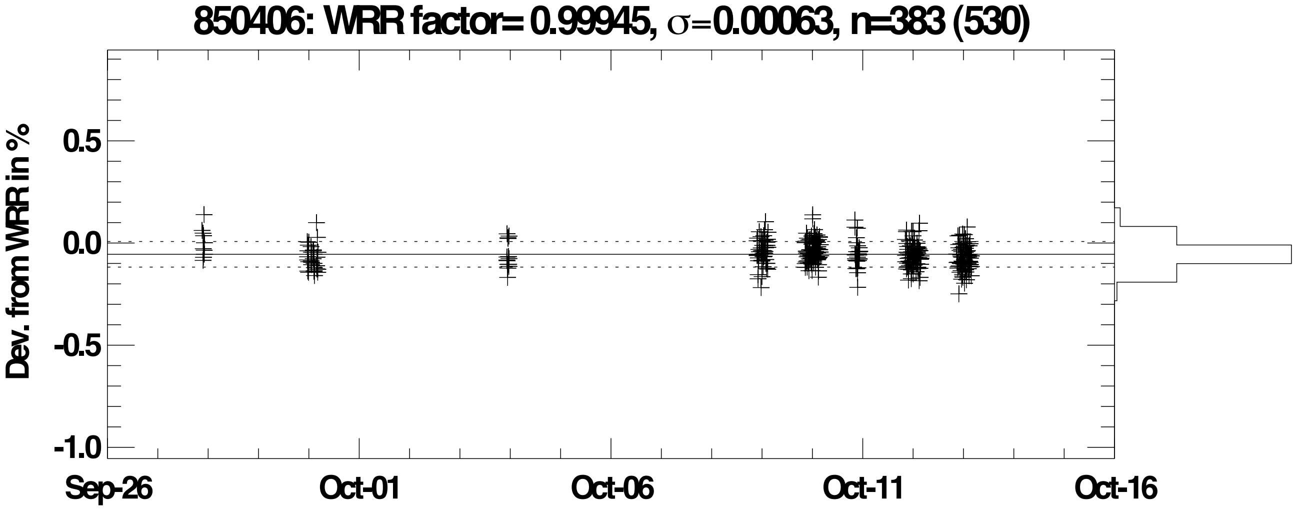
850406: WRR factor= 0.99945, σ=0.00063, n=383 (530)
Dev. from WRR in %
0.5
0.0
-0.5
-1.0
Sep-26
Oct-01
Oct-06
Oct-11
Oct-16

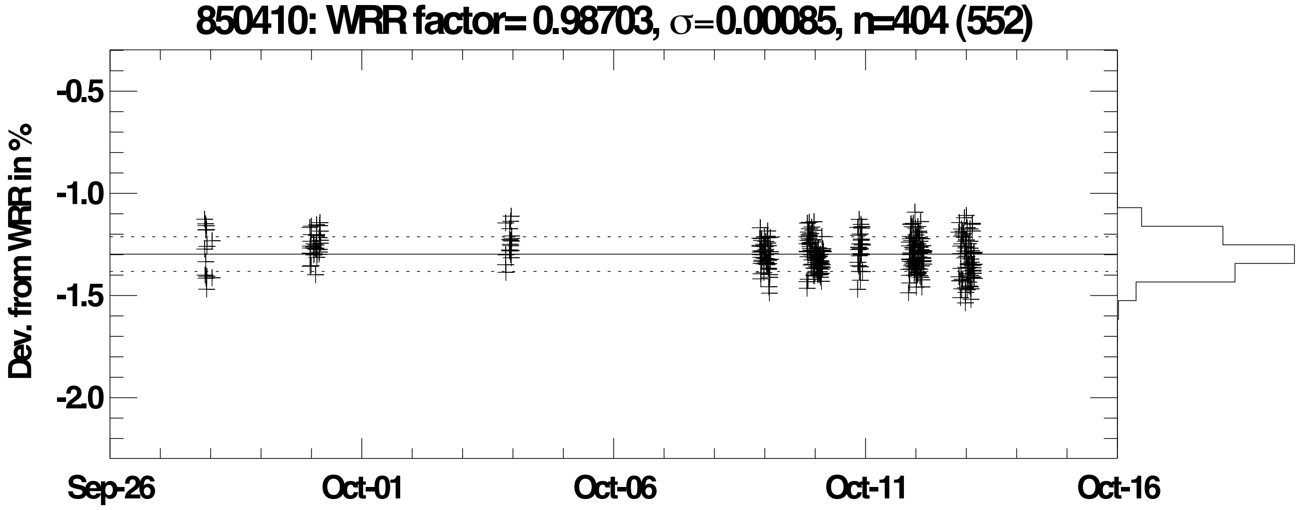
850410: WRR factor= 0.98703, σ=0.00085, n=404 (552)
Dev. from WRR in %
-0.5
-1.0
-1.5
-2.0
Sep-26
Oct-01
Oct-06
Oct-11
Oct-16

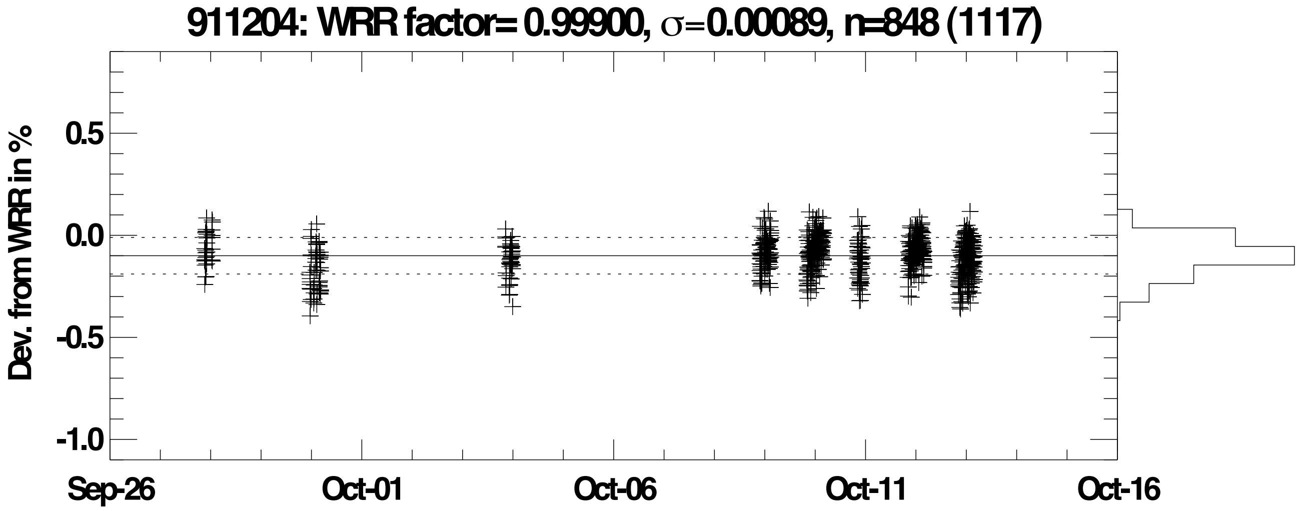
911204: WRR factor= 0.99900, σ=0.00089, n=848 (1117)
Dev. from WRR in %
0.5
0.0
-0.5
-1.0
Sep-26
Oct-01
Oct-06
Oct-11
Oct-16

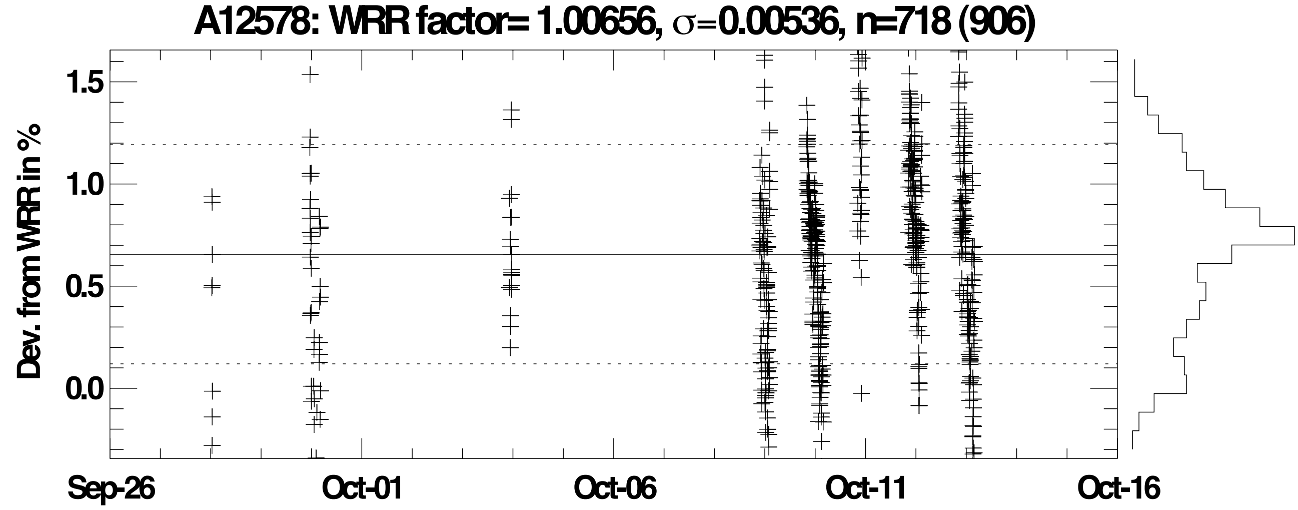
A12578: WRR factor= 1.00656, σ=0.00536, n=718 (906)
Dev. from WRR in %
1.5
1.0
0.5
0.0
Sep-26
Oct-01
Oct-06
Oct-11
Oct-16

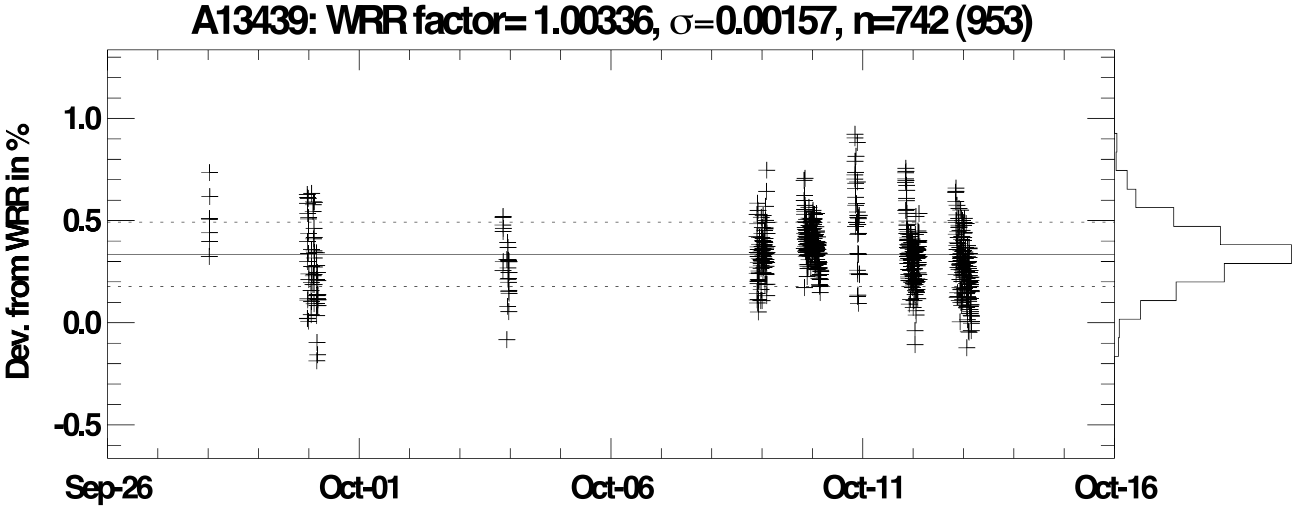
A13439: WRR factor= 1.00336, σ=0.00157, n=742 (953)
Dev. from WRR in %
1.0
0.5
0.0
-0.5
Sep-26
Oct-01
Oct-06
Oct-11
Oct-16

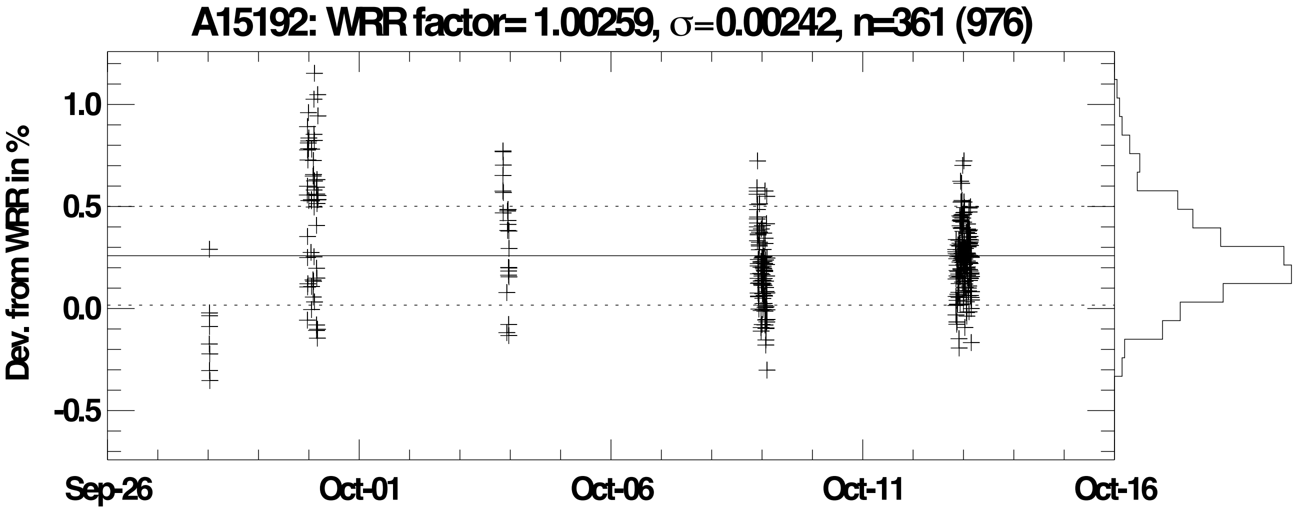
A15192: WRR factor= 1.00259, σ=0.00242, n=361 (976)
Dev. from WRR in %
1.0
0.5
0.0
-0.5
Sep-26
Oct-01
Oct-06
Oct-11
Oct-16

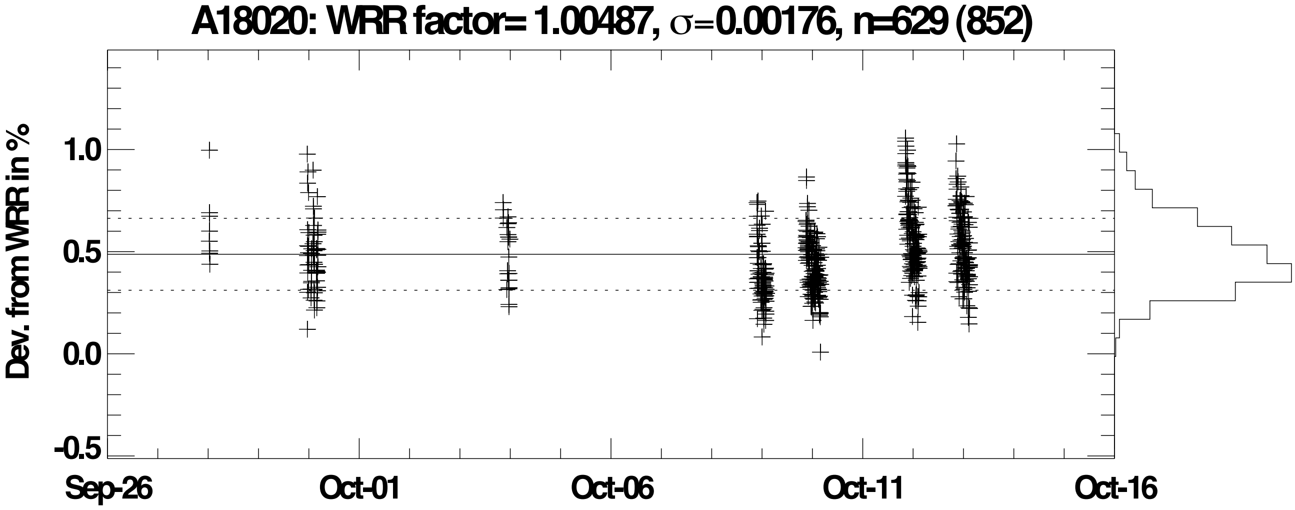
A18020: WRR factor= 1.00487, σ=0.00176, n=629 (852)
Dev. from WRR in %
1.0
0.5
0.0
-0.5
Sep-26
Oct-01
Oct-06
Oct-11
Oct-16

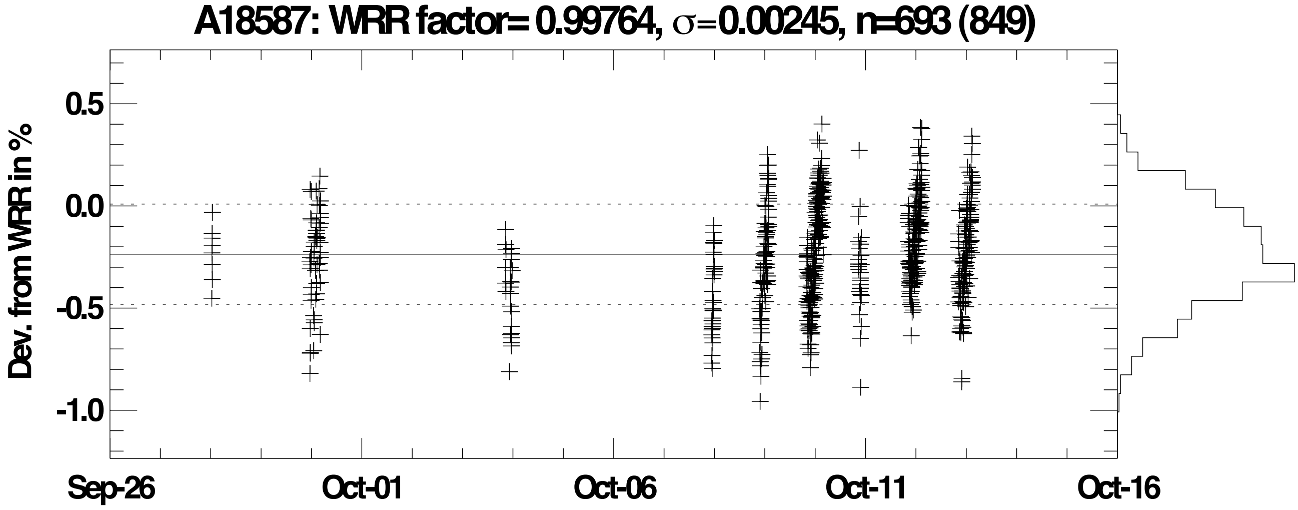
A18587: WRR factor= 0.99764, σ=0.00245, n=693 (849)
Dev. from WRR in %
0.5
0.0
-0.5
-1.0
Sep-26
Oct-01
Oct-06
Oct-11
Oct-16

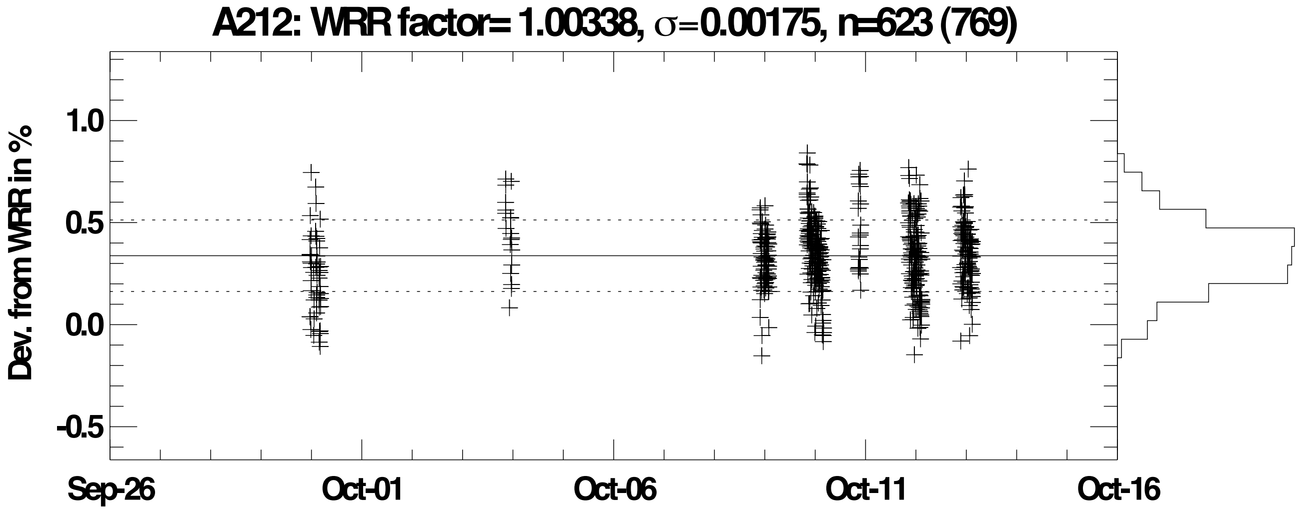
A212: WRR factor= 1.00338, σ=0.00175, n=623 (769)
Dev. from WRR in %
1.0
0.5
0.0
-0.5
Sep-26
Oct-01
Oct-06
Oct-11
Oct-16

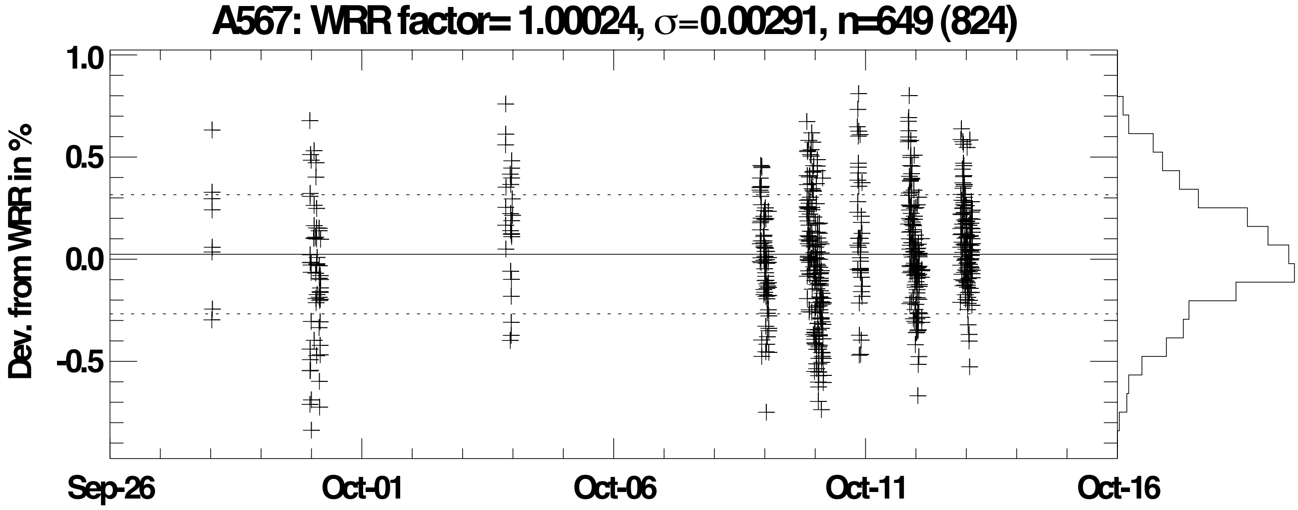
A567: WRR factor= 1.00024, σ=0.00291, n=649 (824)
Dev. from WRR in %
1.0
0.5
0.0
-0.5
Sep-26
Oct-01
Oct-06
Oct-11
Oct-16

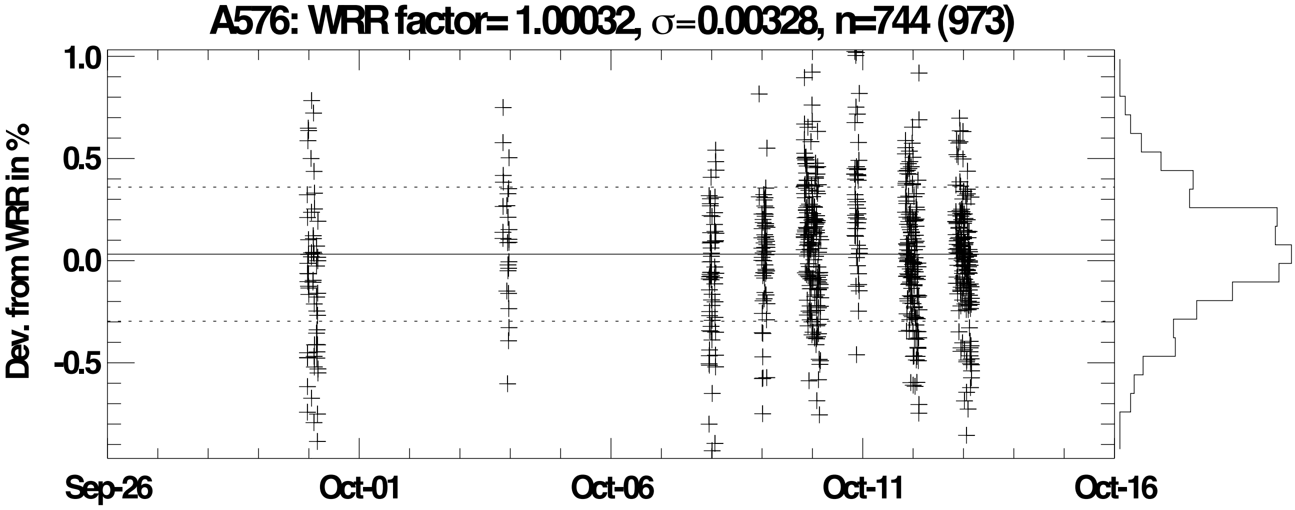
A576: WRR factor= 1.00032, σ=0.00328, n=744 (973)
1.0
0.5
0.0
-0.5
Dev. from WRR in %
Sep-26
Oct-01
Oct-06
Oct-11
Oct-16

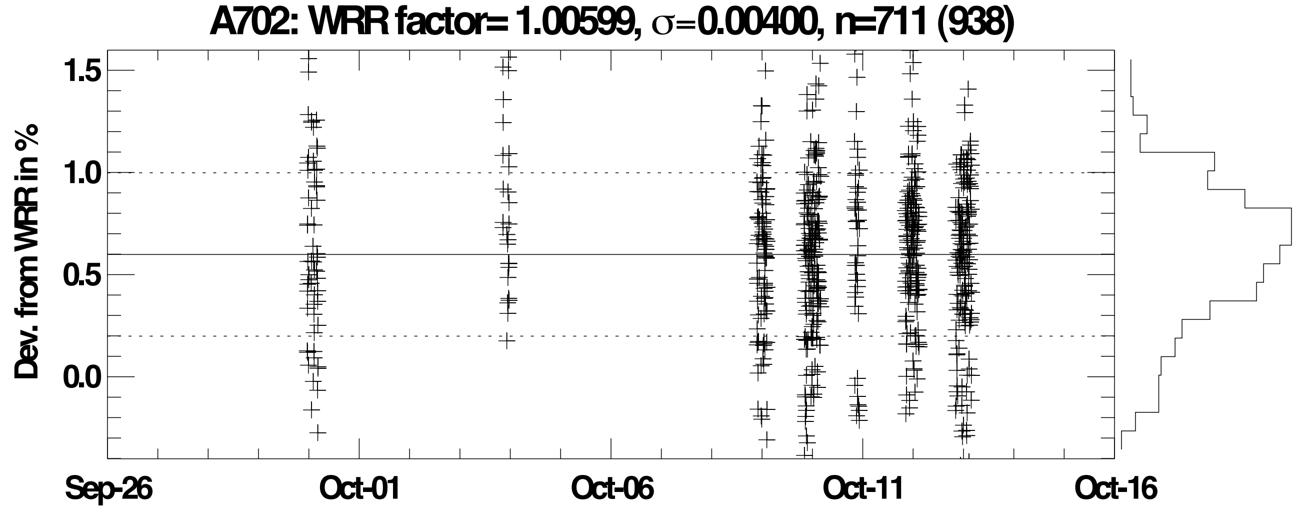
A702: WRR factor= 1.00599, σ=0.00400, n=711 (938)
1.5
1.0
0.5
0.0
Dev. from WRR in %
Sep-26
Oct-01
Oct-06
Oct-11
Oct-16

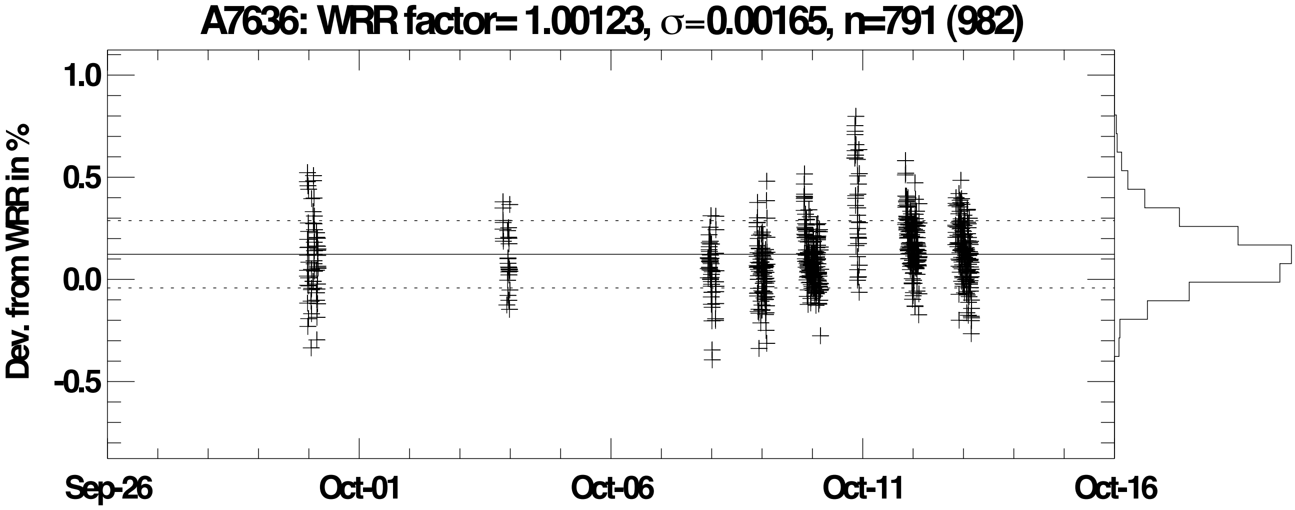
A7636: WRR factor= 1.00123, σ=0.00165, n=791 (982)
1.0
0.5
0.0
-0.5
Dev. from WRR in %
Sep-26
Oct-01
Oct-06
Oct-11
Oct-16

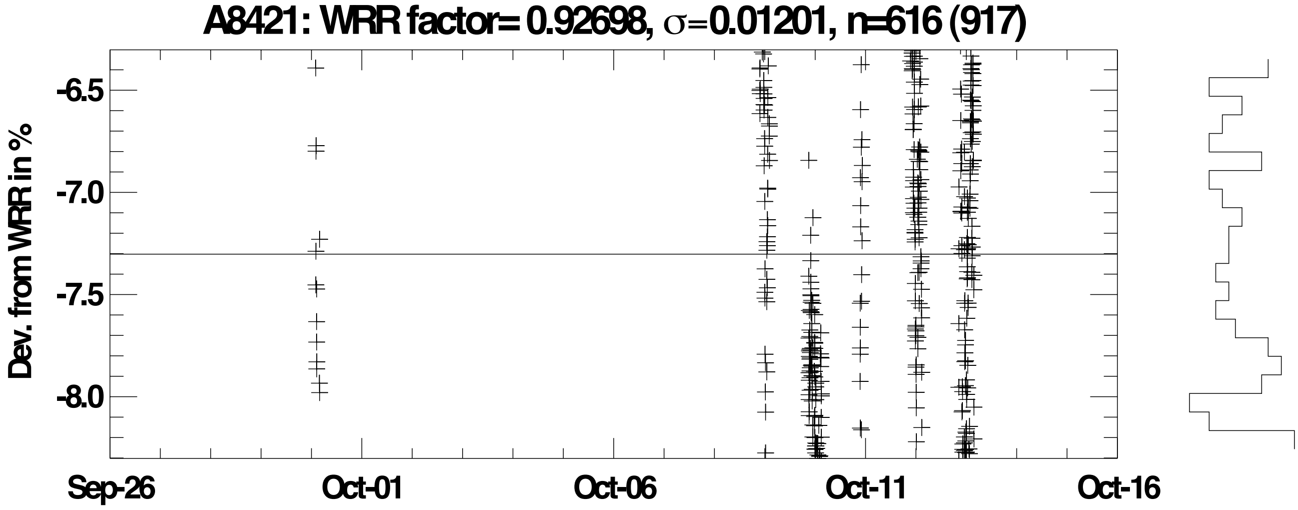
A8421: WRR factor= 0.92698, σ=0.01201, n=616 (917)
Dev. from WRR in %
-6.5
-7.0
-7.5
-8.0
Sep-26
Oct-01
Oct-06
Oct-11
Oct-16

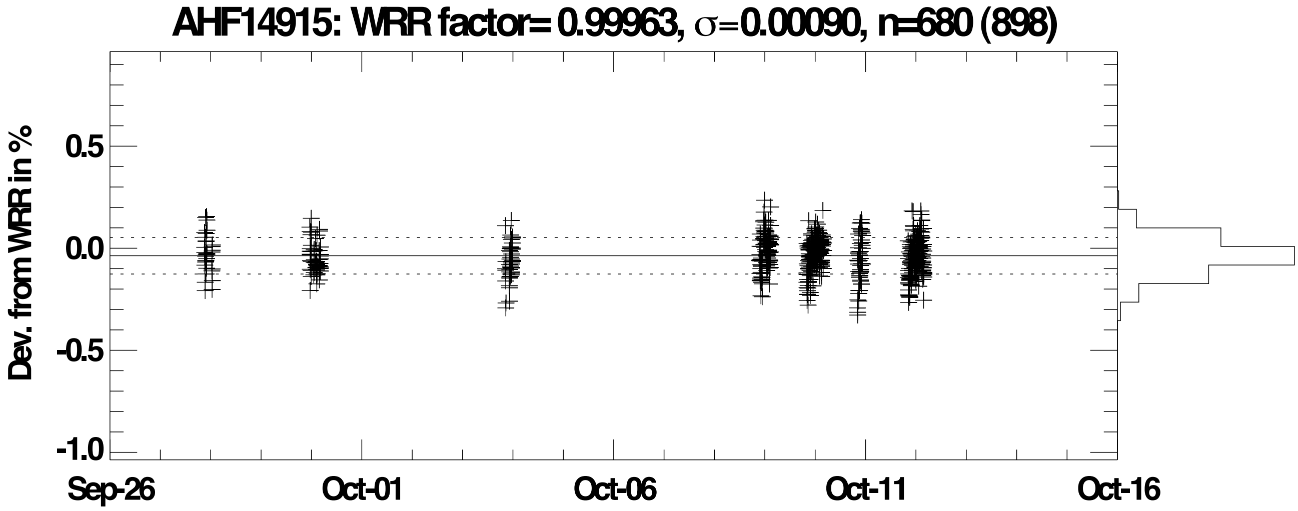
AHF14915: WRR factor= 0.99963, σ=0.00090, n=680 (898)
Dev. from WRR in %
0.5
0.0
-0.5
-1.0
Sep-26
Oct-01
Oct-06
Oct-11
Oct-16

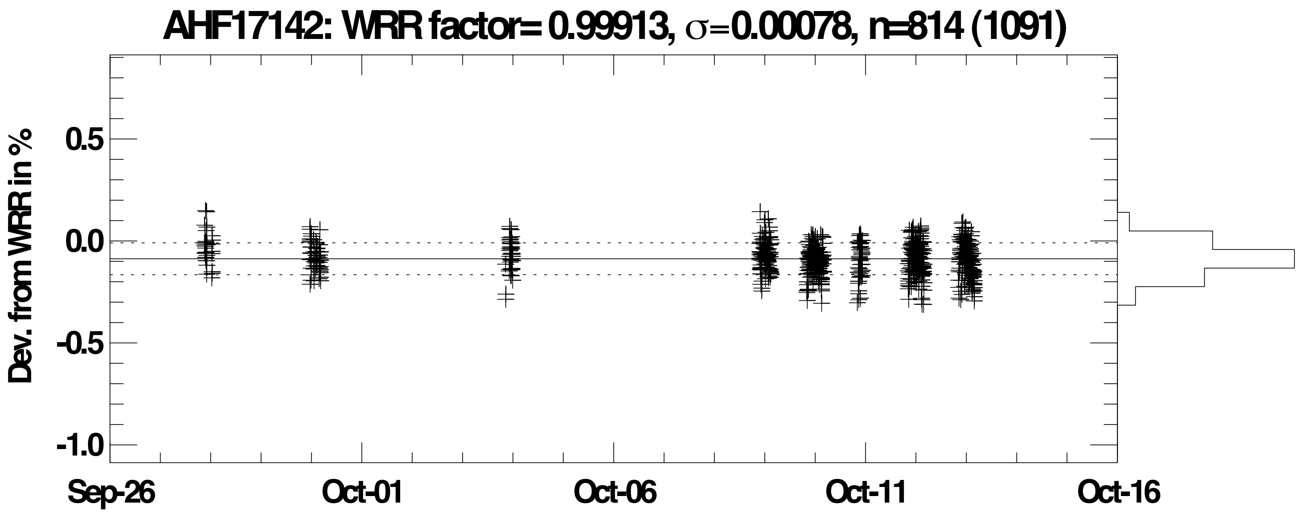
AHF17142: WRR factor= 0.99913, σ=0.00078, n=814 (1091)
Dev. from WRR in %
0.5
0.0
-0.5
-1.0
Sep-26
Oct-01
Oct-06
Oct-11
Oct-16

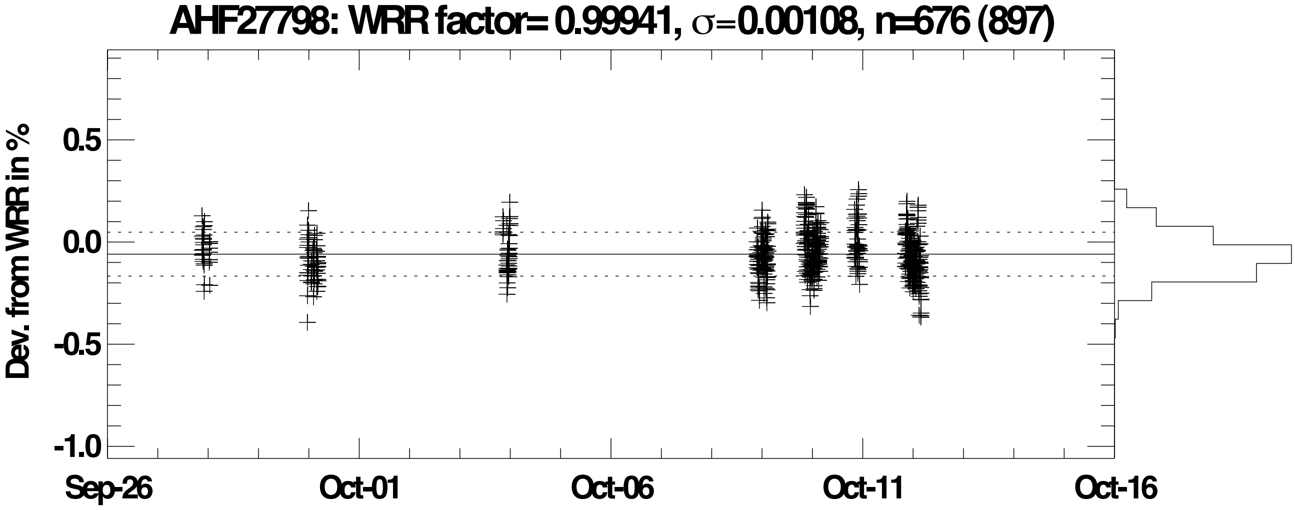
AHF27798: WRR factor= 0.99941, σ=0.00108, n=676 (897)
Dev. from WRR in %
0.5
0.0
-0.5
-1.0
Sep-26
Oct-01
Oct-06
Oct-11
Oct-16

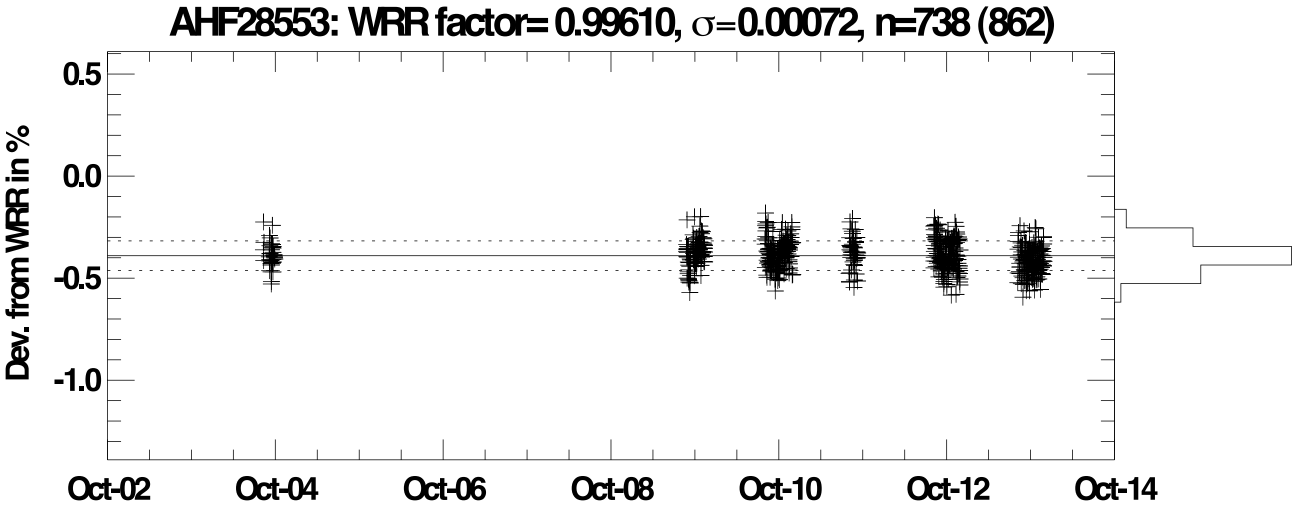
AHF28553: WRR factor= 0.99610, σ=0.00072, n=738 (862)
Dev. from WRR in %
0.5
0.0
-0.5
-1.0
Oct-02
Oct-04
Oct-06
Oct-08
Oct-10
Oct-12
Oct-14

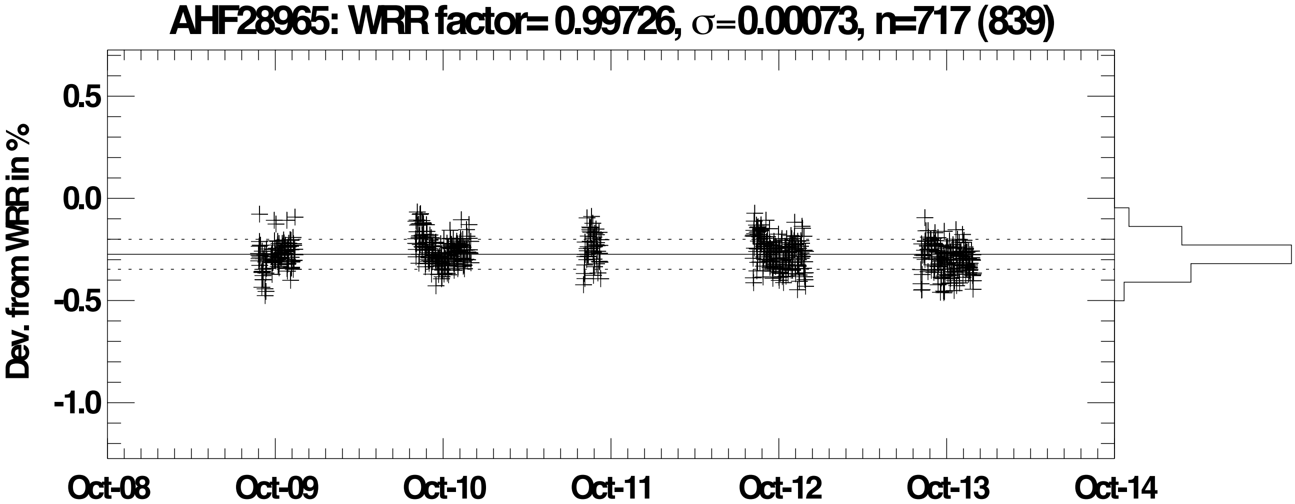
AHF28965: WRR factor= 0.99726, σ=0.00073, n=717 (839)
Dev. from WRR in %
0.5
0.0
-0.5
-1.0
Oct-08
Oct-09
Oct-10
Oct-11
Oct-12
Oct-13
Oct-14

AHF28968: WRR factor= 0.99776, σ=0.00076, n=903 (1146)

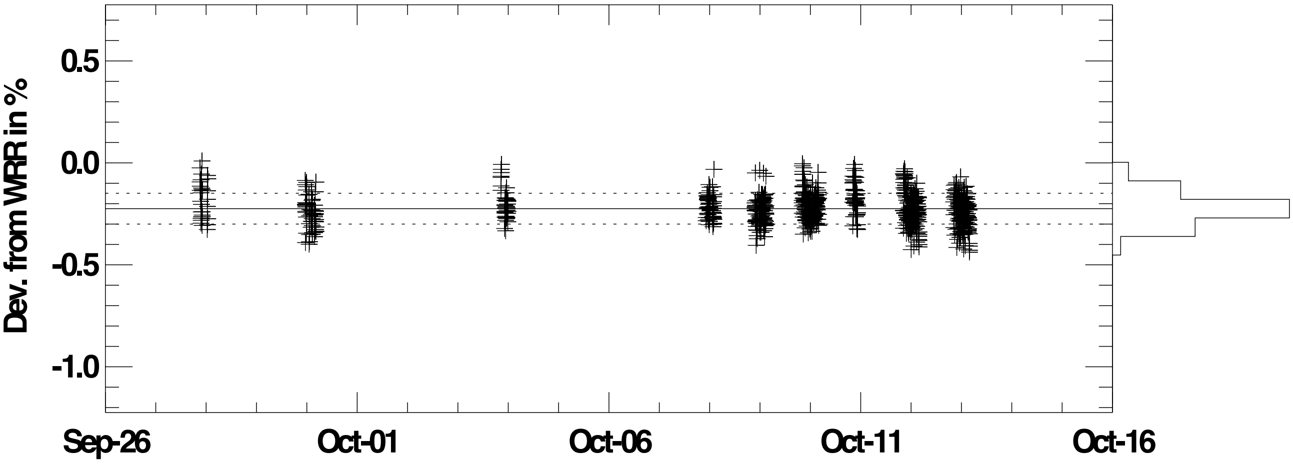

AHF29220: WRR factor= 0.99756, σ=0.00075, n=920 (1158)

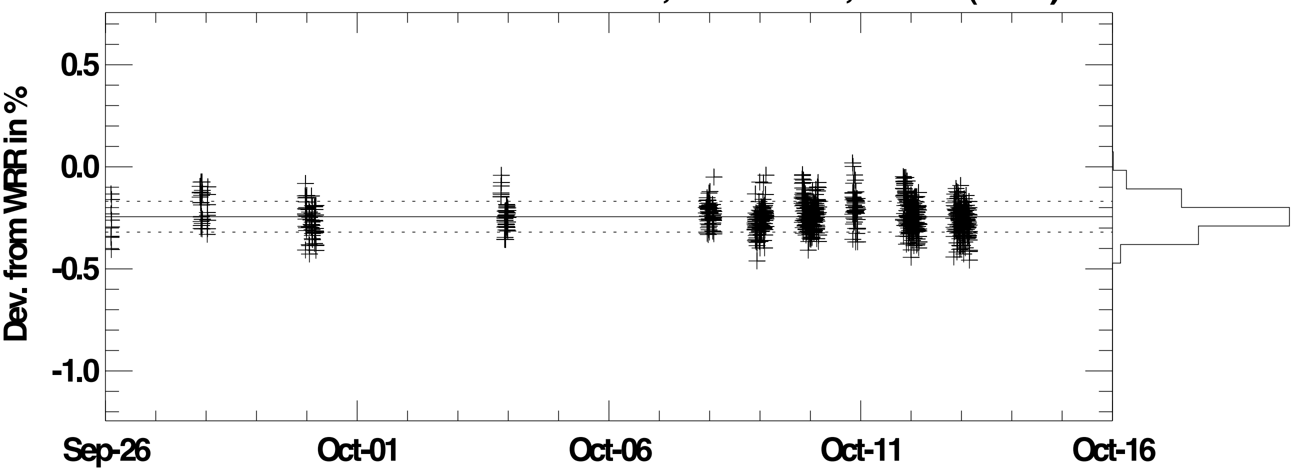

AHF30710: WRR factor= 1.00250, σ=0.00084, n=733 (857)

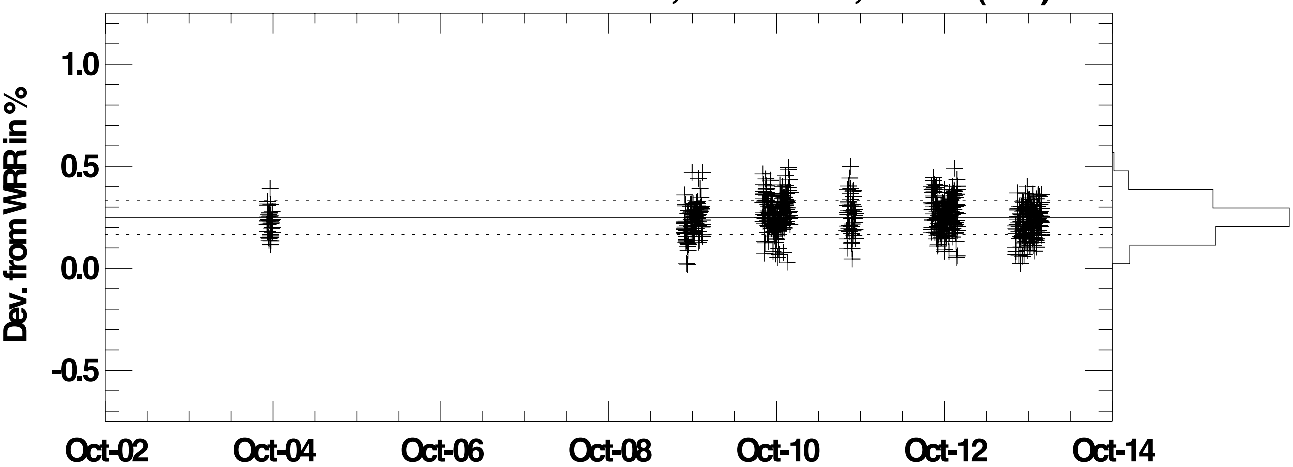

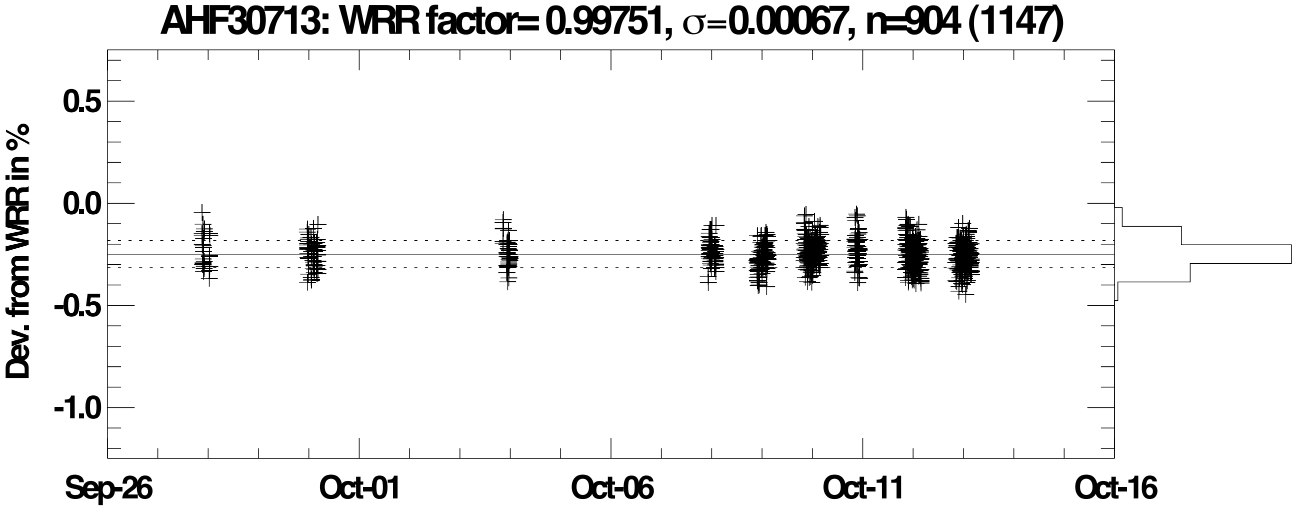
AHF30713: WRR factor= 0.99751, σ=0.00067, n=904 (1147)
Dev. from WRR in %
0.5
0.0
-0.5
-1.0
Sep-26
Oct-01
Oct-06
Oct-11
Oct-16

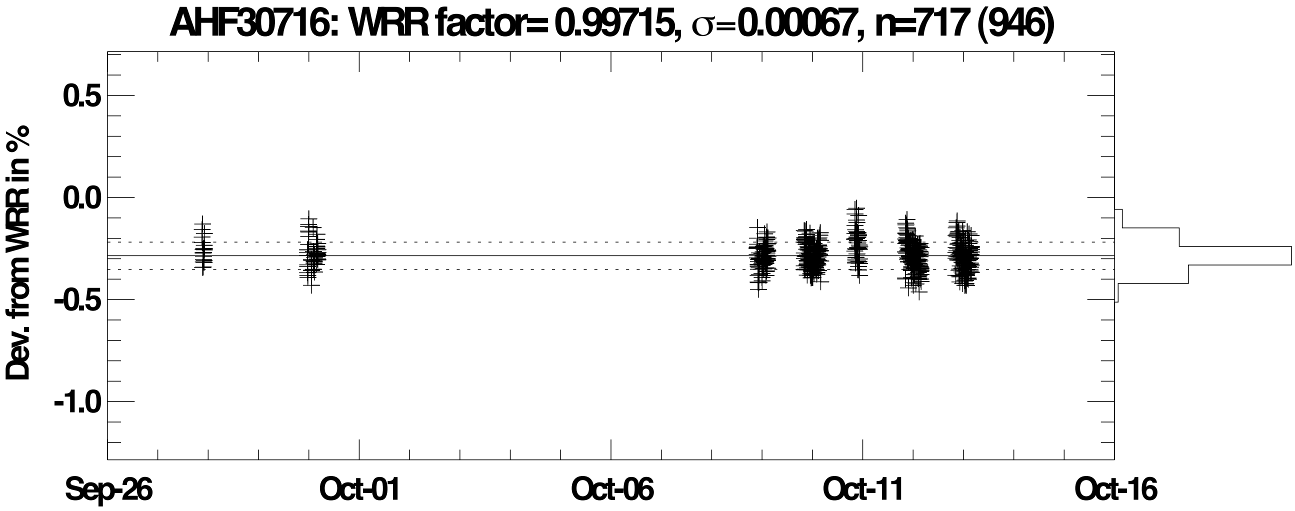
AHF30716: WRR factor= 0.99715, σ=0.00067, n=717 (946)
Dev. from WRR in %
0.5
0.0
-0.5
-1.0
Sep-26
Oct-01
Oct-06
Oct-11
Oct-16

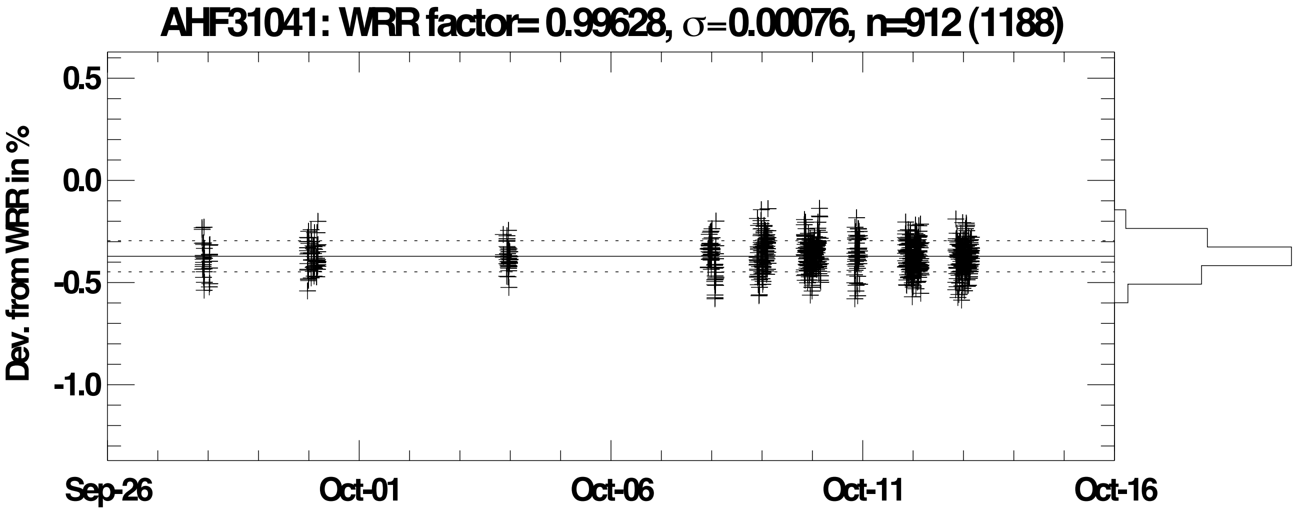
AHF31041: WRR factor= 0.99628, σ=0.00076, n=912 (1188)
Dev. from WRR in %
0.5
0.0
-0.5
-1.0
Sep-26
Oct-01
Oct-06
Oct-11
Oct-16

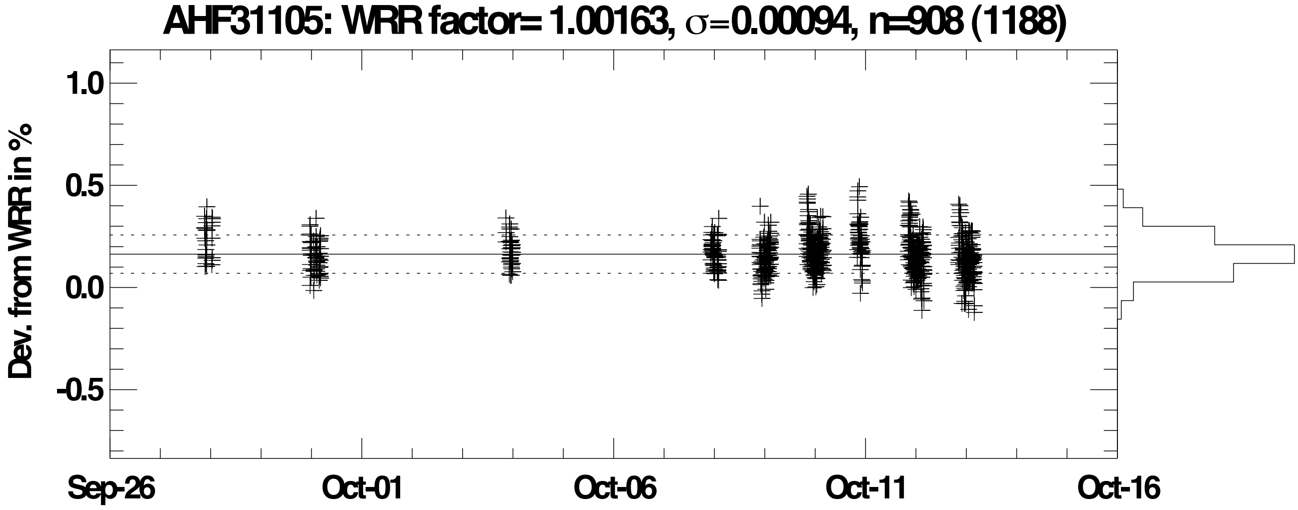
AHF31105: WRR factor= 1.00163, σ=0.00094, n=908 (1188)
Dev. from WRR in %
1.0
0.5
0.0
-0.5
Sep-26
Oct-01
Oct-06
Oct-11
Oct-16

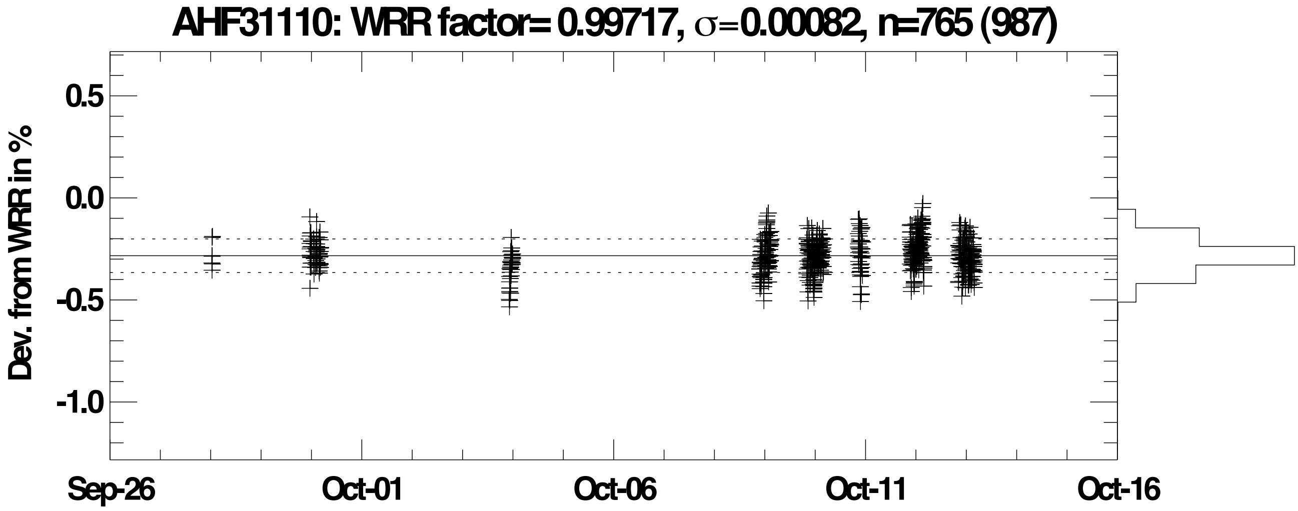
AHF31110: WRR factor= 0.99717, σ=0.00082, n=765 (987)
Dev. from WRR in %
0.5
0.0
-0.5
-1.0
Sep-26
Oct-01
Oct-06
Oct-11
Oct-16

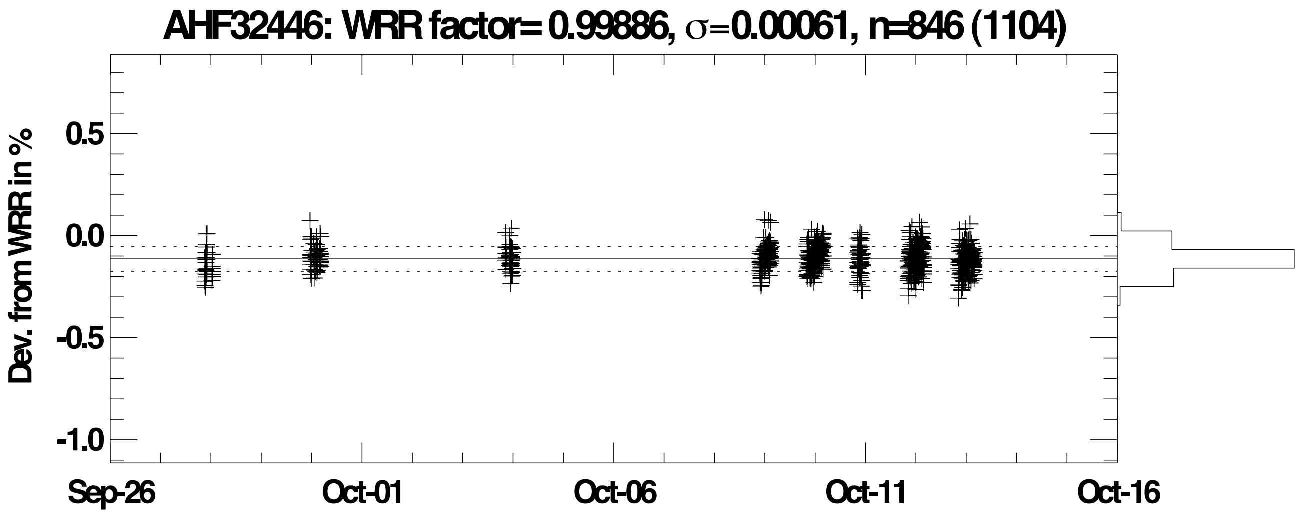
AHF32446: WRR factor= 0.99886, σ=0.00061, n=846 (1104)
Dev. from WRR in %
0.5
0.0
-0.5
-1.0
Sep-26
Oct-01
Oct-06
Oct-11
Oct-16

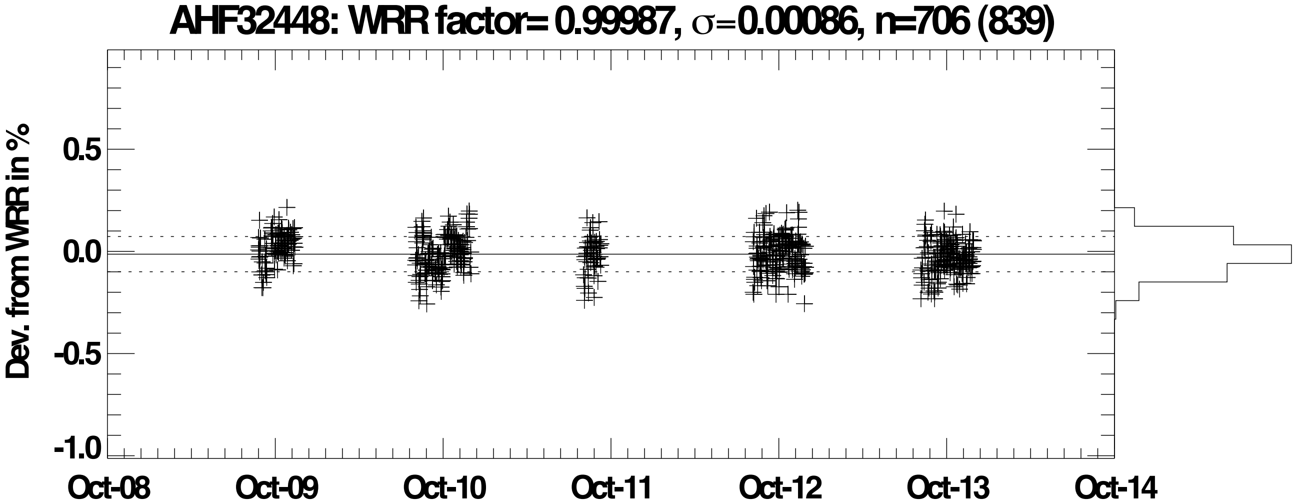
AHF32448: WRR factor= 0.99987, σ=0.00086, n=706 (839)
Dev. from WRR in %
0.5
0.0
-0.5
-1.0
Oct-08
Oct-09
Oct-10
Oct-11
Oct-12
Oct-13
Oct-14

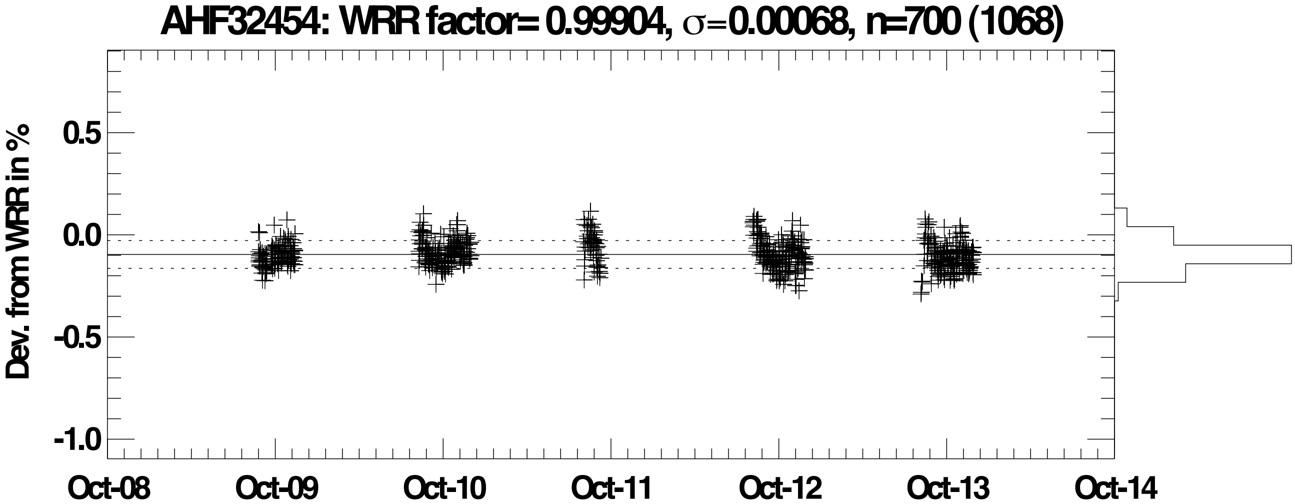
AHF32454: WRR factor= 0.99904, σ=0.00068, n=700 (1068)
Dev. from WRR in %
0.5
0.0
-0.5
-1.0
Oct-08
Oct-09
Oct-10
Oct-11
Oct-12
Oct-13
Oct-14

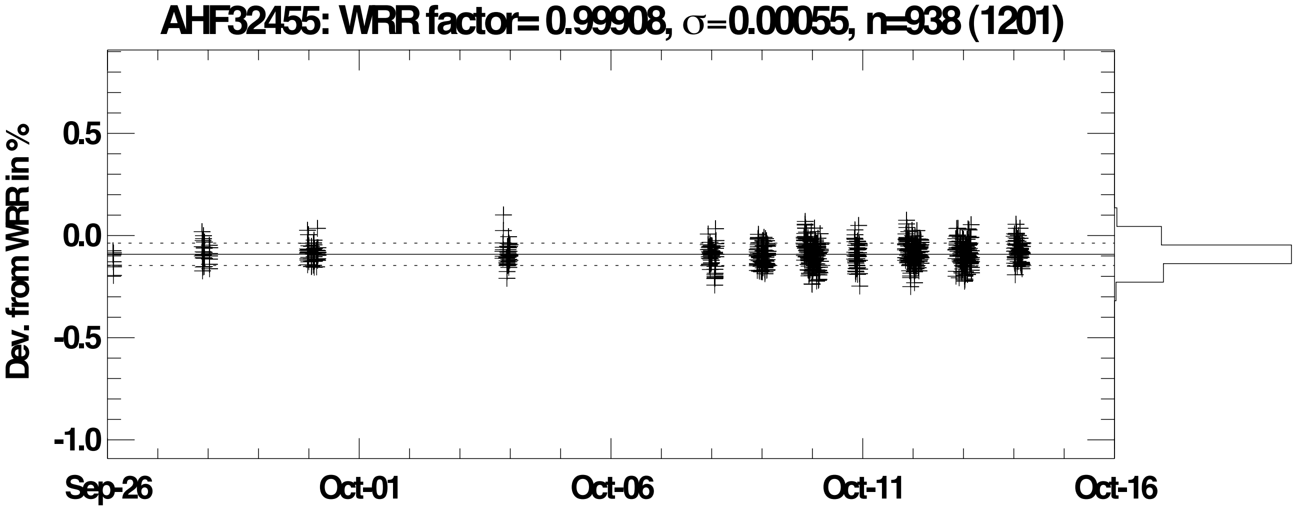
AHF32455: WRR factor= 0.99908, σ=0.00055, n=938 (1201)
Dev. from WRR in %
0.5
0.0
-0.5
-1.0
Sep-26
Oct-01
Oct-06
Oct-11
Oct-16

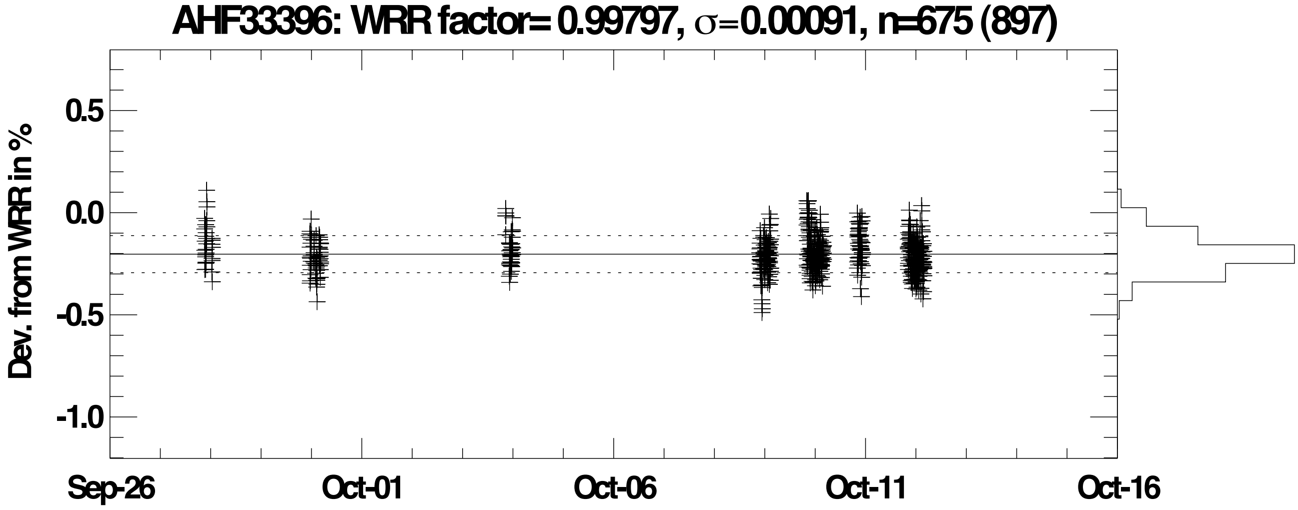
AHF33396: WRR factor= 0.99797, σ=0.00091, n=675 (897)
Dev. from WRR in %
0.5
0.0
-0.5
-1.0
Sep-26
Oct-01
Oct-06
Oct-11
Oct-16

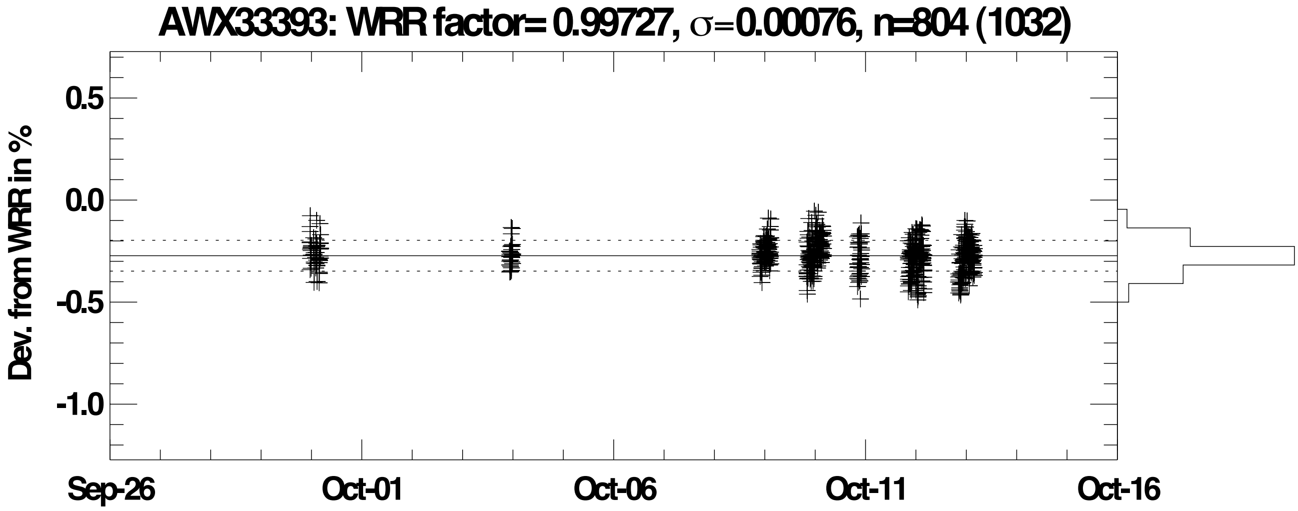
AWX33393: WRR factor= 0.99727, σ=0.00076, n=804 (1032)
Dev. from WRR in %
0.5
0.0
-0.5
-1.0
Sep-26
Oct-01
Oct-06
Oct-11
Oct-16

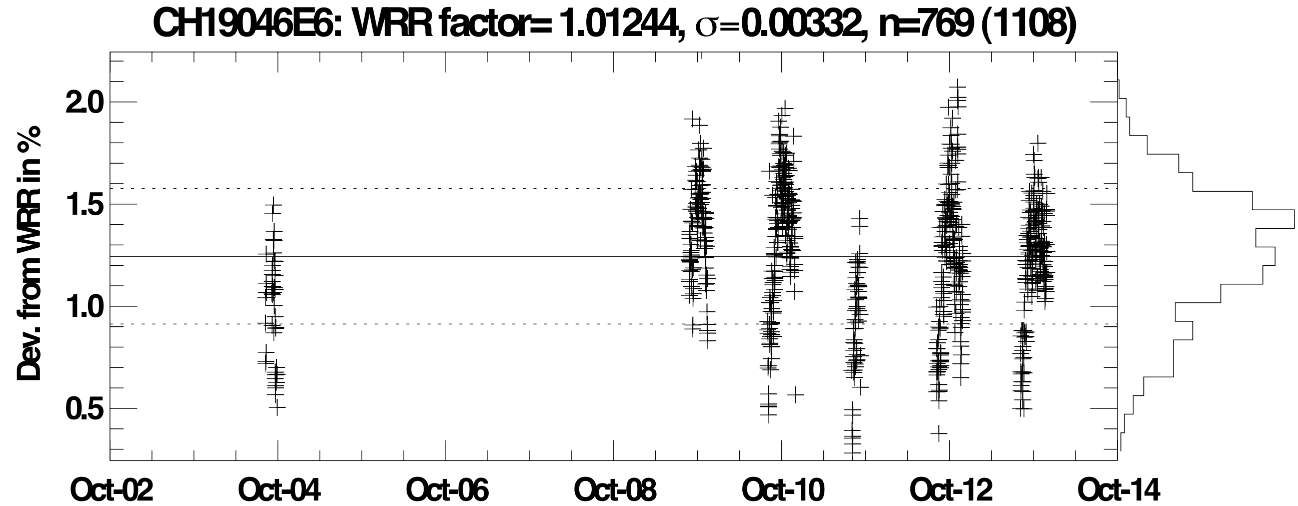
CH19046E6: WRR factor= 1.01244, σ=0.00332, n=769 (1108)
Dev. from WRR in %
2.0
1.5
1.0
0.5
Oct-02
Oct-04
Oct-06
Oct-08
Oct-10
Oct-12
Oct-14

CH1930018: WRR factor= 0.99635, σ=0.00235, n=850 (1056)

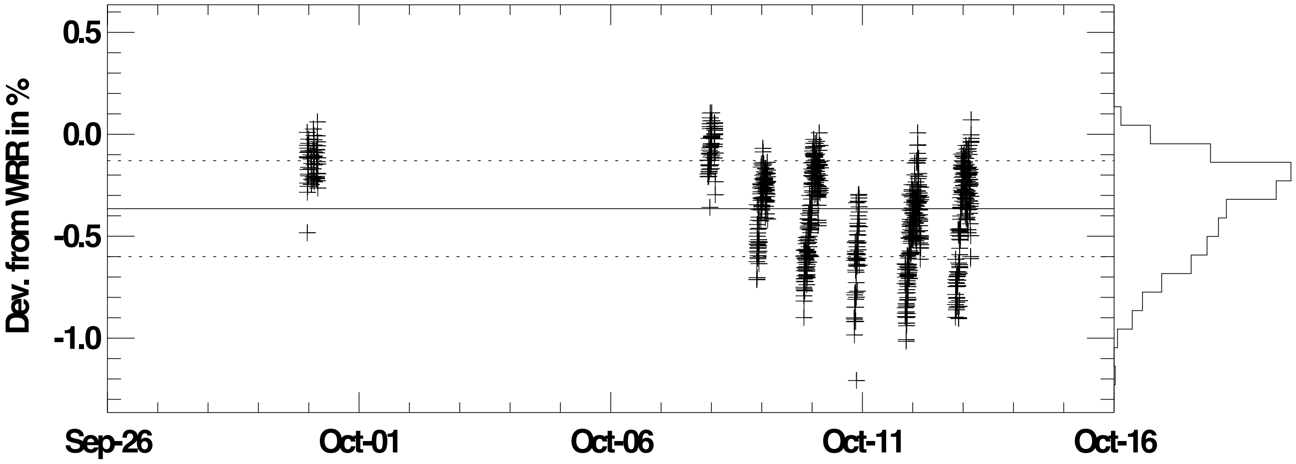

CH1940072: WRR factor= 1.00596, σ=0.00143, n=859 (1114)

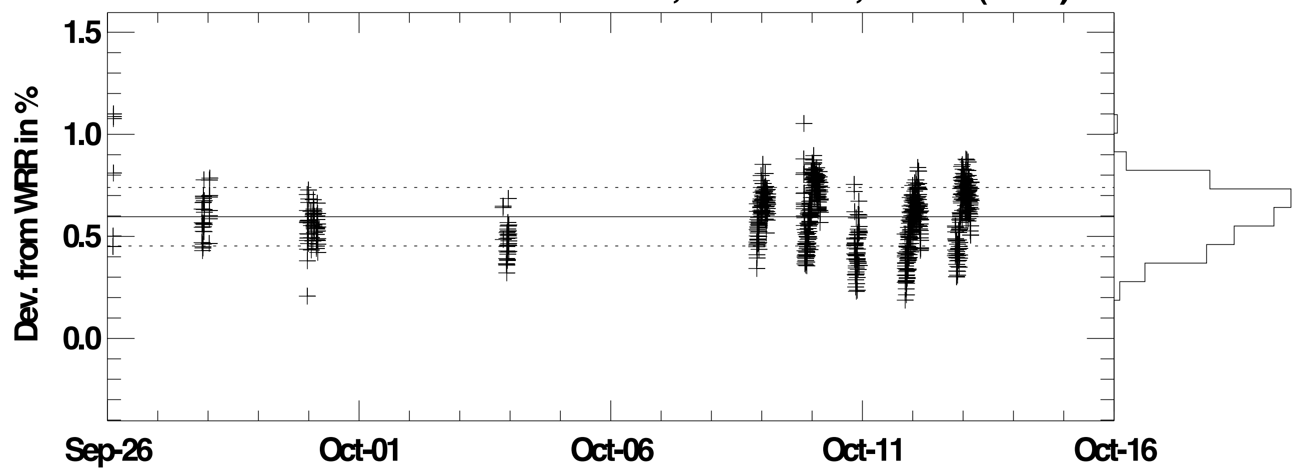

CH1980174: WRR factor= 1.00140, σ=0.00142, n=307 (369)

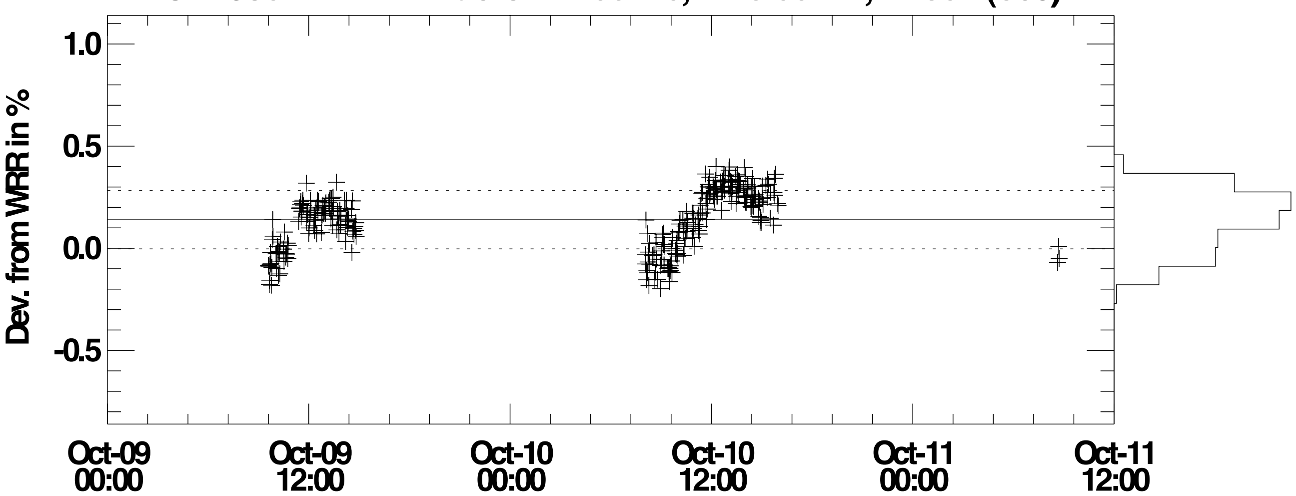

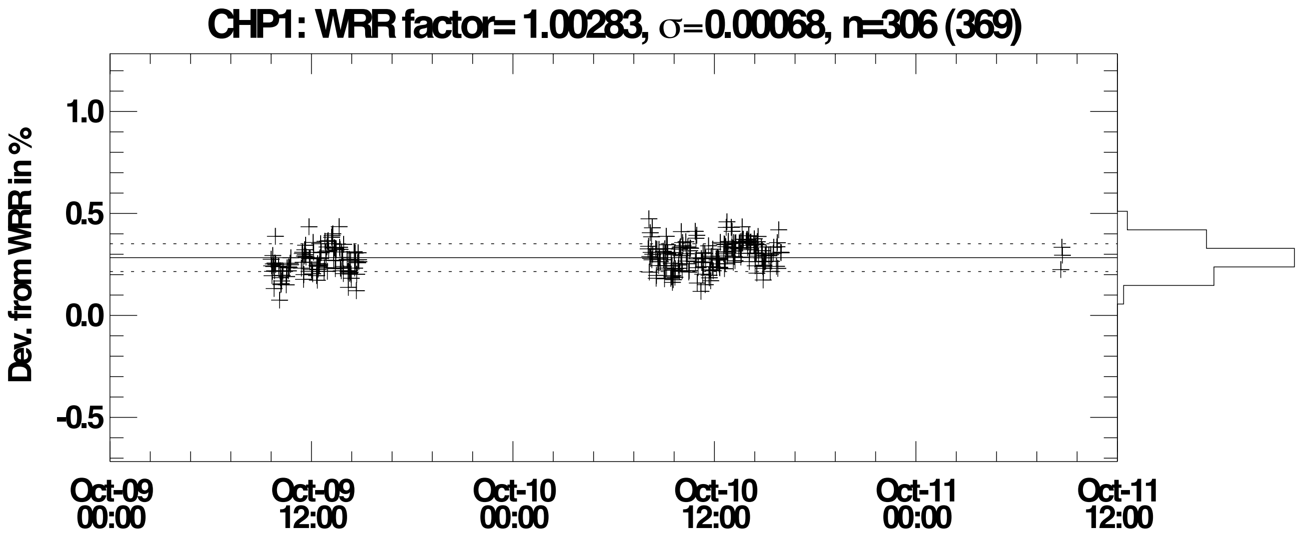
CHP1: WRR factor= 1.00283, σ=0.00068, n=306 (369)
Dev. from WRR in %
1.0
0.5
0.0
-0.5
Oct-09 00:00
Oct-09 12:00
Oct-10 00:00
Oct-10 12:00
Oct-11 00:00
Oct-11 12:00

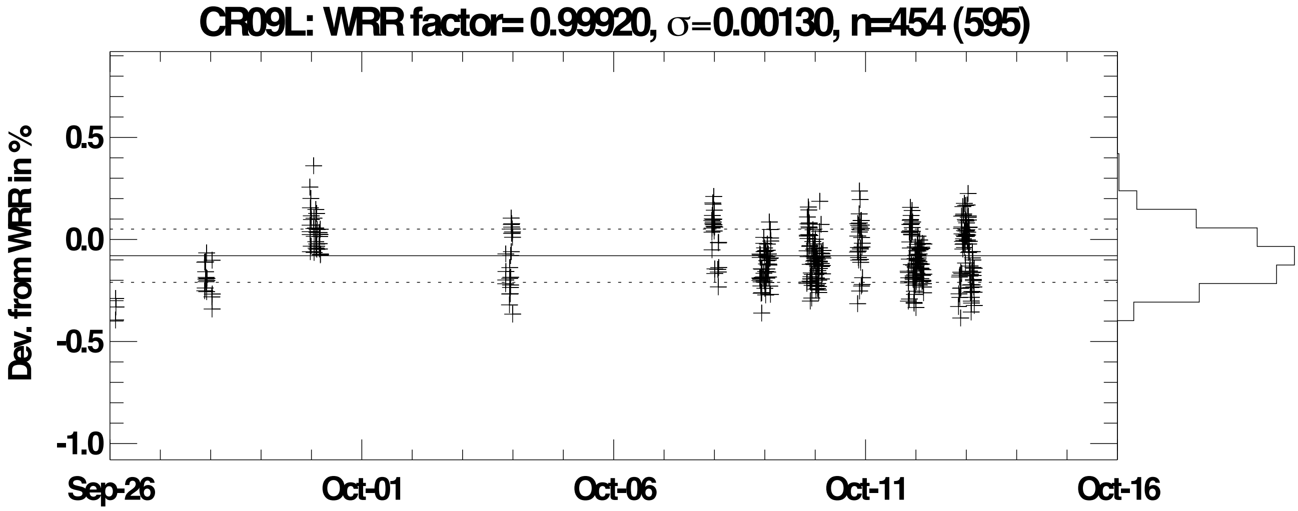
CR09L: WRR factor= 0.99920, σ=0.00130, n=454 (595)
Dev. from WRR in %
0.5
0.0
-0.5
-1.0
Sep-26
Oct-01
Oct-06
Oct-11
Oct-16

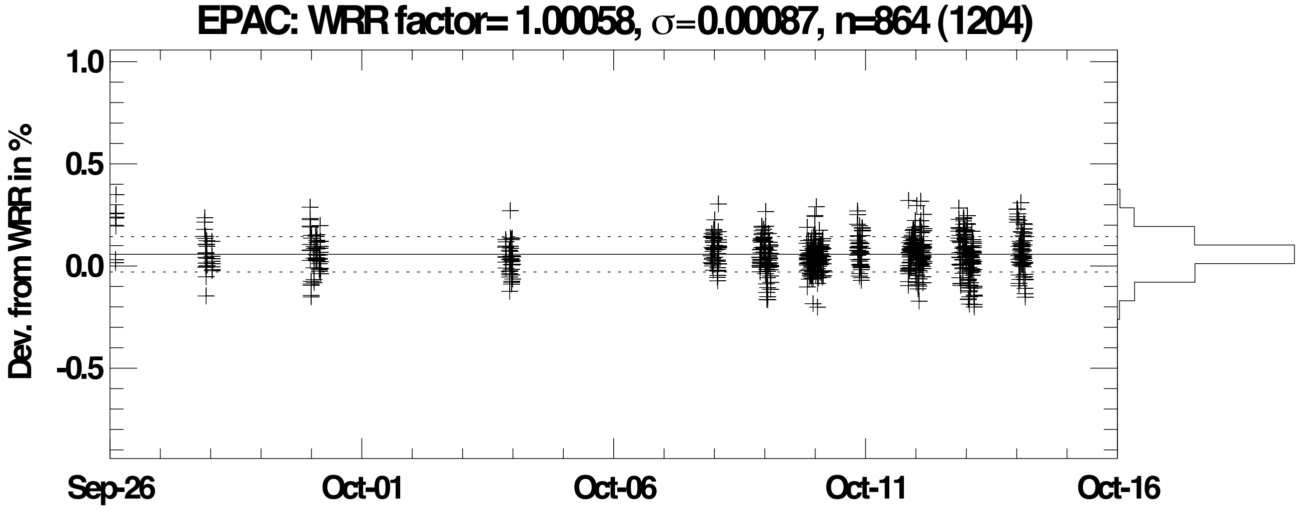
EPAC: WRR factor= 1.00058, σ=0.00087, n=864 (1204)
Dev. from WRR in %
1.0
0.5
0.0
-0.5
Sep-26
Oct-01
Oct-06
Oct-11
Oct-16

HF15744: WRR factor= 0.99803, σ=0.00075, n=768 (1015)

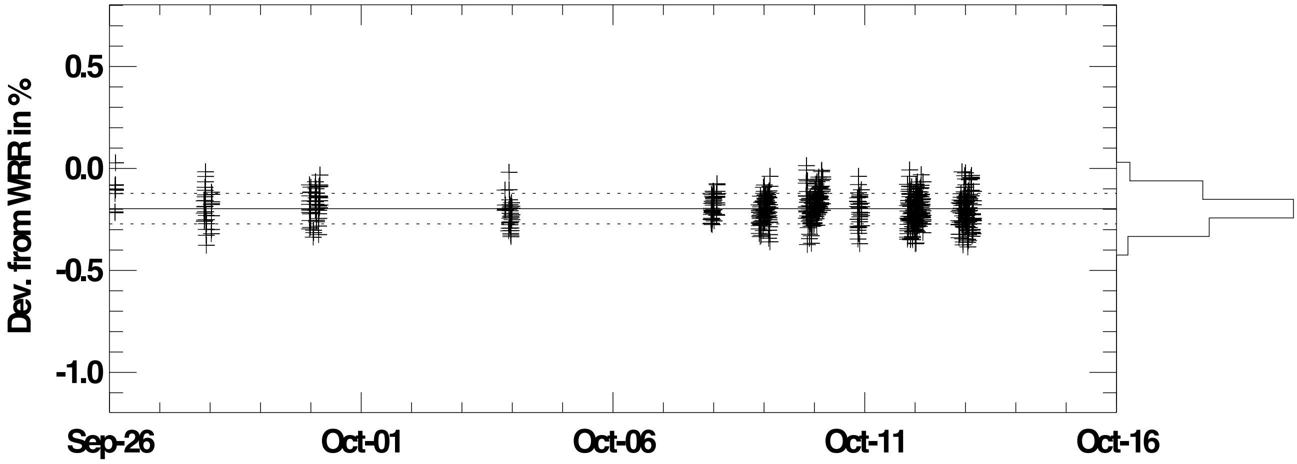

HF18742: WRR factor= 1.00382, σ=0.00278, n=740 (996)

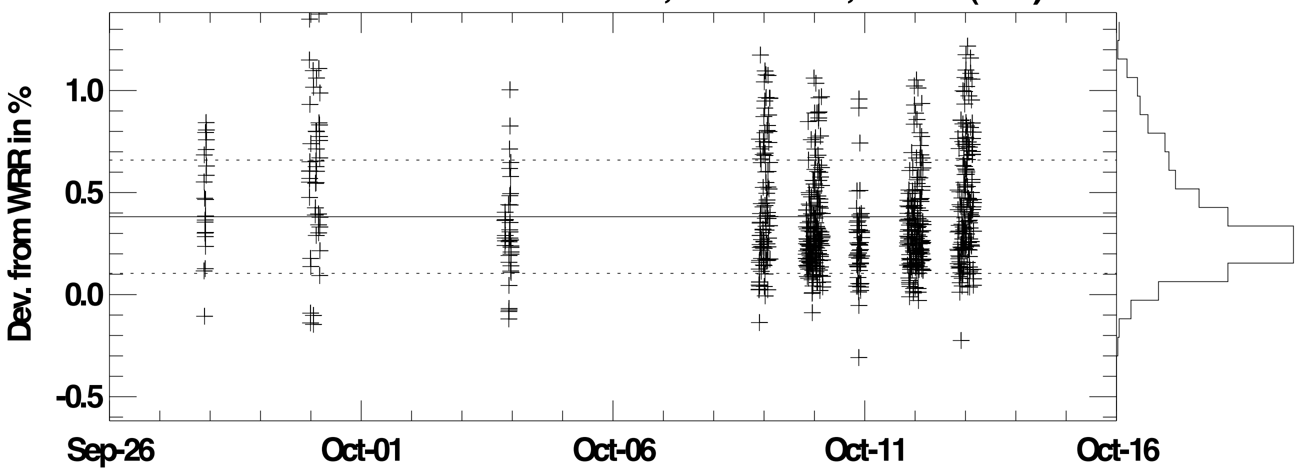

HF18747: WRR factor= 1.00267, σ=0.00063, n=762 (983)

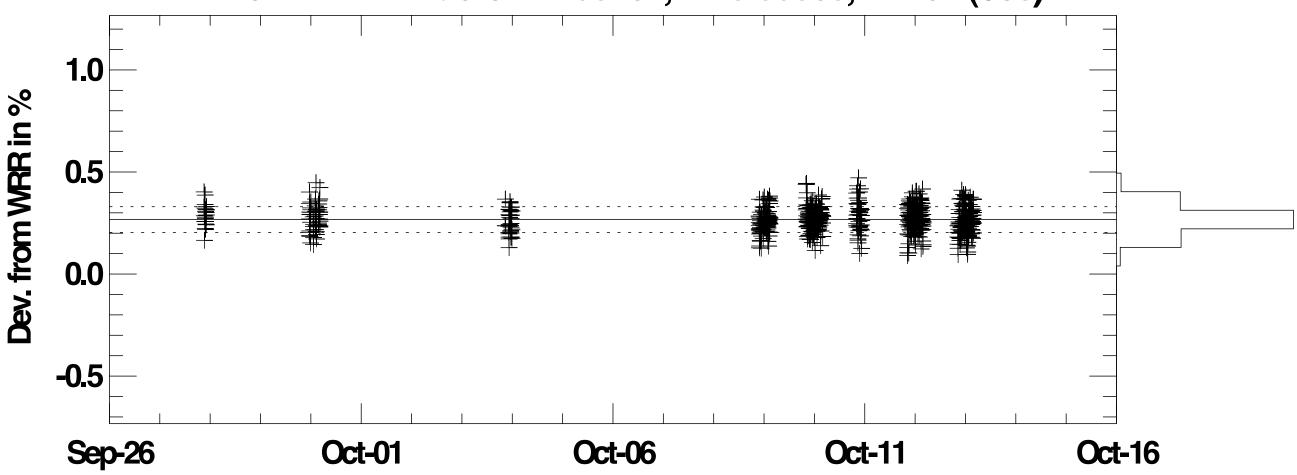

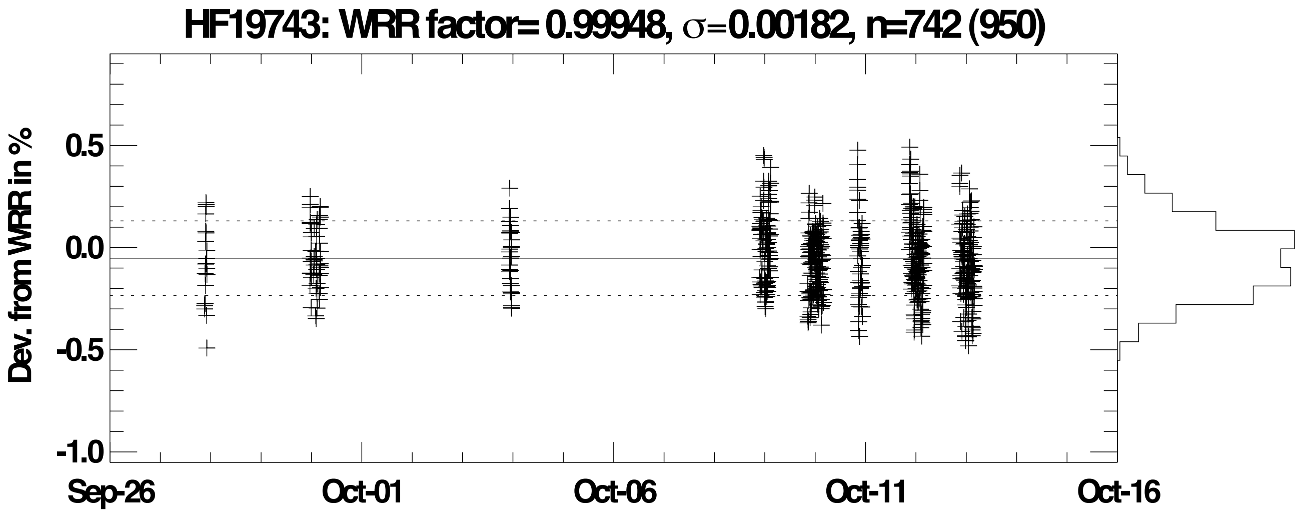
HF19743: WRR factor= 0.99948, σ=0.00182, n=742 (950)
Dev. from WRR in %
0.5
0.0
-0.5
-1.0
Sep-26
Oct-01
Oct-06
Oct-11
Oct-16

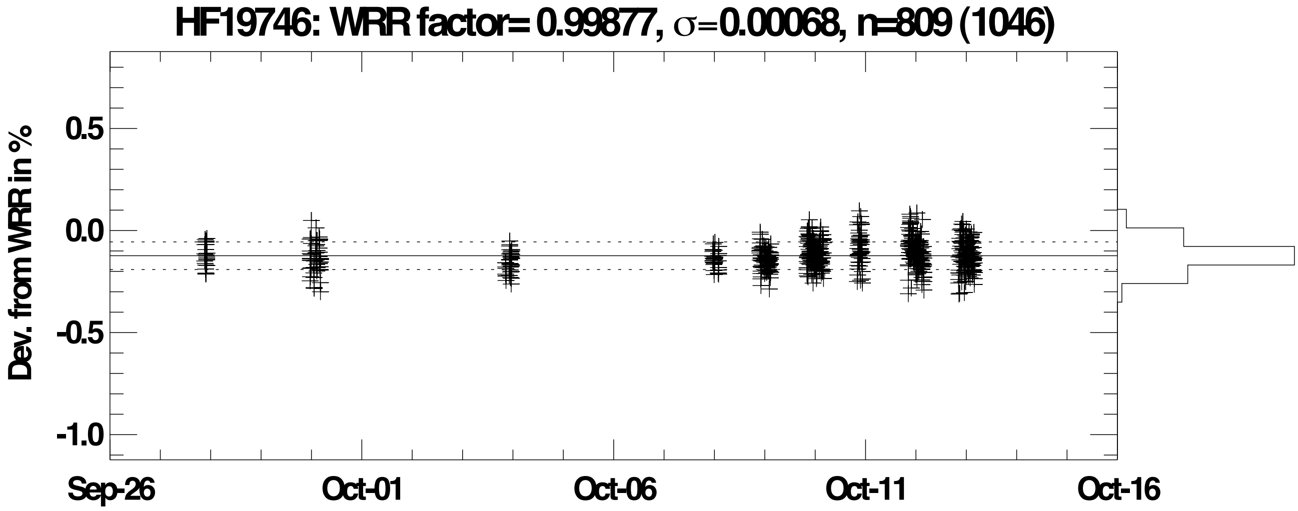
HF19746: WRR factor= 0.99877, σ=0.00068, n=809 (1046)
Dev. from WRR in %
0.5
0.0
-0.5
-1.0
Sep-26
Oct-01
Oct-06
Oct-11
Oct-16

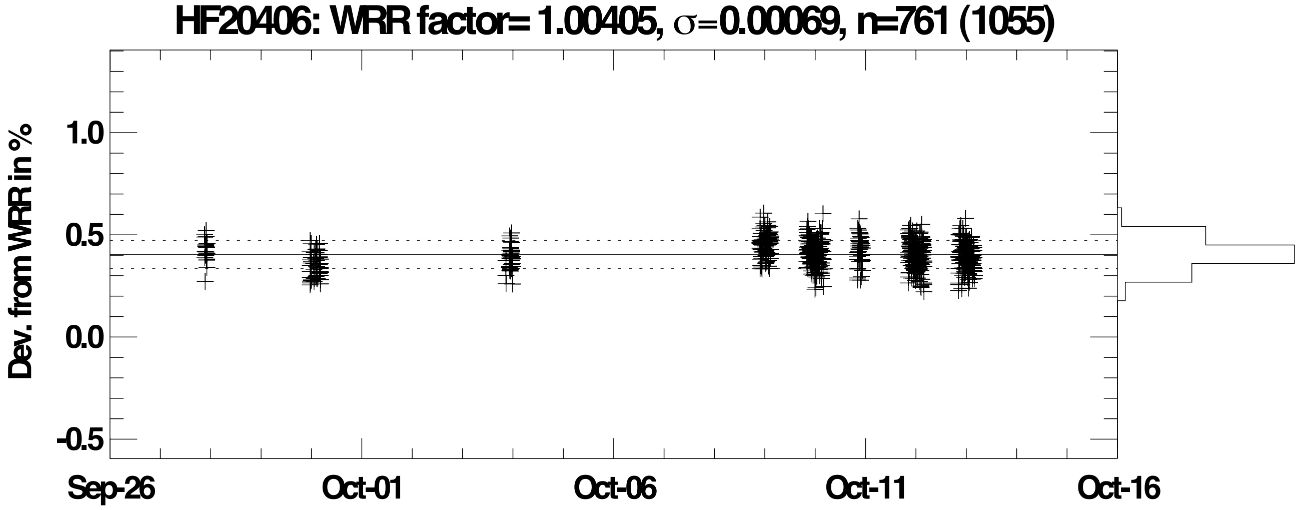
HF20406: WRR factor= 1.00405, σ=0.00069, n=761 (1055)
Dev. from WRR in %
1.0
0.5
0.0
-0.5
Sep-26
Oct-01
Oct-06
Oct-11
Oct-16

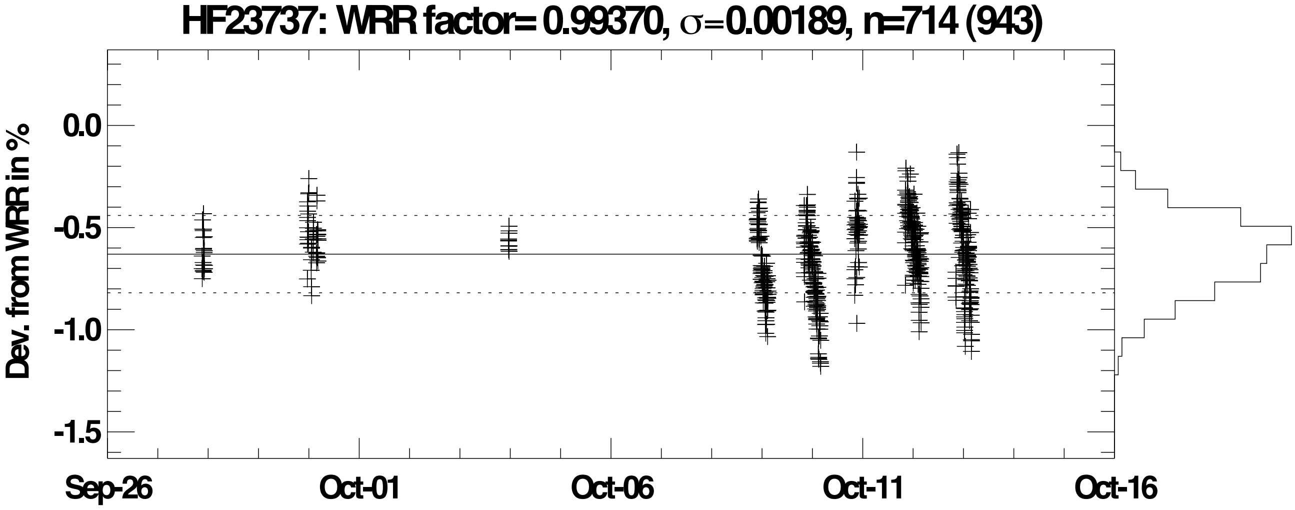
HF23737: WRR factor= 0.99370, σ=0.00189, n=714 (943)
Dev. from WRR in %
0.0
-0.5
-1.0
-1.5
Sep-26
Oct-01
Oct-06
Oct-11
Oct-16

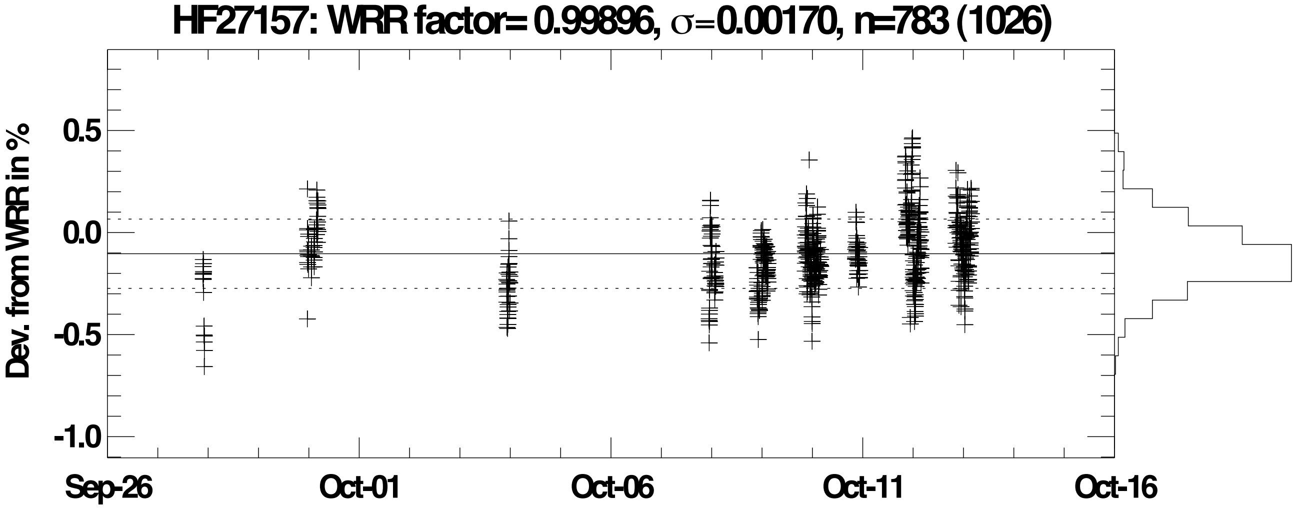
HF27157: WRR factor= 0.99896, σ=0.00170, n=783 (1026)
Dev. from WRR in %
0.5
0.0
-0.5
-1.0
Sep-26
Oct-01
Oct-06
Oct-11
Oct-16

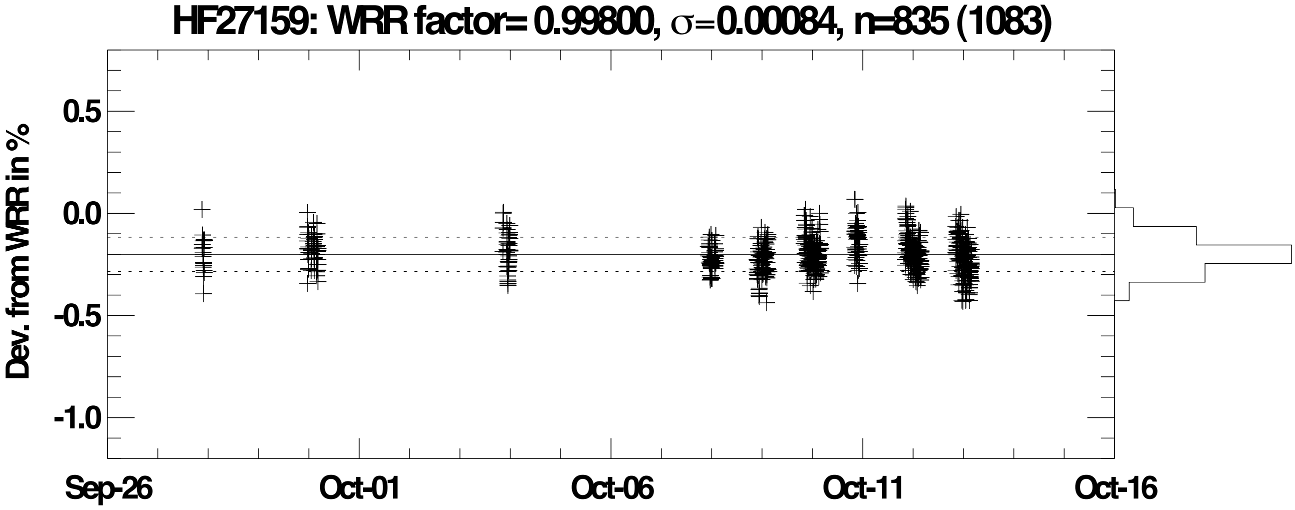
HF27159: WRR factor= 0.99800, σ=0.00084, n=835 (1083)
Dev. from WRR in %
0.5
0.0
-0.5
-1.0
Sep-26
Oct-01
Oct-06
Oct-11
Oct-16

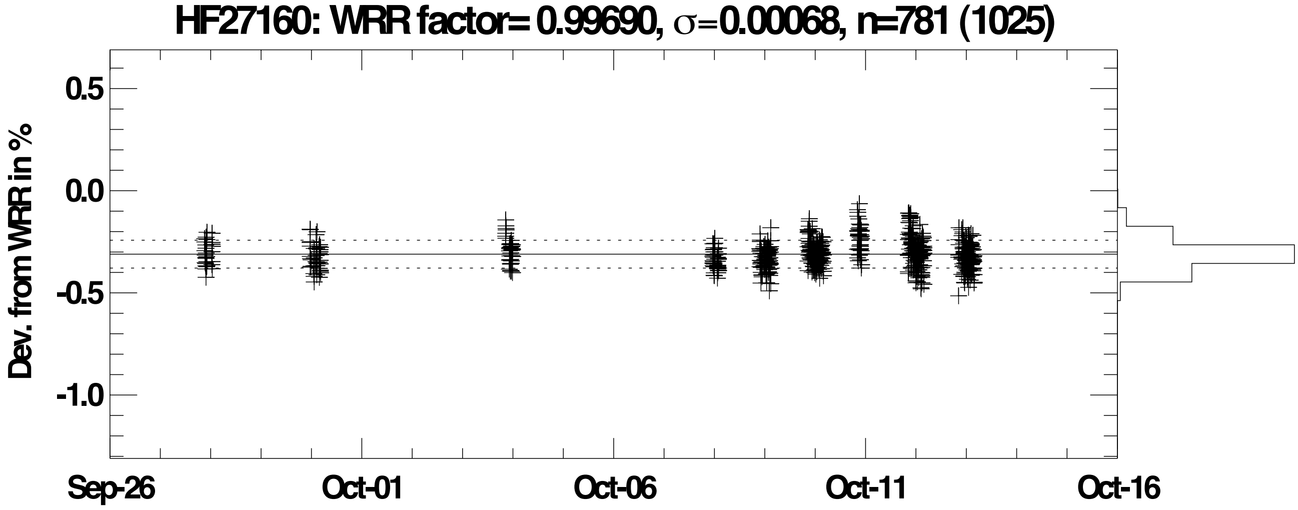
HF27160: WRR factor= 0.99690, σ=0.00068, n=781 (1025)
Dev. from WRR in %
0.5
0.0
-0.5
-1.0
Sep-26
Oct-01
Oct-06
Oct-11
Oct-16

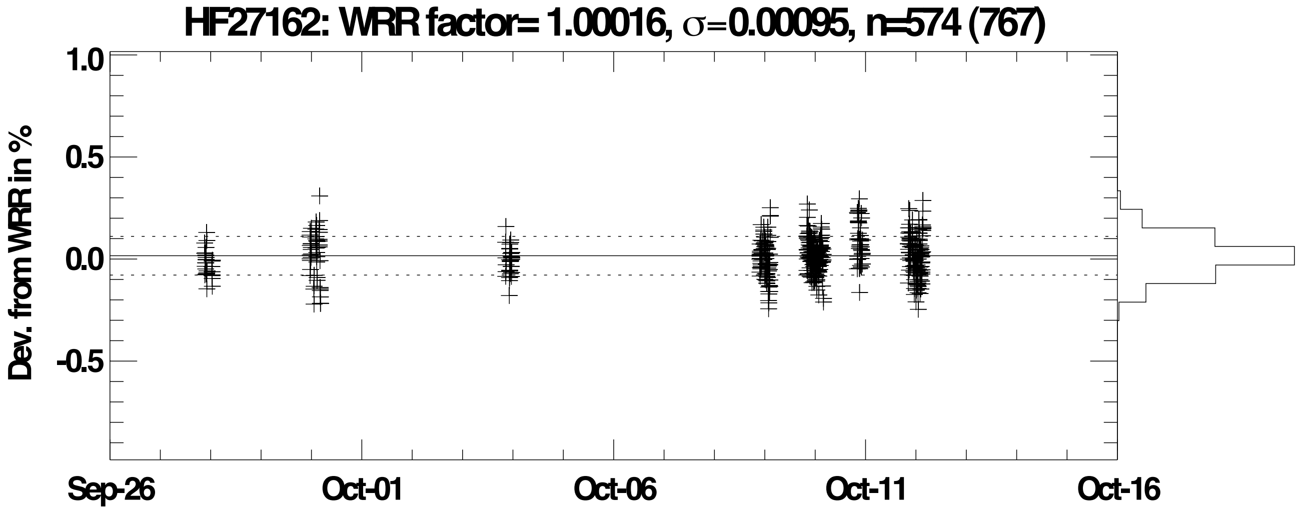
HF27162: WRR factor= 1.00016, σ=0.00095, n=574 (767)
Dev. from WRR in %
1.0
0.5
0.0
-0.5
Sep-26
Oct-01
Oct-06
Oct-11
Oct-16

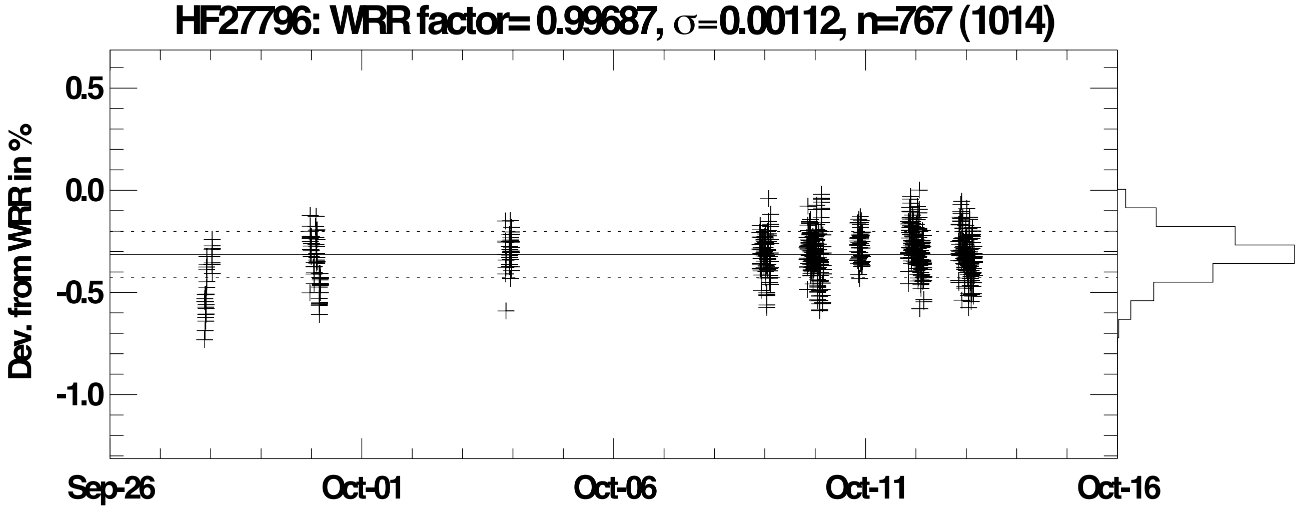
HF27796: WRR factor= 0.99687, σ=0.00112, n=767 (1014)
Dev. from WRR in %
0.5
0.0
-0.5
-1.0
Sep-26
Oct-01
Oct-06
Oct-11
Oct-16

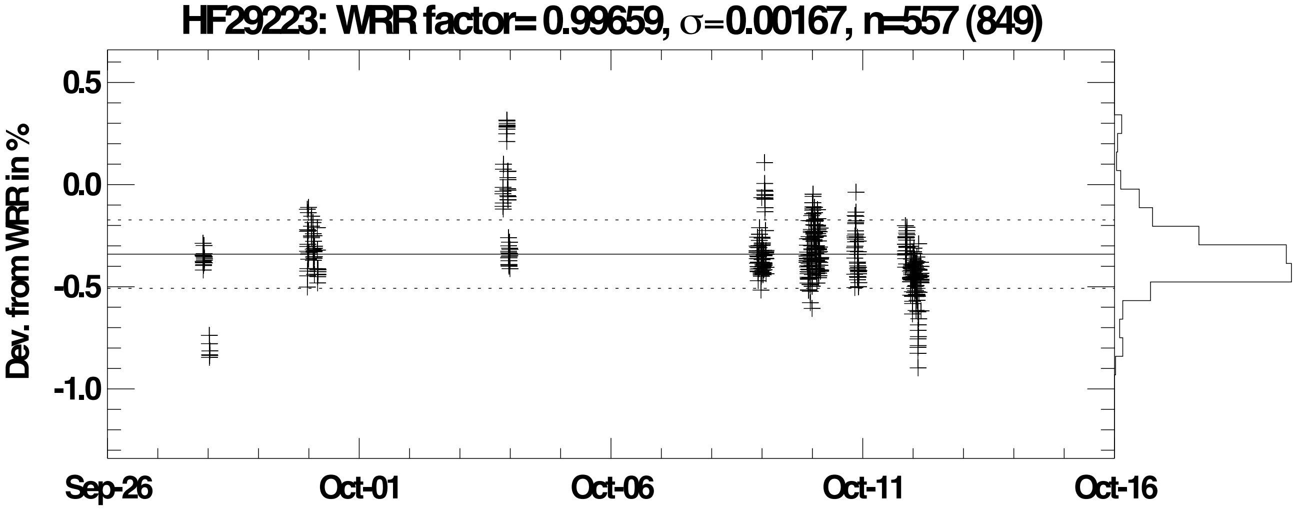
HF29223: WRR factor= 0.99659, σ=0.00167, n=557 (849)
Dev. from WRR in %
0.5
0.0
-0.5
-1.0
Sep-26
Oct-01
Oct-06
Oct-11
Oct-16

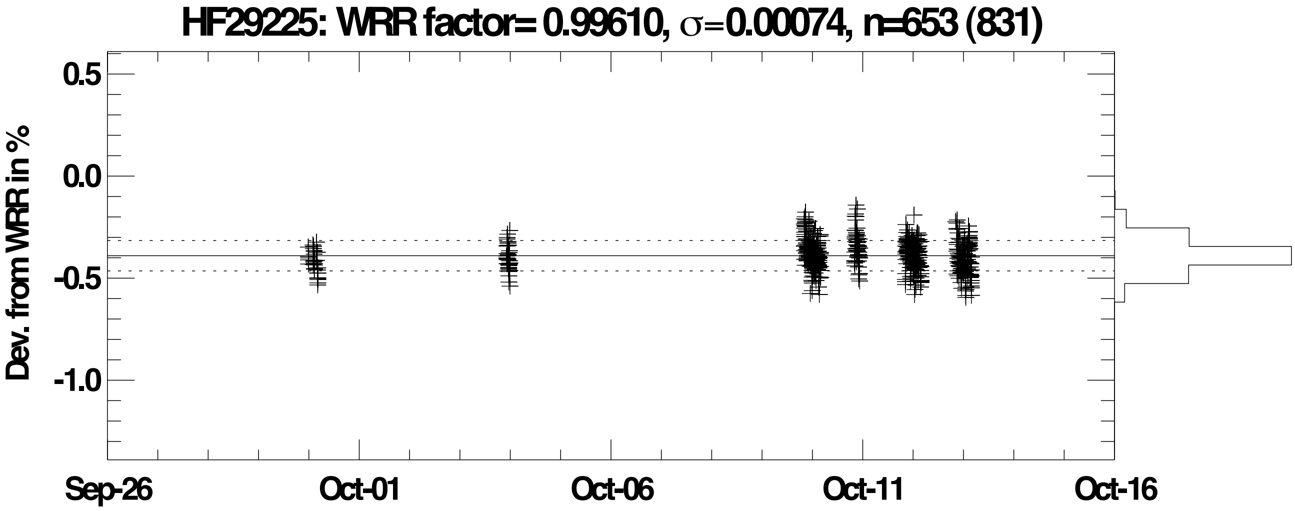
HF29225: WRR factor= 0.99610, σ=0.00074, n=653 (831)
Dev. from WRR in %
0.5
0.0
-0.5
-1.0
Sep-26
Oct-01
Oct-06
Oct-11
Oct-16

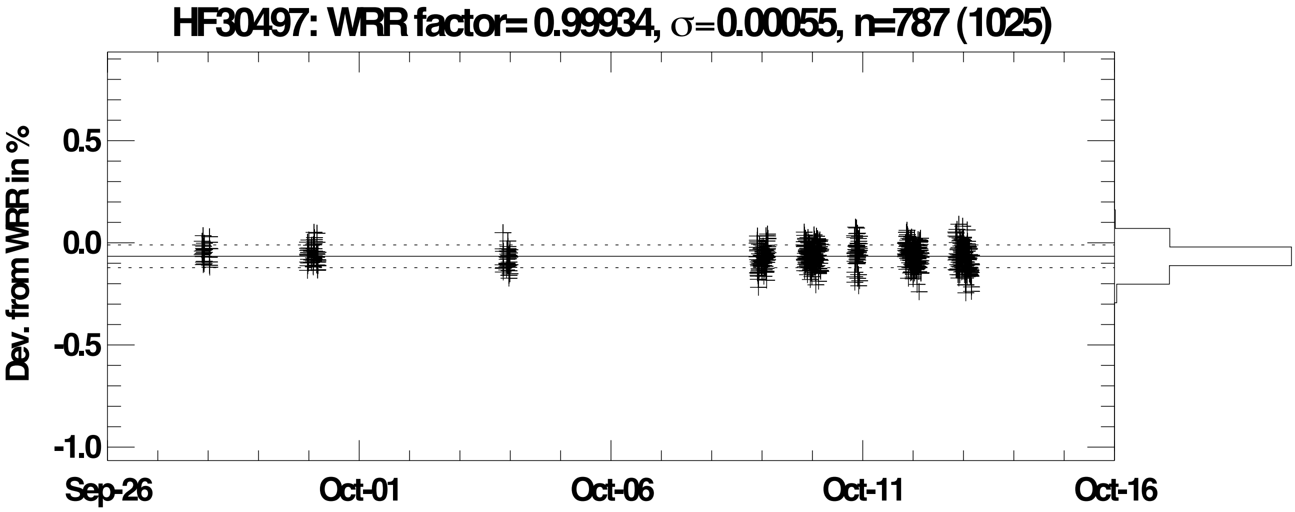
HF30497: WRR factor= 0.99934, σ=0.00055, n=787 (1025)
Dev. from WRR in %
0.5
0.0
-0.5
-1.0
Sep-26
Oct-01
Oct-06
Oct-11
Oct-16

HF31103: WRR factor= 0.99962, σ=0.00068, n=753 (1015)

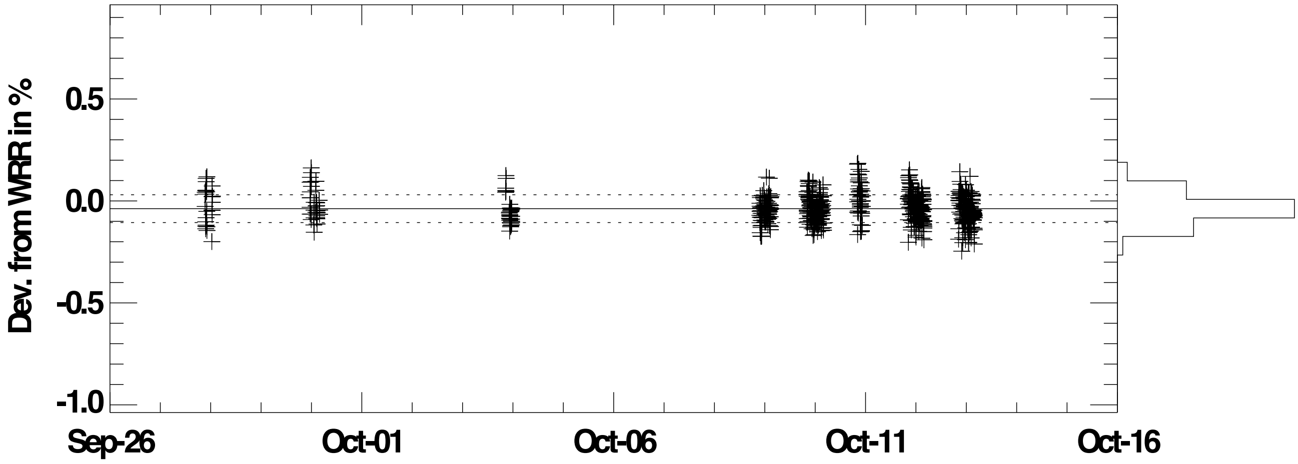

MAR-1-1: WRR factor= 0.99867, σ=0.00084, n=347 (423)

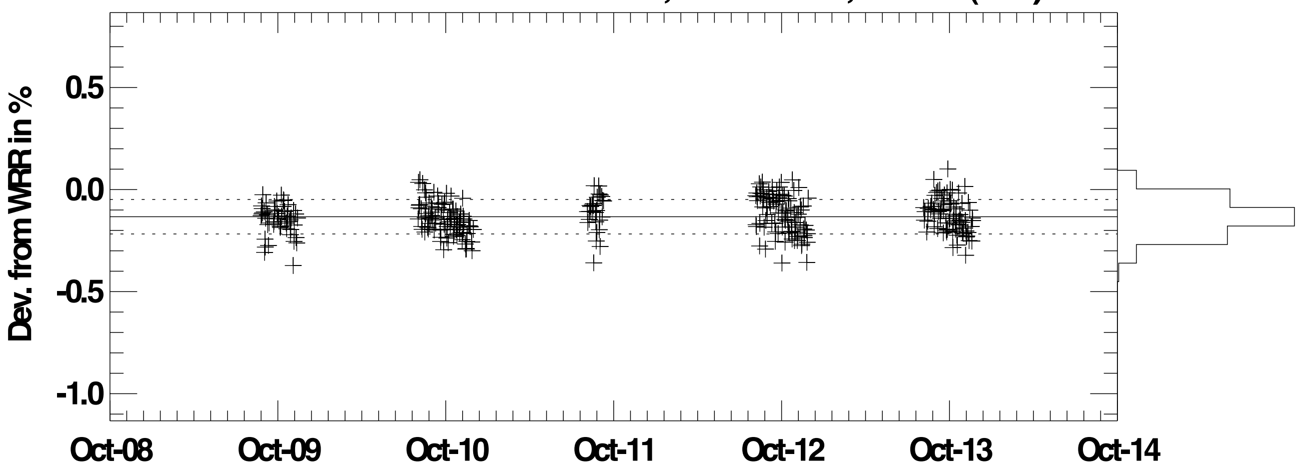

MAR-1-2: WRR factor= 0.99870, σ=0.00126, n=290 (329)

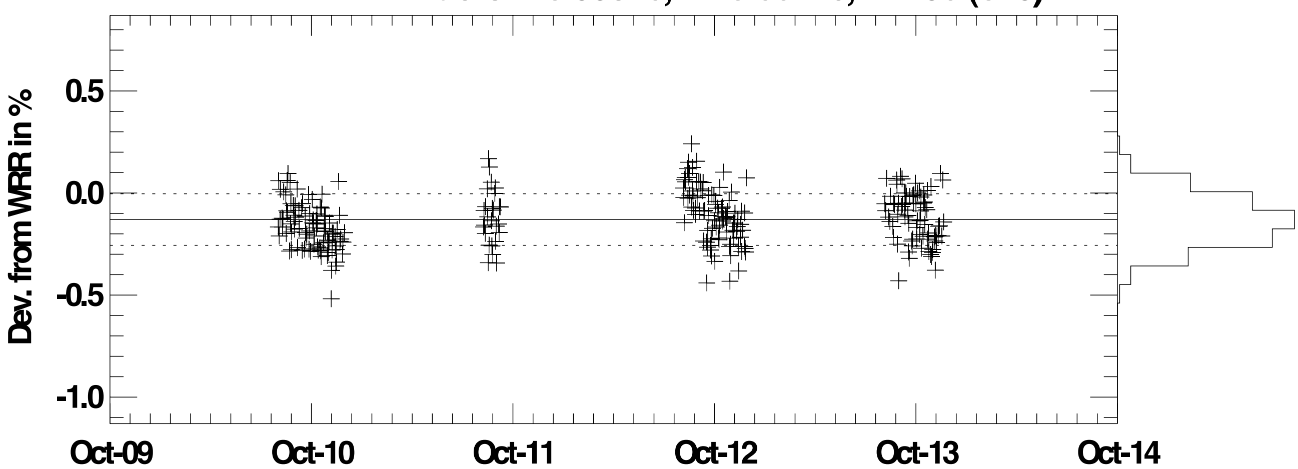

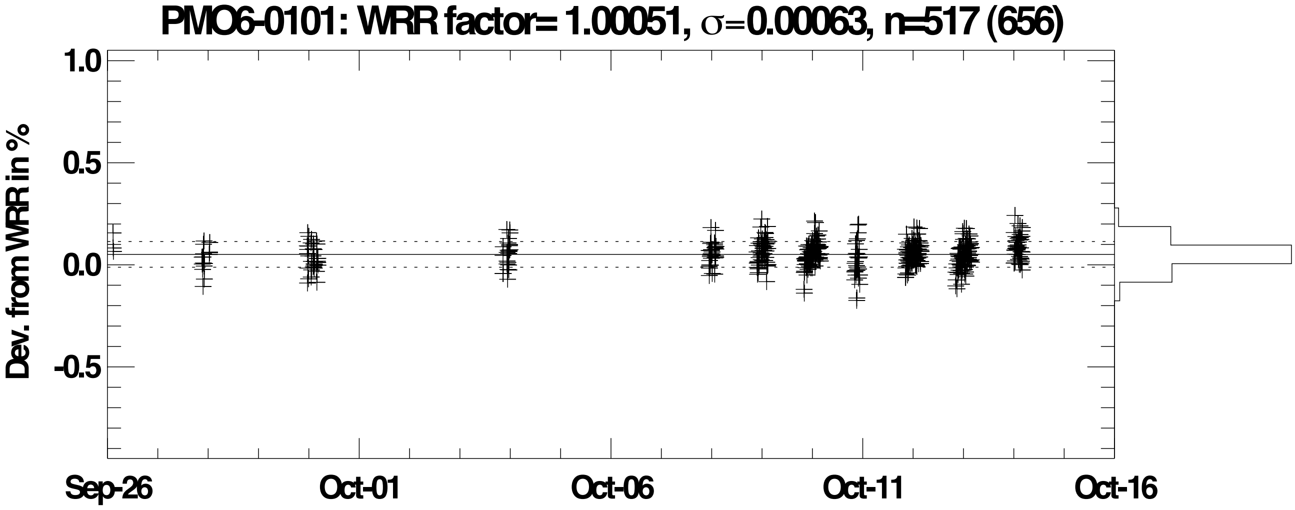
PMO6-0101: WRR factor= 1.00051, σ=0.00063, n=517 (656)
Dev. from WRR in %
1.0
0.5
0.0
-0.5
Sep-26
Oct-01
Oct-06
Oct-11
Oct-16

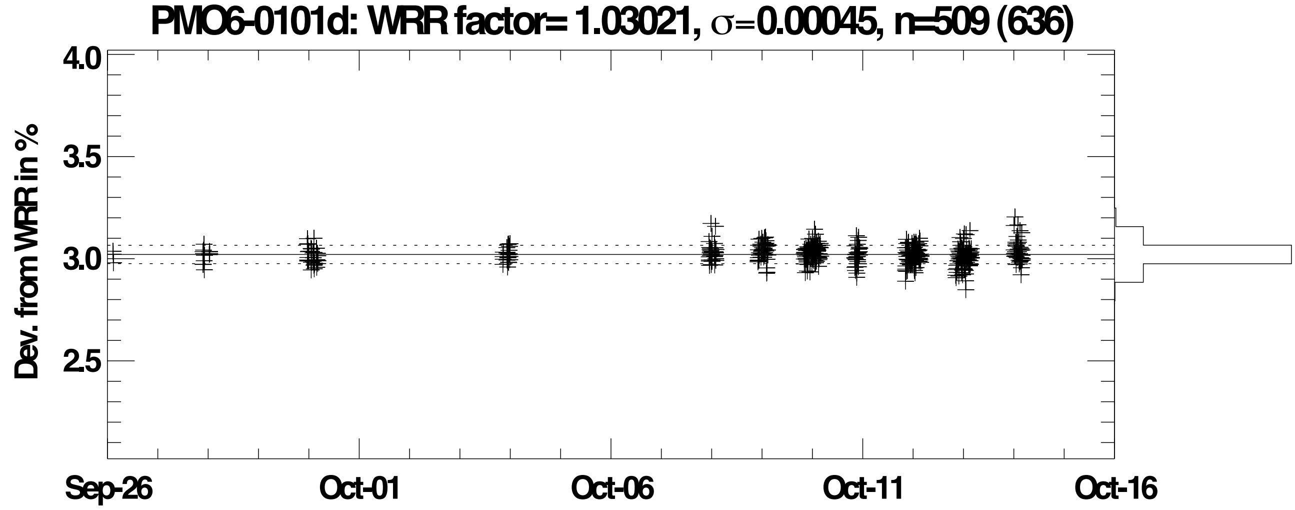
PMO6-0101d: WRR factor= 1.03021, σ=0.00045, n=509 (636)
Dev. from WRR in %
4.0
3.5
3.0
2.5
Sep-26
Oct-01
Oct-06
Oct-11
Oct-16

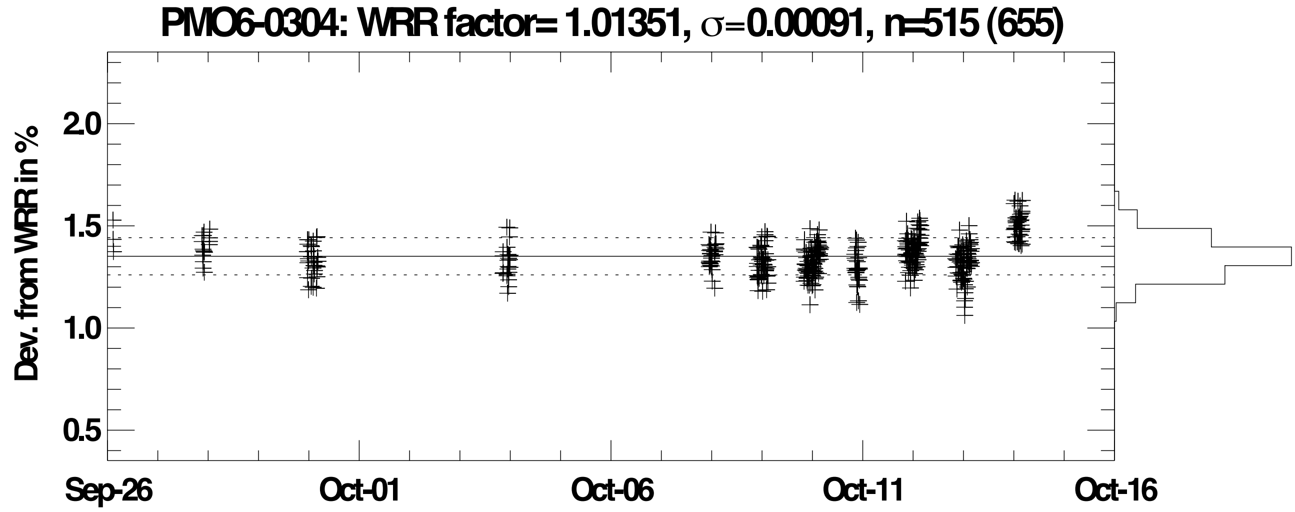
PMO6-0304: WRR factor= 1.01351, σ=0.00091, n=515 (655)
Dev. from WRR in %
2.0
1.5
1.0
0.5
Sep-26
Oct-01
Oct-06
Oct-11
Oct-16

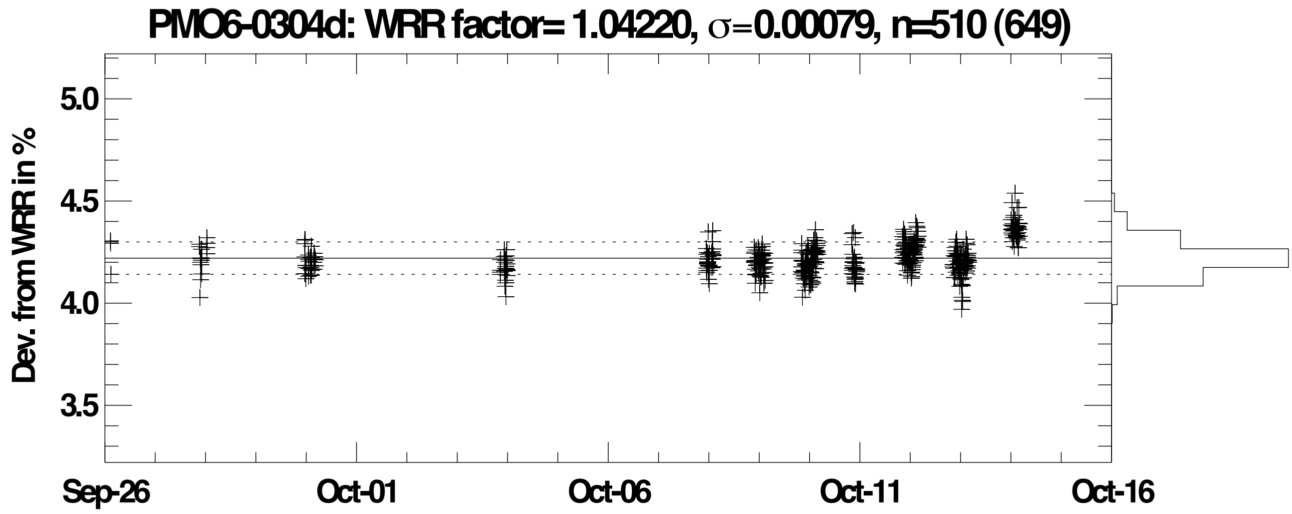
PMO6-0304d: WRR factor= 1.04220, σ=0.00079, n=510 (649)
Dev. from WRR in %
5.0
4.5
4.0
3.5
Sep-26
Oct-01
Oct-06
Oct-11
Oct-16

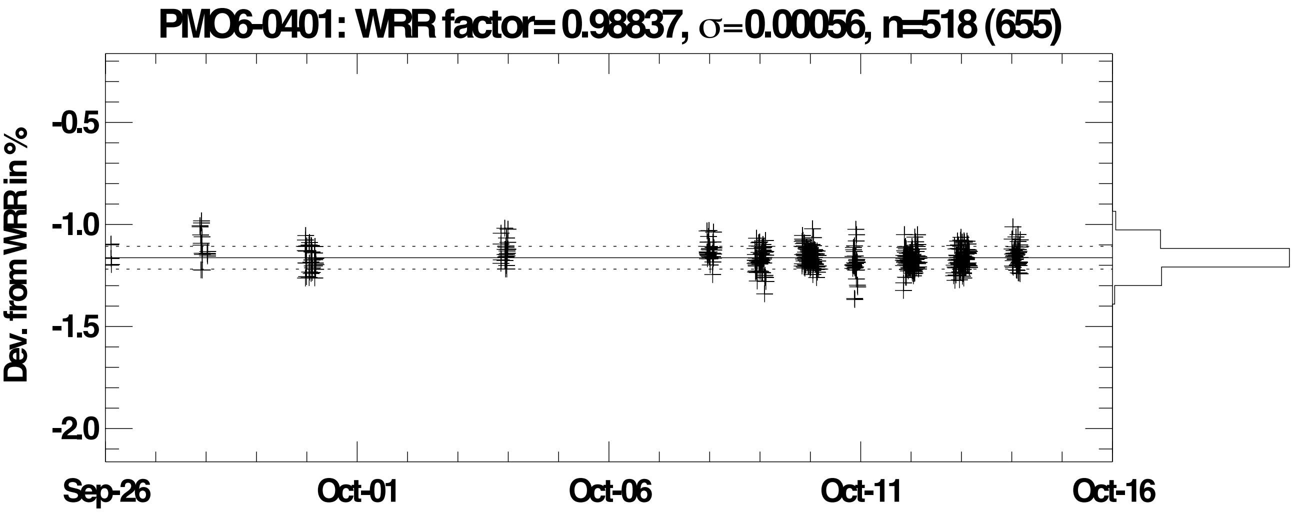
PMO6-0401: WRR factor= 0.98837, σ=0.00056, n=518 (655)
Dev. from WRR in %
-0.5
-1.0
-1.5
-2.0
Sep-26
Oct-01
Oct-06
Oct-11
Oct-16

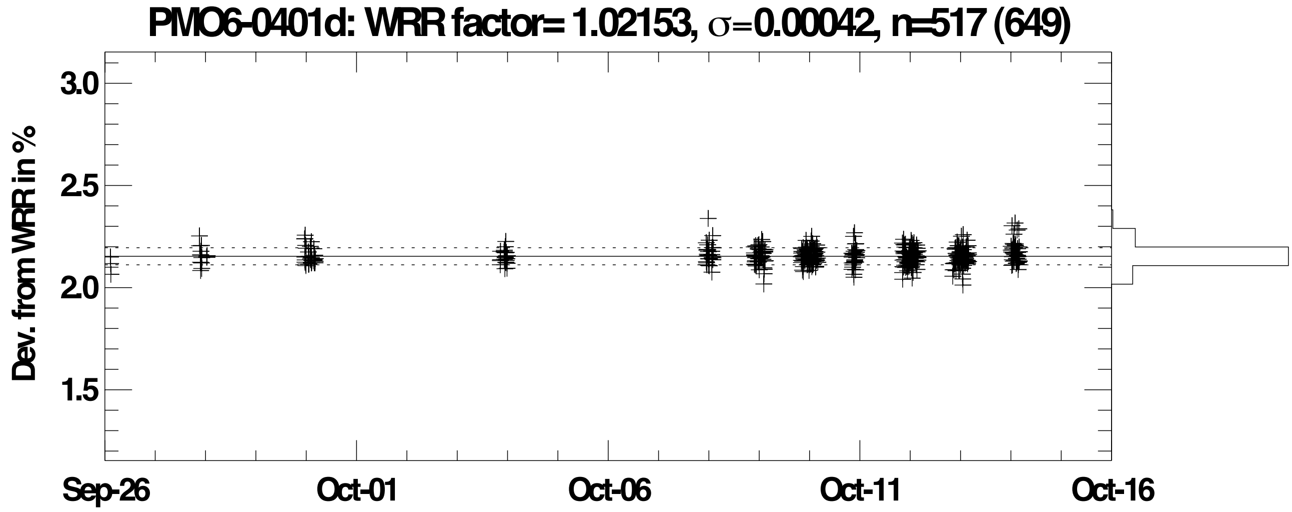
PMO6-0401d: WRR factor= 1.02153, σ=0.00042, n=517 (649)
Dev. from WRR in %
3.0
2.5
2.0
1.5
Sep-26
Oct-01
Oct-06
Oct-11
Oct-16

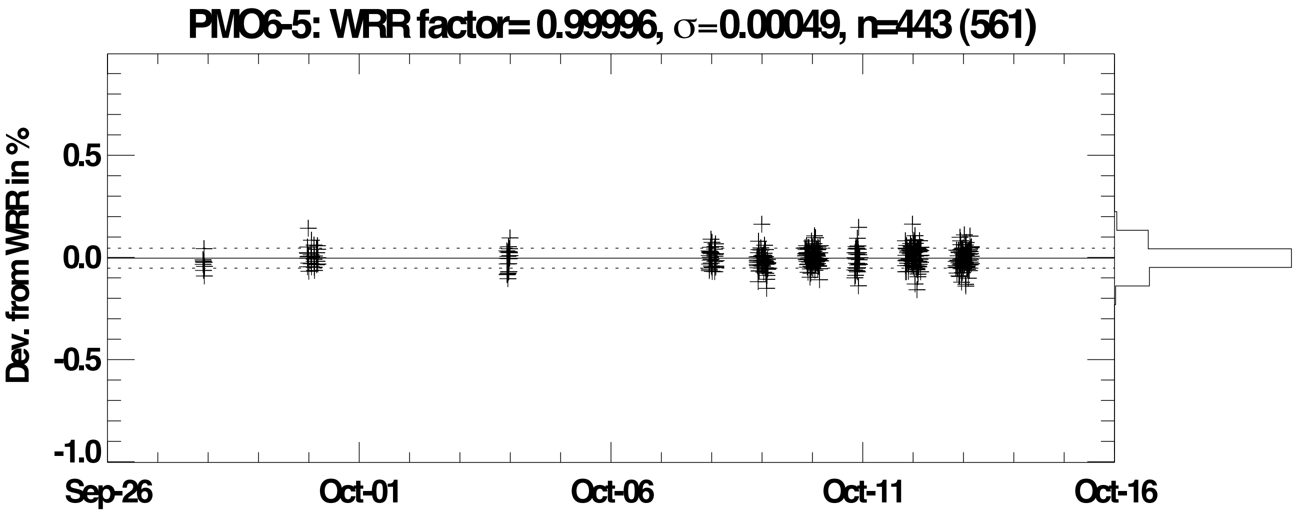
PMO6-5: WRR factor= 0.99996, σ=0.00049, n=443 (561)
Dev. from WRR in %
0.5
0.0
-0.5
-1.0
Sep-26
Oct-01
Oct-06
Oct-11
Oct-16

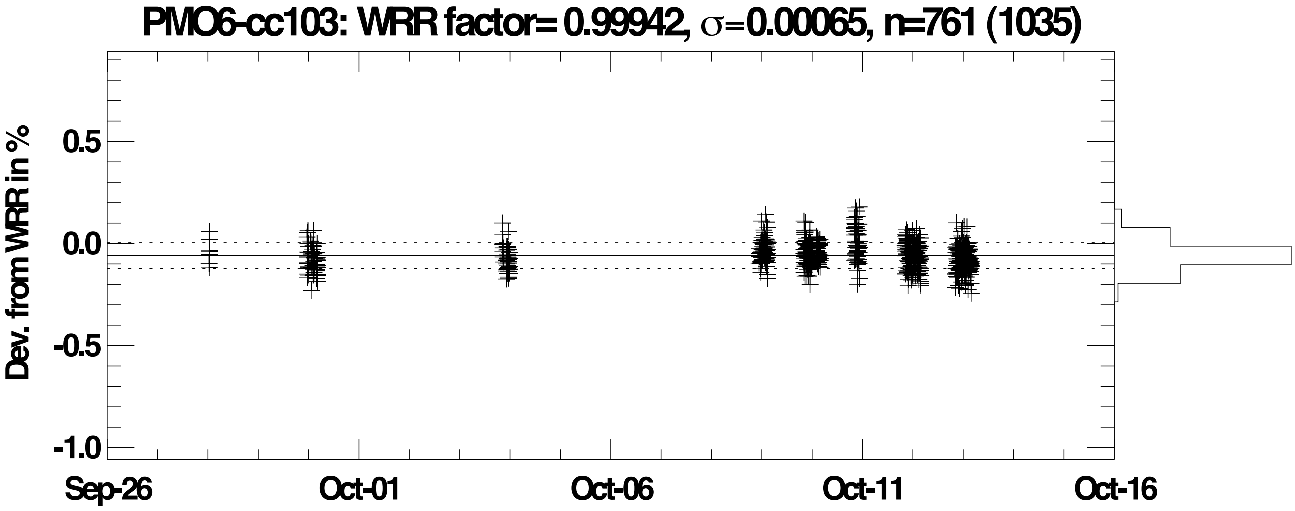
PMO6-cc103: WRR factor= 0.99942, σ=0.00065, n=761 (1035)
Dev. from WRR in %
0.5
0.0
-0.5
-1.0
Sep-26
Oct-01
Oct-06
Oct-11
Oct-16

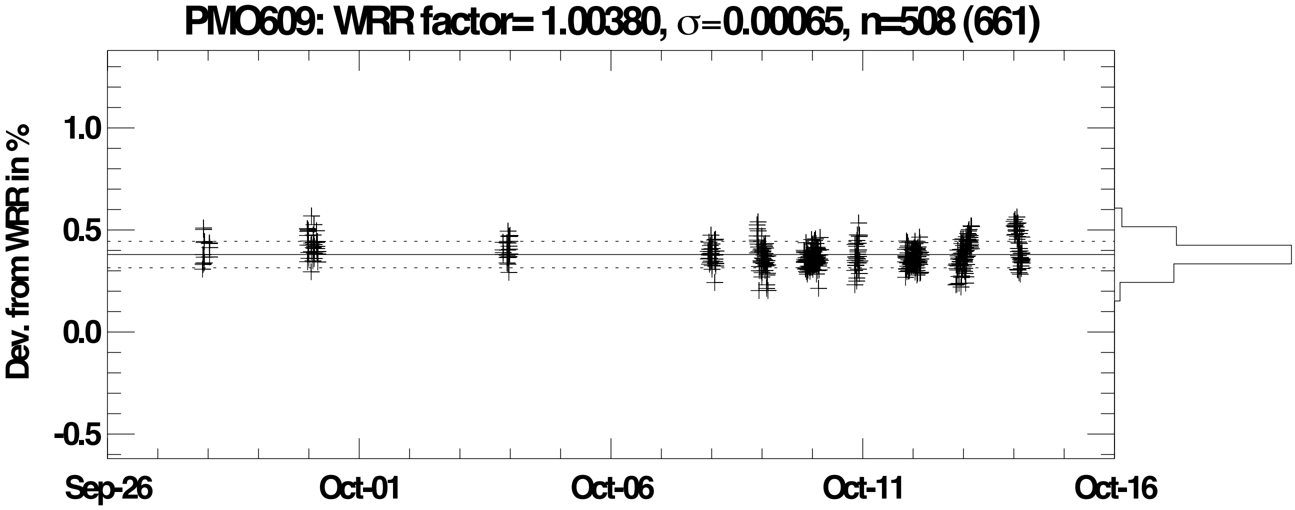
PMO609: WRR factor= 1.00380, σ=0.00065, n=508 (661)
Dev. from WRR in %
1.0
0.5
0.0
-0.5
Sep-26
Oct-01
Oct-06
Oct-11
Oct-16

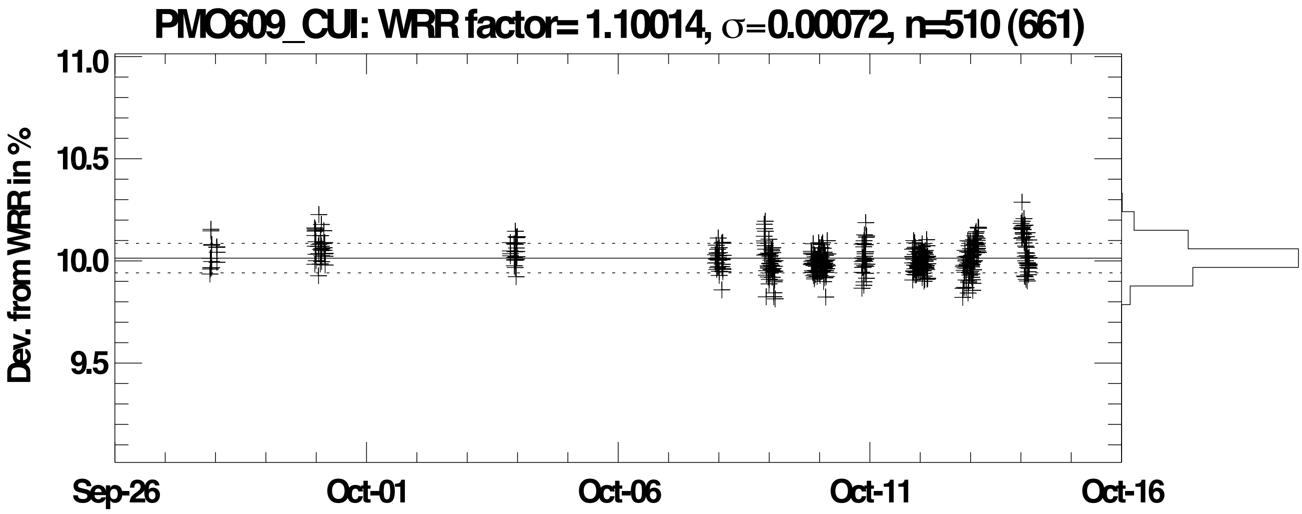
PMO609_CUI: WRR factor= 1.10014, σ=0.00072, n=510 (661)
Dev. from WRR in %
11.0
10.5
10.0
9.5
Sep-26
Oct-01
Oct-06
Oct-11
Oct-16

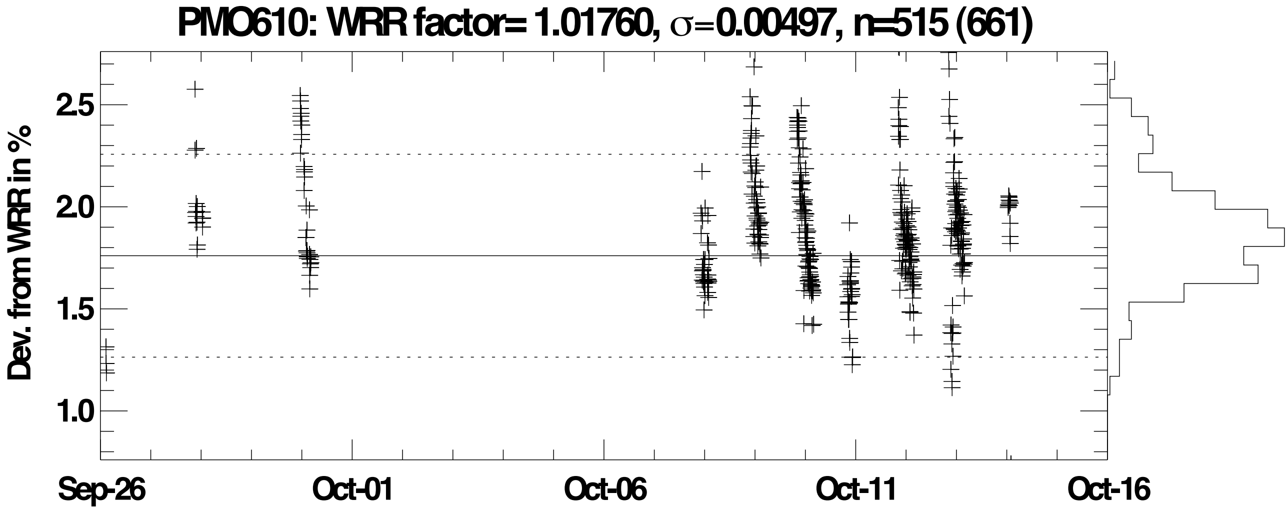
PMO610: WRR factor= 1.01760, σ=0.00497, n=515 (661)
Dev. from WRR in %
2.5
2.0
1.5
1.0
Sep-26
Oct-01
Oct-06
Oct-11
Oct-16

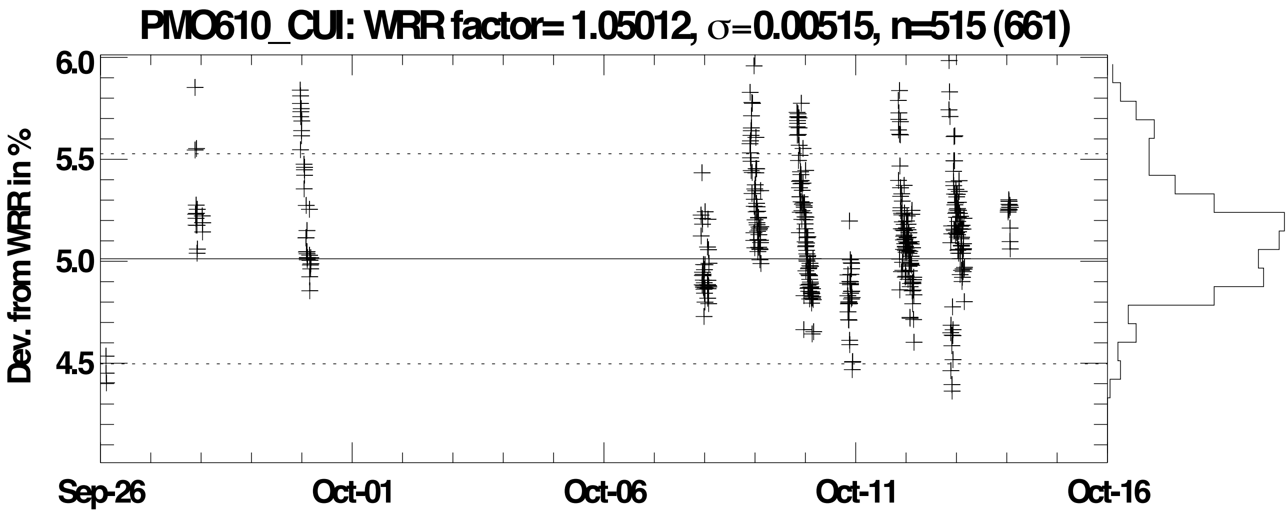
PMO610_CUI: WRR factor= 1.05012, σ=0.00515, n=515 (661)
Dev. from WRR in %
6.0
5.5
5.0
4.5
Sep-26
Oct-01
Oct-06
Oct-11
Oct-16

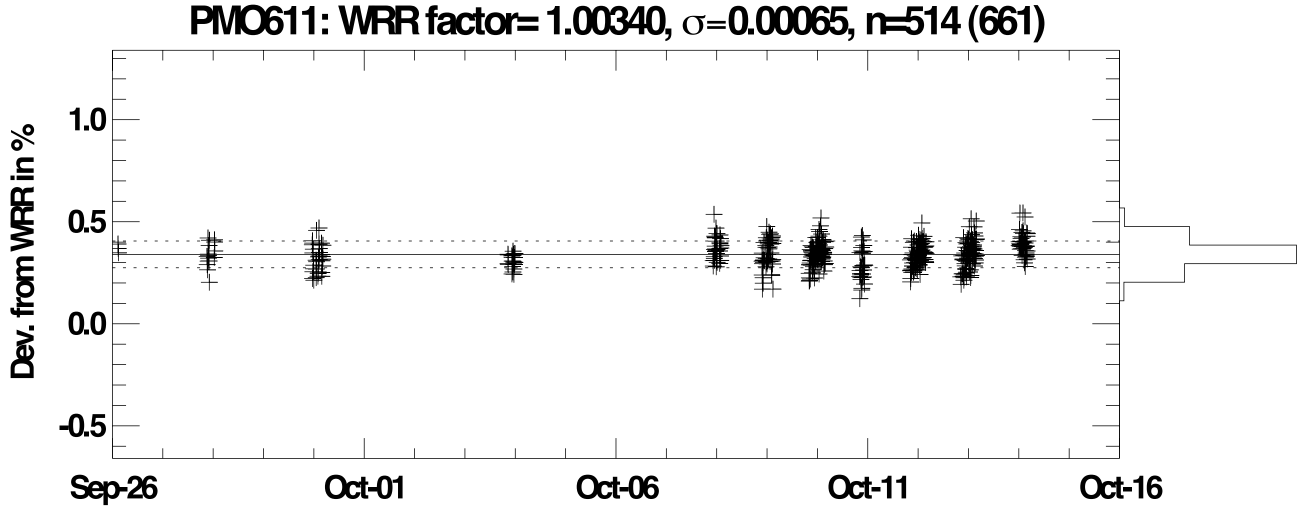
PMO611: WRR factor= 1.00340, σ=0.00065, n=514 (661)
Dev. from WRR in %
1.0
0.5
0.0
-0.5
Sep-26
Oct-01
Oct-06
Oct-11
Oct-16

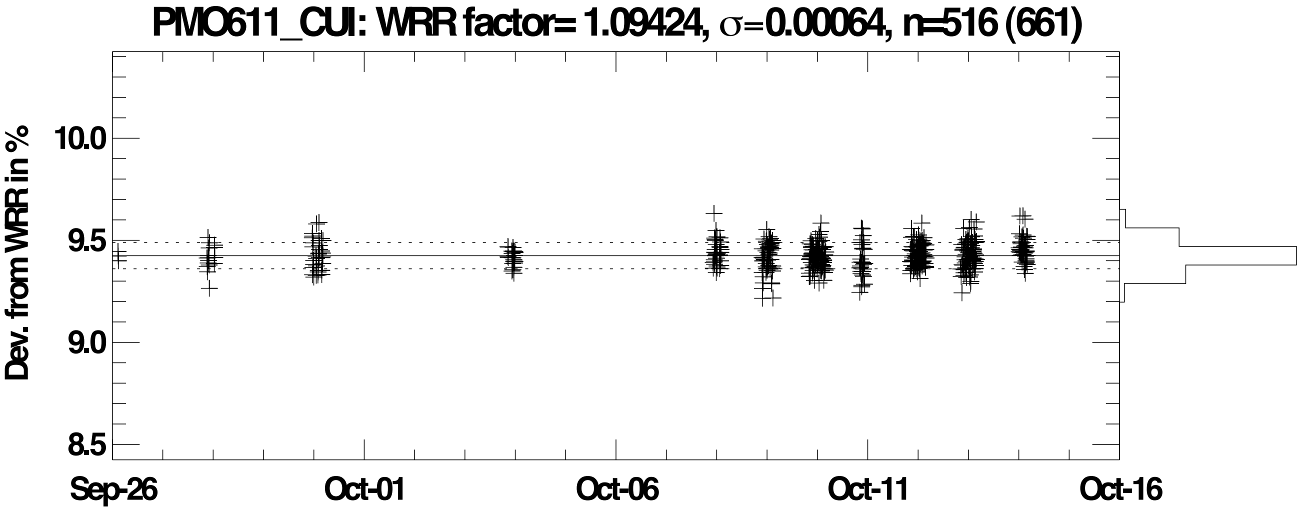
PMO611_CUI: WRR factor= 1.09424, σ=0.00064, n=516 (661)
Dev. from WRR in %
10.0
9.5
9.0
8.5
Sep-26
Oct-01
Oct-06
Oct-11
Oct-16

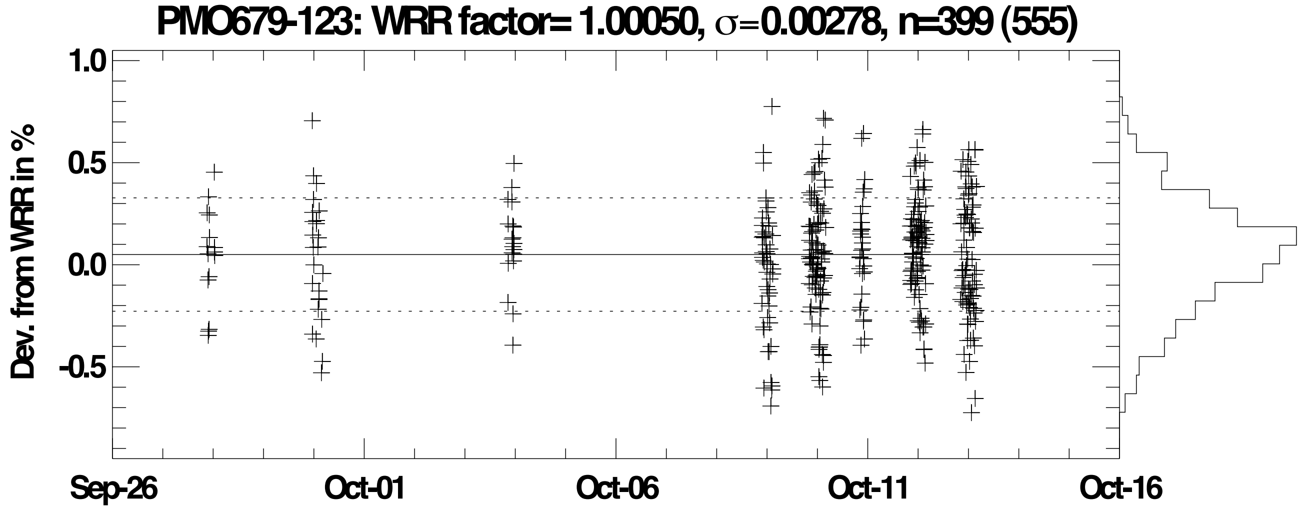
PMO679-123: WRR factor= 1.00050, σ=0.00278, n=399 (555)
Dev. from WRR in %
1.0
0.5
0.0
-0.5
Sep-26
Oct-01
Oct-06
Oct-11
Oct-16

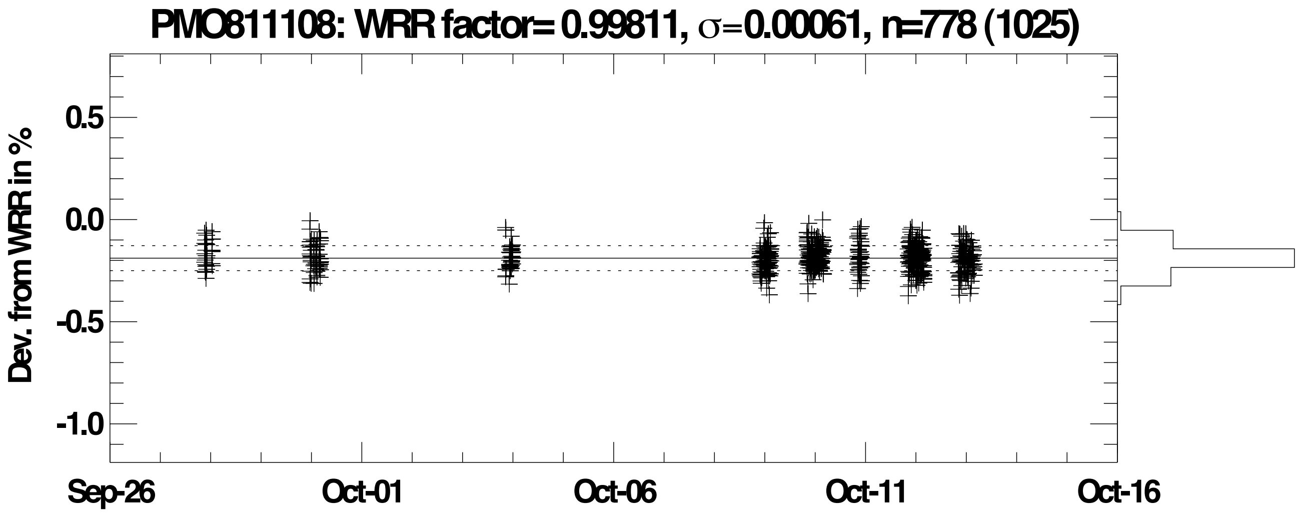
PMO811108: WRR factor= 0.99811, σ=0.00061, n=778 (1025)
Dev. from WRR in %
0.5
0.0
-0.5
-1.0
Sep-26
Oct-01
Oct-06
Oct-11
Oct-16

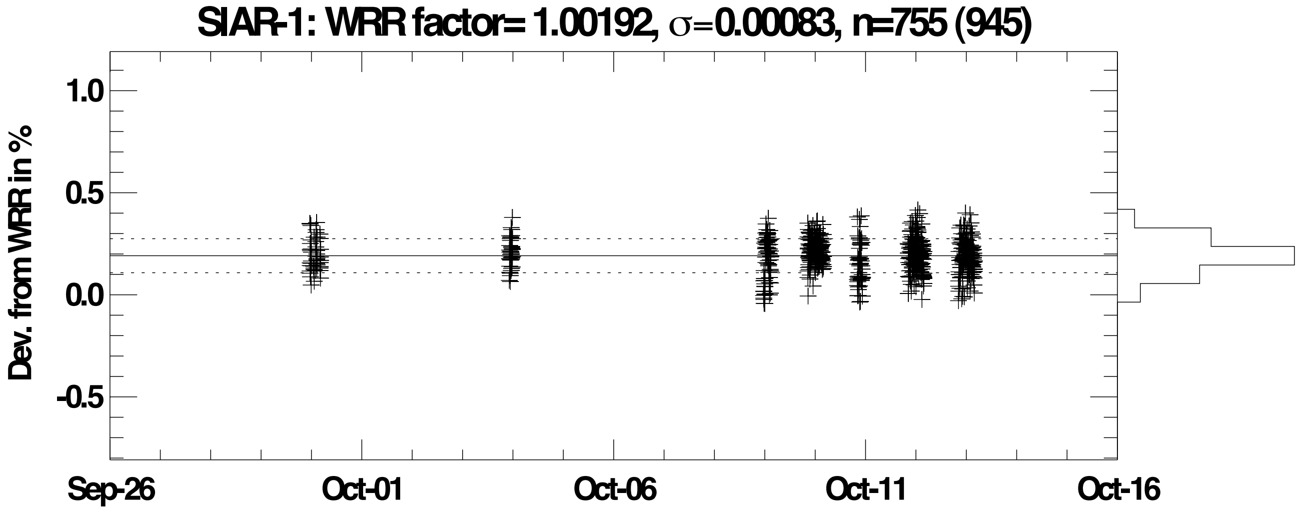
SIAR-1: WRR factor= 1.00192, σ=0.00083, n=755 (945)
Dev. from WRR in %
1.0
0.5
0.0
-0.5
Sep-26
Oct-01
Oct-06
Oct-11
Oct-16

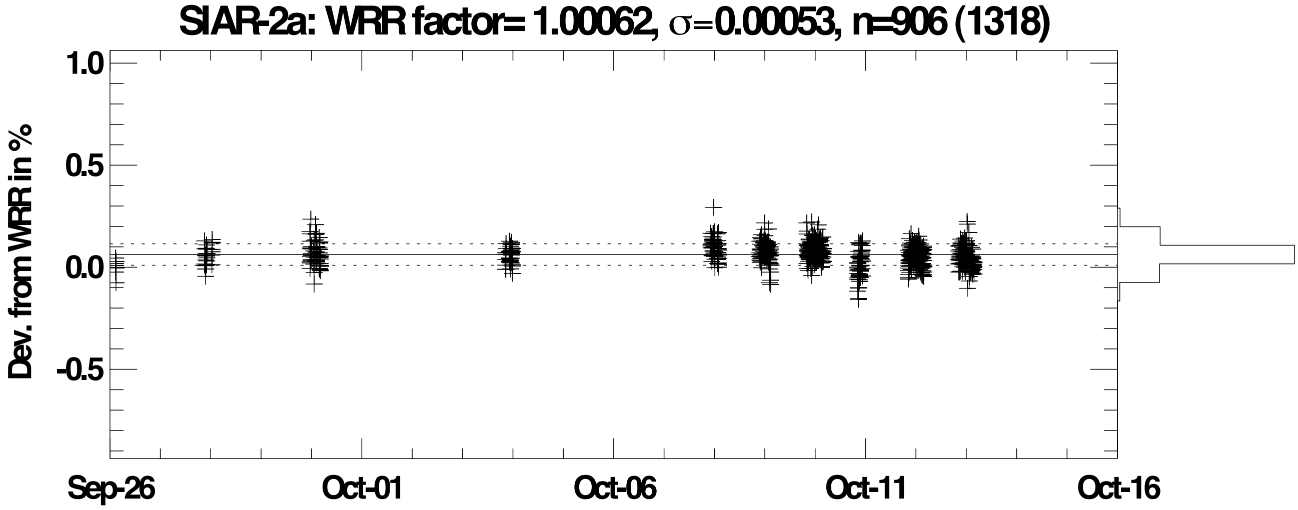
SIAR-2a: WRR factor= 1.00062, σ=0.00053, n=906 (1318)
Dev. from WRR in %
1.0
0.5
0.0
-0.5
Sep-26
Oct-01
Oct-06
Oct-11
Oct-16

SIAR-2b: WRR factor= 0.99862, σ=0.00051, n=970 (1318)

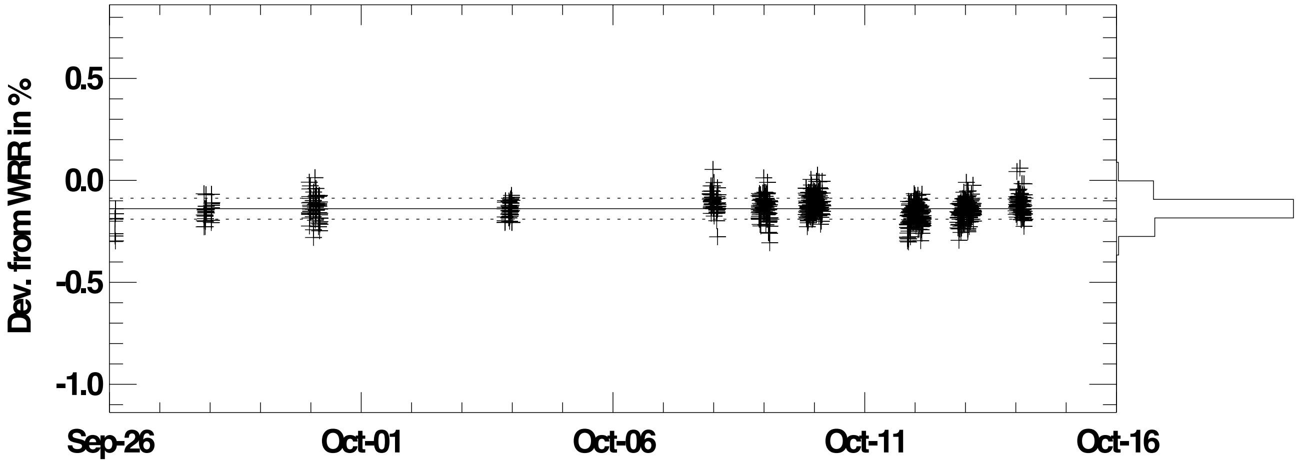

SIAR-2c: WRR factor= 1.00001, σ=0.00093, n=760 (956)

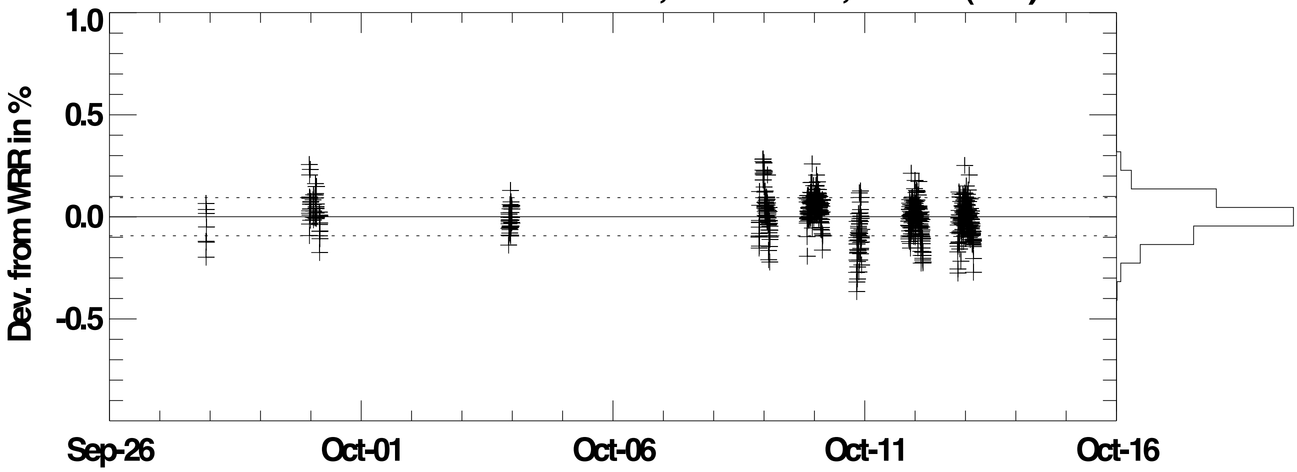

TMI67502: WRR factor= 0.99947, σ=0.00091, n=552 (660)

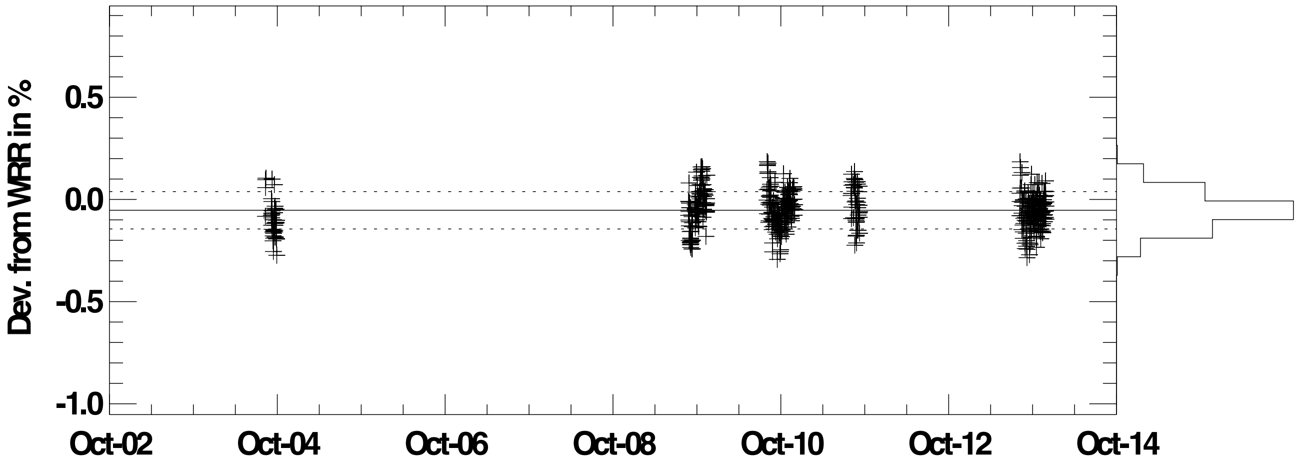

TMI67604: WRR factor= 0.99879, σ=0.00073, n=805 (1014)

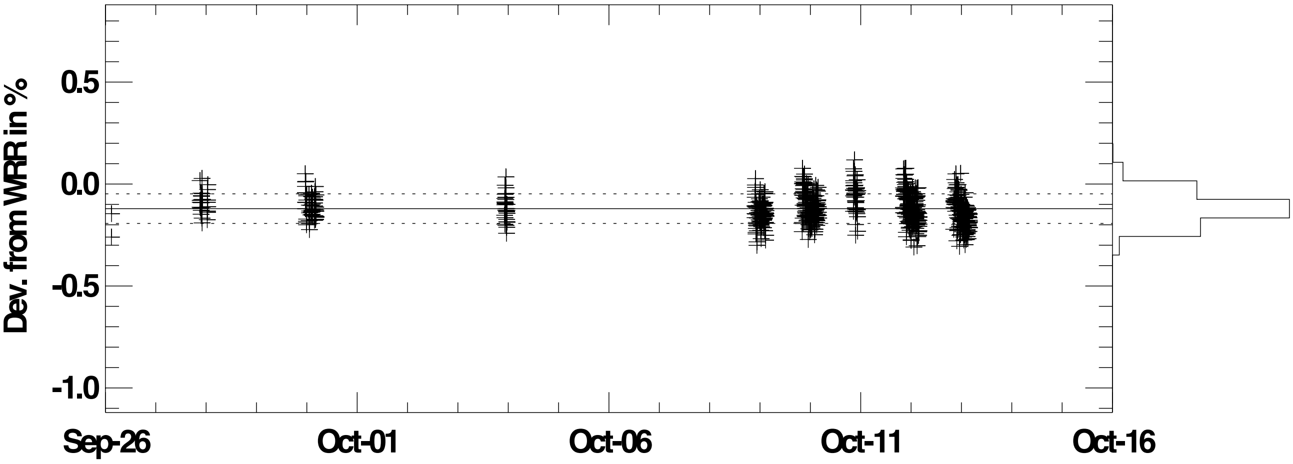

TMI68016: WRR factor= 1.00009, σ=0.00072, n=73 (1039)

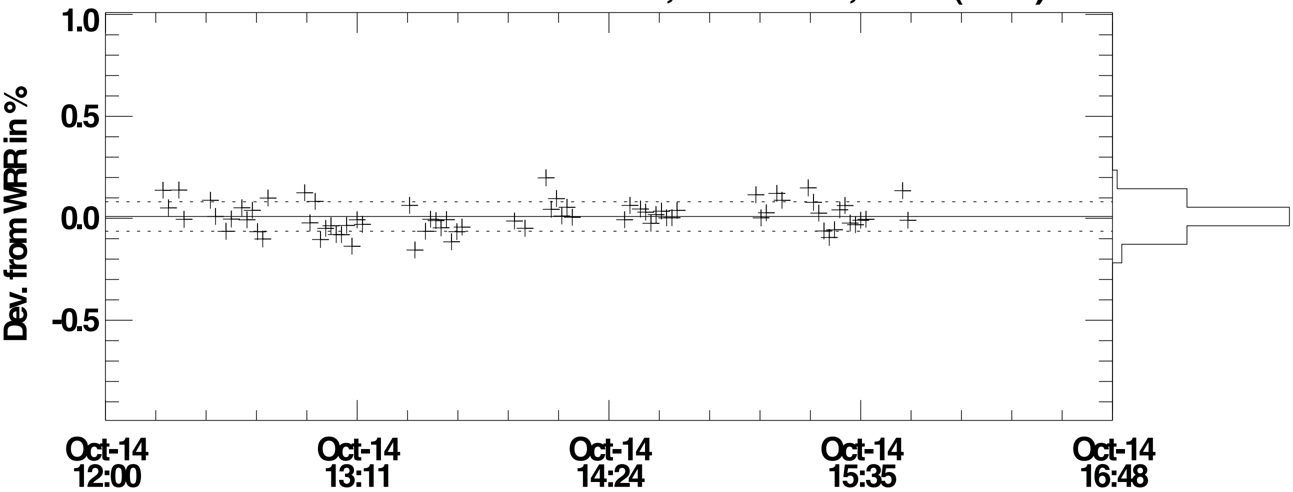

TMI68018: WRR factor= 0.99712, σ=0.00069, n=894 (1147)

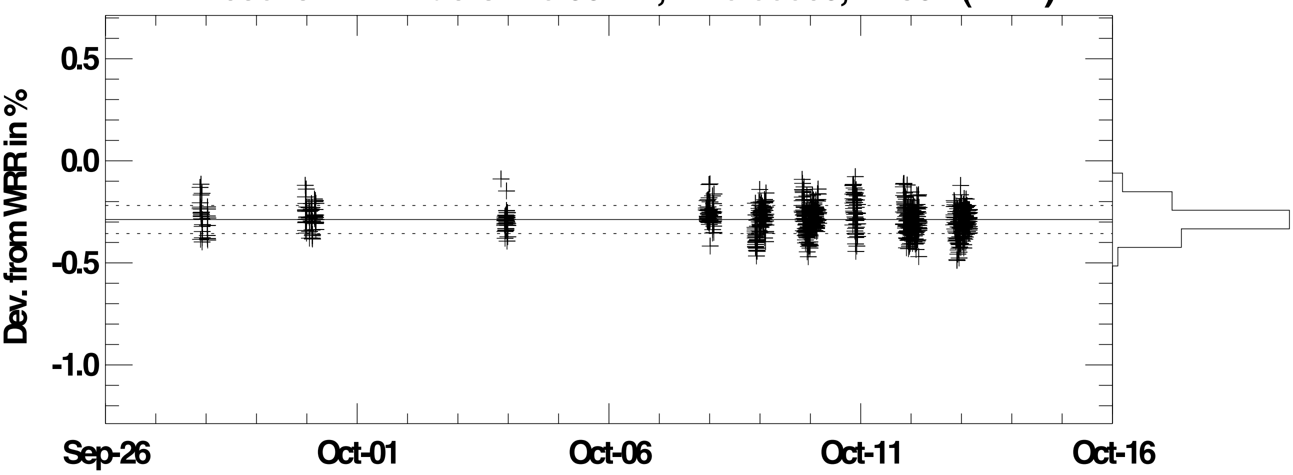

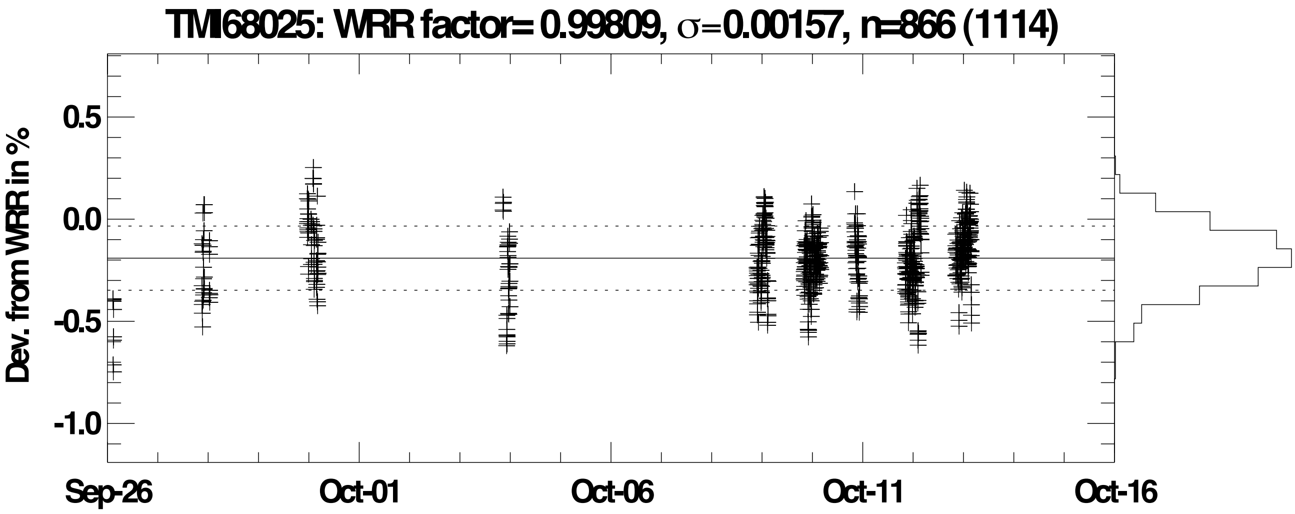
TMI68025: WRR factor= 0.99809, σ=0.00157, n=866 (1114)
Dev. from WRR in %
0.5
0.0
-0.5
-1.0
Sep-26
Oct-01
Oct-06
Oct-11
Oct-16

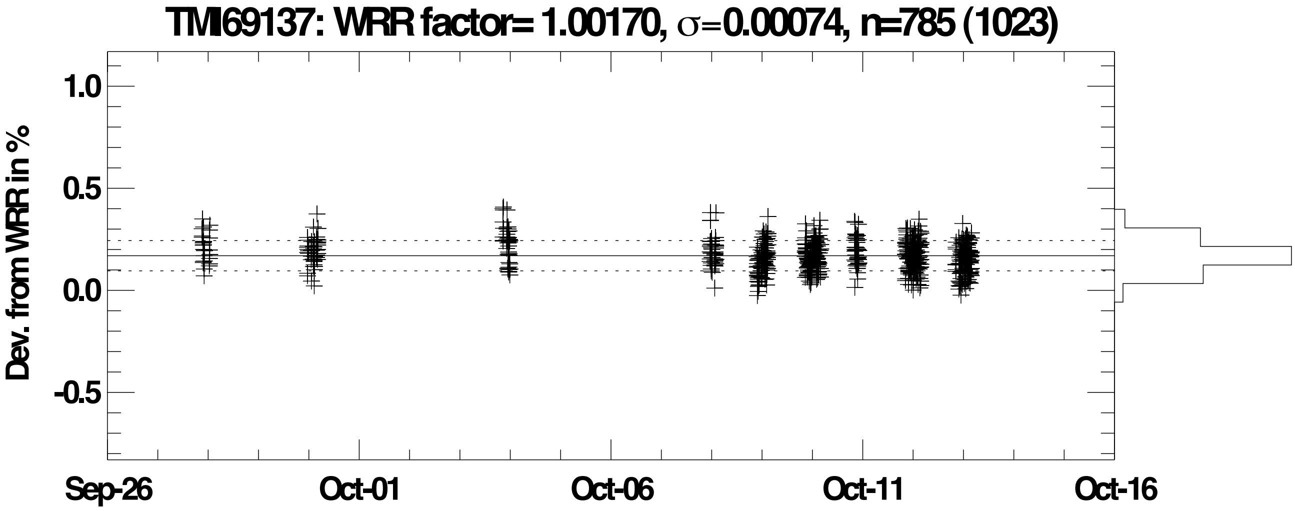
TMI69137: WRR factor= 1.00170, σ=0.00074, n=785 (1023)
Dev. from WRR in %
1.0
0.5
0.0
-0.5
Sep-26
Oct-01
Oct-06
Oct-11
Oct-16

3.2 Auxiliary Data

3.2.1 Direct, Global and Diffuse Irradiance

3.2.2 Meteorological Data

3.2.3 Airmass and Aerosol Optical Depth

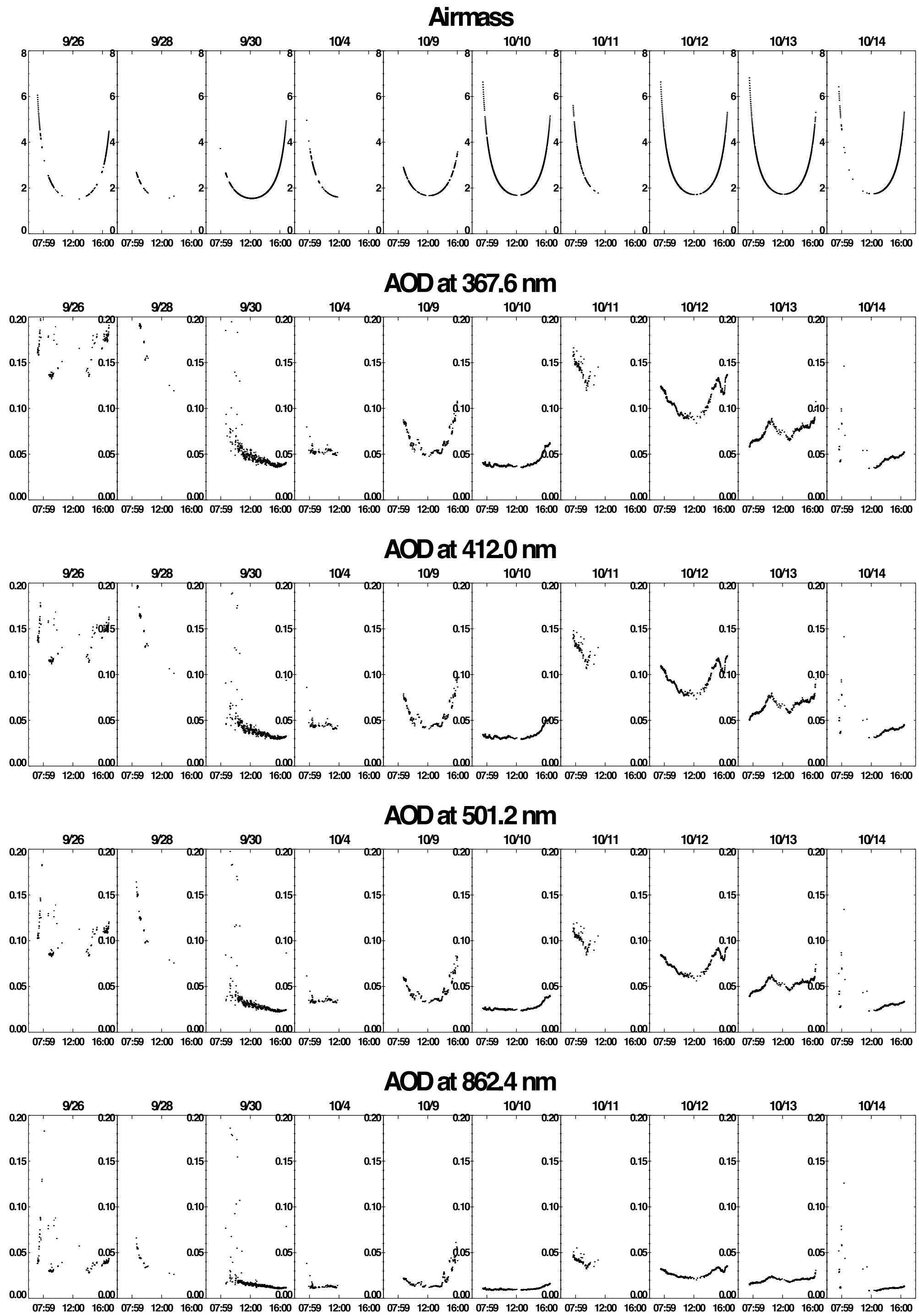

Part II

SYMPOSIUM